REPUBLIC OF IRAQ
MINISTRY OF HIGHER EDUCATION AND
SCIENTIFIC RESEARCH
AL-FURAT AL-AWSAT TECHNICAL UNIVERSITY
ENGINEERING TECHNICAL COLLEGE - NAJAF

ENHANCED DETECTION OF COVID-19 USING FUZZY LOGIC AND INDEPENDENT COMPONENT ANALYSIS TECHNIQUES

MOHANAD SAREM ABDULLAH

(M. Sc. In Communications Techniques Eng.)

2022

ENHANCED DETECTION OF COVID-19 USING FUZZY LOGIC AND INDEPENDENT COMPONENT ANALYSIS TECHNIQUES

THESIS

SUBMITTED TO THE COMMUNICATIONS TECHNIQUES ENGINEERING DEPARTMENT

IN PARTIAL FULFILLMENT OF THE REQUIREMENTS FOR THE DEGREE OF MASTER

IN

COMMUNICATION ENGINEERING

BY

MOHANAD SAREM ABDULLAH

Supervised by

Asst. Prof. Dr. Ahmed Kareem Prof. Dr. Faris Mohammed

November /2022

Supervisor Certification

We certify that this thesis titled " **Enhanced Detection of COVID-19 using Fuzzy Logic and Independent Component Analysis Techniques** " which is being submitted by Mohanad Sarem Abdullah was prepared under my/our supervision at the Communication Techniques Engineering Department, Engineering Technical College-Najaf, AL-Furat Al-Awsat Technical University, as partial fulfillment of the requirements for the of Technical Master degree Communication Engineering.

Signature

Name: Asst. Prof. Dr. Ahmed Kareem

(Supervisor)

Date: / 11 / 2022

Signature:

Name: Prof. Dr. Faris Mohammed

(Co-Supervisor)

Date: / 11 / 2022

In view of the available recommendation, I/we forward this thesis for debate by the examining committee.

Signature:

Name: **Prof. Dr. Ahmad T. Abdulsadda**

(Head of Comm Tech. Eng. Dept.)

Date: / / 2022

Committee Report

We certify that we have read this thesis titled "**Enhanced Detection of COVID-19 using Fuzzy Logic and Independent Component Analysis Techniques** " which is being submitted by **Mohanad Sarem Abdullah** and as Examining Committee, examined the student in its contents. In our opinion, the thesis is adequate for award of degree of Master.

Signature:
Name: Asst. Prof. Dr. Ahmed Kareem
(Supervisor)
Date: / / 2022

Signature:
Name: Prof. Dr. Faris Mohammed
(Co-Supervisor)
Date: / / 2022

Signature:
Name: Asst. Prof. Dr Ahmed M. Z. Al Hilli
(Member)
Date: / / 2022

Signature:
Name: Asst. Prof. Dr Salam Mahdi Azooz
(Member)
Date: / / 2022

Signature:
Name: Prof. Dr. Hikmat Najem Abdullah
(Chairman)
Date: / / 2022

Approval of the Engineering Technical College- Najaf

Signature:
Name: Asst. Prof. Dr. Hassanain Ghani Hammet
(Dean of Engineering Technical College- Najaf)
Date: / / 2022

Linguistic Certification

This to certify that this thesis entitled "**Enhanced Detection of COVID-19 using Fuzzy Logic and Independent Component Analysis Techniques**" was reviewed linguistically. Its language was amended to meet the style of the English language.

Signature:

Name:

Date: / / 2022

Abstract

The diagnosis of the COVID-19 virus (Coronavirus) is a major health issue worldwide. There are many ways to diagnose this disease, among them the PCR test, which is used world widely. Together of being this test are slow in its results, also its accuracy is questionable, as it is associated with high false negative/positive results. Accordingly, chest x-ray (CXR) consider to be important investigation method in reaching the diagnosis. The objectives of this research are enhancement detection of COVID-19 through fuzzy logic technique in two ways (fuzzy edge images detection, expression of the proportion of lung damage) and the use of independent component analysis (ICA) for the dimensionality reduction (unnecessary features reduction) process.

The methodology of this research involve collecting of CXR images from different trusted dataset sources then using the proposed technique (fuzzy logic, ICA) as image pre-pressing, after that use the convolution neural network (CNN) specifically deep learning networks are used to train the data come from previous pre-processing, study the results of the impact of the proposed techniques related, are done by using model analysis. Finally, a practical testing for the final model on a mini-computer hardware (Raspberry Pi) was don to be used as webserver. The results of fuzzy logic technique shows that 97% of area under curve (AUC) when using ResNet152V2 and 96% AUC in using DenseNet121.While during using ICA technique the result shows 97% of area under curve (AUC) when using ResNet152V2 and 94% AUC in using DenseNet121.In combination with both techniques, the result shows 99% of AUC when using InceptionV3 and 99% of AUC in using EfficientNetB3, based on the performance results obtained. The proposed techniques show high performance in terms of AUC, accuracy, precision, and training

time when compared with recent techniques present in the previous literature. Finally, the proposed system has been applied for this work, through the creation of a web application, where the patient's image is entered on the trained model using a smart device (mobile or tablet) via a graphical user interface (GUI) with using IOT technique for uploading the images to the cloud for the verification purpose then sent confirmation state to the patient.

Acknowledgments

In the name of Allah, the Most Gracious, the Most Merciful. Praise be to Allah for His guidance throughout this work, and blessings and peace be upon His Prophet Muhammad and his honorable family.

First, I would like to thank Allah Almighty for His kindness and mercy and for all His blessings upon us, for allowing me the opportunity to complete my studies.

I extend my heartfelt thanks to my family as they have been the best help to me in my scientific career.

I would like to appreciate the efforts made by my supervisor Prof. Dr. Ahmed Al-Bakri and Prof. Dr. Faris Al-Jaifari, who had the greatest impact in meeting the requirements of the current study.

I will always try to live up to your expectations.

DECLARATION

I hereby declare that that the work in this thesis is my own except for quotation and summaries which have been duly acknowledged.

1Nov 2022 **Mohanad Sarem Abdullah**

LIST OF TABLES

List of Figures

List of Abbreviation

1D	One Dimensions
2D	Two Dimensions
3D	Three Dimensions
ARDS	Acute Respiratory Distress Syndrome
AI	Artificial Intelligence
ANN	Artificial Neural Network
AUC	Area Under the Curve
BRISQUE	Blind/referenceless image spatial quality evaluator
BSS	Blind signal separation
CAD	Computer-Aided Diagnostic
CNNs	Convolutional Neural Networks
COVID-19	Coronavirus Disease of 2019
CT-Scan	Computed tomography Scans
CXR	Chest x-ray
DL	Deep Learning
DNN	Deep Neural Networks
FCL	Fully Connected Layer
FIS	Fuzzy Inference Systems
FN	False Negatives
FP	False Positives
GUI	Graphical user interface
HTML	Hypertext Markup Language
ICA	Independent Component Analysis
ICU	Intensive Care Unit
IOT	Internet of Things
LOM	Largest of maxima
ML	Machine Learning
MRI	Magnetic Resonance Imaging
MSCN	Mean Subtracted Contrast Normalized
PCA	Principle Component Analysis
ResNet	Residual Network
ROC	Receiver Operating Characteristic
RT-PCR	Reverse transcription polymerase chain reaction
SARS	Severe Acute Respiratory Syndrome
SOM	Small of maxima
TN	True Negatives
TP	True Positives
VGG	Visual Geometry Group

List of Symbols

S(I(x,y))	Binary decision of picture
F	Convolutional kernel is size
X_i	Demonstrates the result
D(*I*)	Detection Function
A	Fuzzy Sets
Gl(n)	General linear group
G	Gold standard
h_i	Image's height
w_i	Image's width
Z	Input size
I(m,n)	Intensity image
k^{th}	layer's input
μ(m,n)	Local mean
σ(m,n)	Local variance
I(x,y)	Medical image
A	Mixing matrix
i^{th}	No. layer's
W	Non-singular matrices
n	Objects of interest
R	Outcome
P	Padding value
M	picture
R_i	Represents the i^{th} layer
s	Signal source vector
p	Source signals
S	Step size
μ_{output}	The Max operator

CHAPTER ONE

INTRODUCTION

1. 1 Background

Coronavirus (COVID-19) in recent years is considered one of the most dangerous and fastest-spreading diseases because it affects the respiratory system (lung) directly, as the damage that occurs in the lung may worsen, causing suffocation and usually leading to death. The outbreak of this virus also disrupted economic life all over the world. Therefore, researchers in the field of artificial intelligence and health are looking to develop a low-cost and quick-detection tool to limit its spread by diagnosing it with high efficiency. Although the use of examination by chest X-ray (CXR) is one of the useful candidate methods, it must be analyzing the images resulting from the sigmoidal scanning devices, and a large number of assessments must be processed. The CXR is a vital step for researchers to combat COVID-19. Therefore, the diagnosis by CXR has become an important diagnostic tool for detecting the presence of COVID-19, by detecting cloudy incomplete white (glass-ground) spots in the lung [1].

It is sometimes seen in the shape and distribution in the vicinity of the lungs. Using CXR, many Deep Learning (DL) approaches were able to detect COVID-19 patients with high accuracy. [2,3] Since most health centers and hospitals contain X-ray machines, a lung x-ray examination is one of the most important and fastest types of examination to detect COVID-19 patients. Because specialist radiologists are hard to find and frequently

booked during epidemics, automatic diagnosis of COVID-19 from chest pictures is particularly desirable. Despite the fact that the vast majority of machine learning models may be incorrect, so the disease can be initially predicted until a radiologist is available to confirm the case by looking at the database of the person to be examined through the cloud and Internet of Things (IoT) [4]. Medical image analysis is done by segmentation techniques, which will help clinicians and patients obtain basic and necessary information for 2D and 3D visualization, and early disease detection [5]. The classification of areas of interest (ROIs), such as bronchopulmonary segments, lobes, the lung, and infected areas or lesions at computed tomography (CT) or CXR images, is referred to as segmentation. It is possible to extract features from the segmented areas for description and other purposes [6].

Given the vast number of patients, automated computer-aided diagnostic (CADx) tools supported by artificial intelligence (AI) techniques to detect and distinguish COVID-19-associated nasal anomalies must be tremendously beneficial. These instruments are especially useful in areas without easy access to CT scans or with limited radiological knowledge. The CXR facilitates quicker triage and higher throughput in mass casualty situations. These tools use a combination of radiological image processing and computer vision to recognize common illness indicators and pinpoint problems. Currently, the DL techniques are based on convolutional neural networks (CNNs),have shown encouraging results in recognizing, classifying, and quantifying illness patterns in medical imagery in CXRs and CT scans [7-9].

Fuzzy logic has played an important role in several fields of research in recent decades [10]. Fuzzy logic is a branch of fuzzy set theory that simulates reasoning and human thought to improve the procedure's efficacy while dealing with unclear or ambiguous data [11]. Especially when adding the ICA technique to get impressive results in the field of image processing and data analysis [12, 13]. Applying the FastICA algorithm to reduce image dimensions, greatly helped in accelerating the training process without affecting the image properties.

1.2 Problem statement

1- Generally, the current methods that are used for COVID-19 detection by CXR images do not give a comprehensive evaluation of the COVID -19 case.

2- The patient's state becomes more complicated if there was a late diagnosis, by using traditional diagnosis like PCR and may be the event of the virus exacerbating, which leads to severe dyspnea and thus directly affects human life.

3- The lack of intervention by a specialist doctor in artificial intelligence systems may cause danger to human life in some cases.

1.3 Research Objectives

The objective of the thesis is summarized as follows:

1. Enhancement detection of COVID-19 through fuzzy logic technique in two ways:

1.1 - Applying the fuzzy filter on CXR images as pre-processing, to obtain models of classification with high performance metrics such as recall, precision, and accuracy.

1.2 - Expression of the proportion of lung damage after prediction in the same way as decision-making in humans.

2. Use ICA as dimensionality reduction process by reducing unnecessary features.
3. Design and implementation of a practical device for the purpose of early diagnosis by using Raspberry Pi and work as a web server to access webpage Graphic User Interface (GUI), which can be connected directly with internet for IOT.

1.4 General Methodology

The methodology was explained in general in flowchart Figure (1.1) to show the main objective of this work:

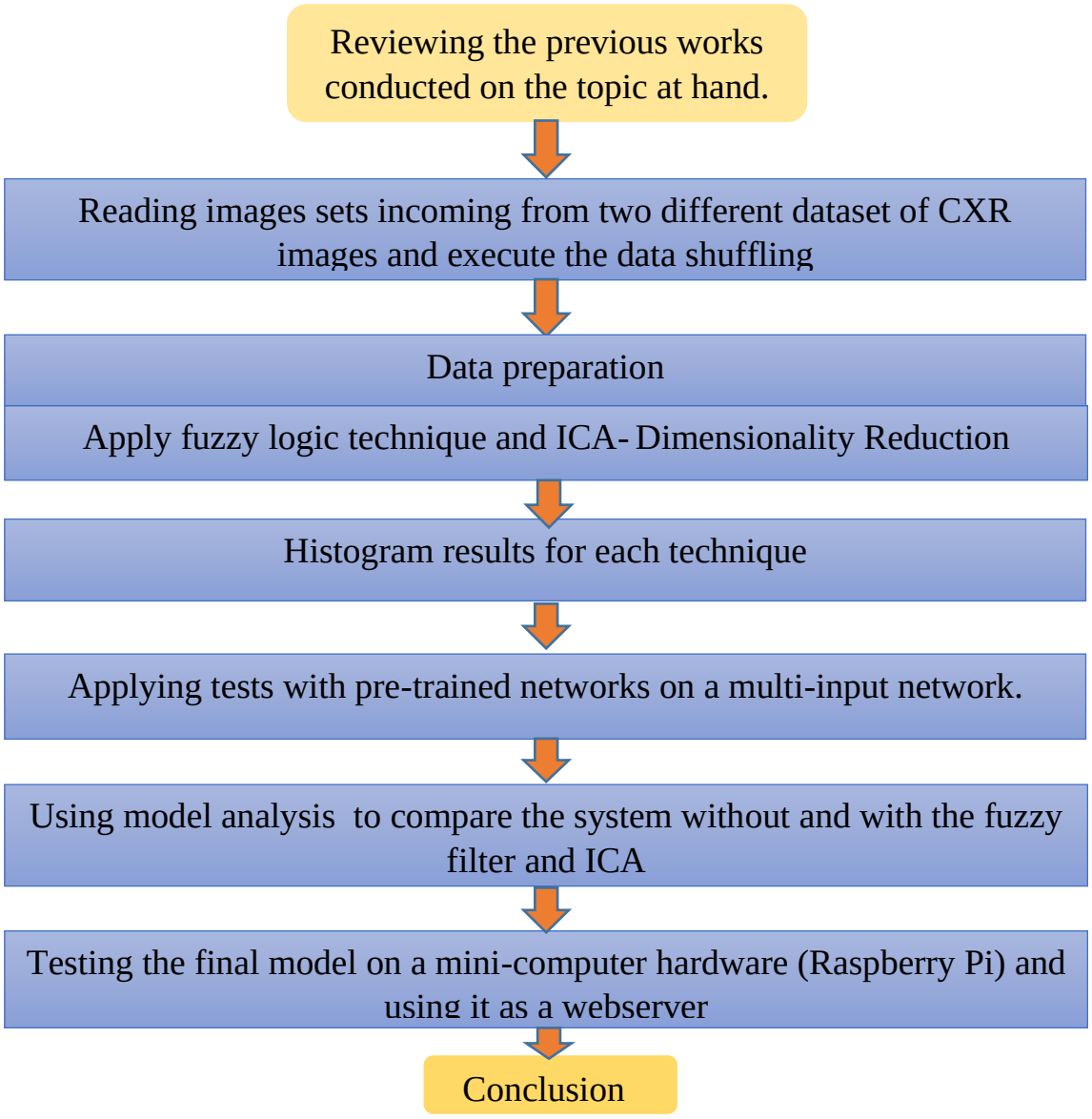

Figure 1.1. Flow of the General Methodology

1.5 Research Contribution

The following are the study's most important contributions:

1. The fuzzy logic technique was used in two ways, the first for images preparation by generating the fuzzy edge of the COVID-19 CXR images, when applied the trapezoidal membership function and the second is to use the if-then rule to give the damage ratio after the prediction.

2. Study the effect of dimensionality reduction for two-dimensional CXR images of Covid-19 patients, where the results illustrate that the pre-processed dataset obtained after dimension reduction gives a high performance in training rate and best accuracy by comparison with the original datasets.

3. Design and implementation hardware device by using mini-computer (Raspberry Pi), and it is called through a graphical user interface (GUI) designed by (HTML and Python) programming language, in addition to uploading the diagnostic results to the cloud using Internet of Things (IoT) technologies.

1.6- Research Layout

This thesis has been divided into five chapters. Each chapter is an introduction that highlights the main topics. Below is a brief overview of the five chapters:

Chapter One: Is an introductory chapter that discusses the background of this study. It explains the problem that the study is attempting to solve. It also clarifies the research objectives and purpose, as well as the study general methodology and contribution.

Chapter Two: Gives a general background on COVID-19, a general introduction to COVID-19 detection methods, types of algorithms for classifying CXR images, considers some image enhancement techniques and covers a literature review of relevant previous work.

Chapter Three: Tackles the general description of the fuzzy logic technique, ICA, and our contribution to the method of merging both techniques and explains the mathematical relationships related to proposed approaches.

Chapter Four: Illustrates the findings from a comparison of the fuzzy logic filter's performance and Dimensionality Reduction with ICA. by measuring the performance of the proposed model using the area under the curve (AUC), accuracy, precision, and recall of each model.

Chapter Five: Discusses the conclusion of the research and suggestions for the work that will be in the future.

1.7- Literature Review

It has been summarized numerous significant papers that discuss the increased identification of Covid using a variety of approaches. Boudrioua [14] classified Covid-19 cases through deep learning by fine-tuning CNNs models using training information. Ozturk et al. [15] achieved 98.1 % and 87.0 % accuracy in binary (Covid-19 against standard) and multi-class (Covid-19 vs average) classification using a CNN-based DarkNet system. Khan and his associates [16] CoroNet was proposed as a deep convolutional neural network based on the exception model capable of discriminating Covid-19 from X- ray. They conducted two multi-classifications and observed that Covid-19 pneumonia had an accuracy of 89.6 % when compared to bacterial pneumonia, viral pneumonia, and ordinary pneumonia, and 95.0 % when compared to non-Covid-19 pneumonia. Wang et al. [17] focused their efforts on developing COVID-Net, which achieved a 93.3 % accuracy rate in multiclassifying patients with Covid-19, non-Covid-19 infection (e.g., Pneumocystis, Streptococcus, ARDS), and standard infection. Marques et al. [18] identified Covid-19 using the Efficient Net design two-way classification, with claimed accuracies of 99.6 % for binary classification (Covid-19 vs. normal) and 96.7 % for multiclassification (Covid-19 vs. pneumonia vs. regular) (Covid-19 vs. pneumonia vs. regular).

Ezzat et al. [19] proposed the gravitational search optimization-DenseNet121-Covid-19 to perform binary classification between non-Covid-19 (Normal) and Covid-19

pneumonia cases (included pneumonia, normal, Streptococcus, Pneumocystis, Streptococcus, ARDS, SARS), with the goal of achieving the (93.4 % accuracy) (93.4 %accuracy) (93.4 % accuracy). Babu Karthik et al. [20] used chest x-ray images to train a genetic deep CNN to discriminate between Covid-19 and normal lungs, reporting a high degree of accuracy (98.8 %). (98.8%). Minaeea and her cohorts [21] SqueezeNet, DenseNet-121, ResNet18, and ResNet50 were trained using transfer learning to distinguish Covid-19 pneumonia from non-Covid-19 pneumonia in chest x-ray images. COVINet, a convolutional neural network developed by Umer et al. [22], is a classification system that operates in binary (normal vs Covid-19), three-way (Covid-19 vs normal vs viral pneumonia), and four-way (standard vs Covid-19 vs bacterial pneumonia vs virus pneumonia).The three-way categorization devised by Keles and his colleagues (normal, viral, Covid-19, and pneumonia) may be resolved by using the COV19-ResNet model, which has a 97 % accuracy rate when employed [23]. Li et al. [24] conducted a survey of patients infected with the coronavirus COVID-19. Clinical signs and symptoms were analysed, as well as alterations in chest x-ray pictures. Lesions were discovered in the lungs' peripheral areas. Table 1.1 contains an overview and evaluation of the relevant literature of different approaches to CXR pictures.

Table 1.1 Summarizes and reviews for Covid-19 detection

Reference	Method	Classification	Accuracy
[14]	CNNs	Three-classification	99.5%
[15]	DarkNet	Two - classification	98.08%.

[16]	DarkNet	Two - classification Tree-classification	98.1%. 87.0%.
[17]	CoroNet	Four-classification three-classification	89.6% 95.0%
[18]	COVID-Net	Three-classification	93.3%
[19]	Efficient Net + CNN	Two-classification Three-classification	99.6% 96.7%
[20]	GSA, DenseNet	Two-classification	93.4%
[21]	Genetic.deep, CNN	Two-classification	98.8%
[22]	DenseNet121, ResNet50, ResNet18,and.SqueezeNet	Two-classification	90.0%
[23]	COVINet	Two-classification, Three-way, Four-way	97%, 90%,85%
[24]	COV19-ResNet	Three-classification	97.6%

CHAPTER TWO
Theoretical Background

2.1- Introduction:

The coronavirus-2, dubbed the SARS2 grounds for Covid-19, is an infectious ailment [25]. According to the 15th of October 2021, about 240 million infections worldwide as of the COVID-19 dashboard from John Hopkins University [26]. The most frequent symptoms include a high fever, exhaustion, dumpiness of breath, and a defeat of smell or taste [27]. Depending on the severity of the infection, hospitalization and placement in an intensive care unit may be necessary and significant respiratory effects such as pneumonia intensive care unit (ICU). It's, unfortunately, the case that many healthcare systems are overwhelmed since ICU ward capacity is limited [28].

National lockdowns, for example, are standard practices in many countries. Covid-19's primary diagnostic method is RTPCR. CT scans and CXR are often utilized in clinical practice for screening and identifying Covid-19 in patients [29]. It takes a long time and a great deal of work for radiologists to manually analyze the images. Computer-aided diagnostic approaches are thus being pursued, notably for detecting Covid-19-related pneumonia in medical photographs. Damage to the lungs caused by Covid-19 may be visible on CXR and CT images. It is thus possible to see a Covid-19 infection by looking at CXR images of patients with multiple air-space illnesses.

According to recent studies, lung hilum, texture thickening, and pulmonary fibrosis may aid in CXR image diagnosis [30]. Again, undetected instances may have devastating implications owing to COVID-19's fast exponential proliferation [31]. Other diagnostic techniques must be developed for Covid-19 sufferers that may be identified early. Rapid and early identification of COVID-19 patients has become of great importance to prevent rapid infection and disease progression. The computing methods used in artificial intelligence (AI) like fuzzy logic, neural networks, and genetic networks are useful in disease diagnosis [32, 33]. They can help patients make decisions, provide instant seclusion, and deliver appropriate therapy [34].

2.2 History of AI in disease detection

Alan Turing proposed the idea of using computers to mimic intelligent behavior and rational thought in 1950 [35]. In his book "Computers and Intelligence" outlined a simple test (later known as the "Turing test") to determine whether computers are capable of human intelligence [36]. Six years later, John McCarthy outlined the definition of artificial intelligence (AI) as "the science and engineering of creating intelligent machines." [37, 38]. When AI first started, it was just a straightforward sequence of “if-then rules”. It has developed over many years to include increasingly powerful algorithms that operate like the human brain. There are many specialized areas of AI, including machine learning, deep learning, and computer vision.

Machine learning (ML) is the use of particular characteristics to find patterns that can be used to examine a specific situation. The computer can then "learn" from this information and use it to predict similar situations in the future. This prediction technique can be used in real-time in medical decision-making to personalize patient care, rather than adhere to a fixed algorithm.ML has developed into what is now referred to as deep learning (DL), which is made up of algorithms to produce an artificial neural network (ANN) that is then capable of learning and acting independently, resembling a human brain [39, 40]. Computer vision is the method by which a computer derives knowledge and comprehension from a collection of pictures or videos as shown in Figure (2.1).

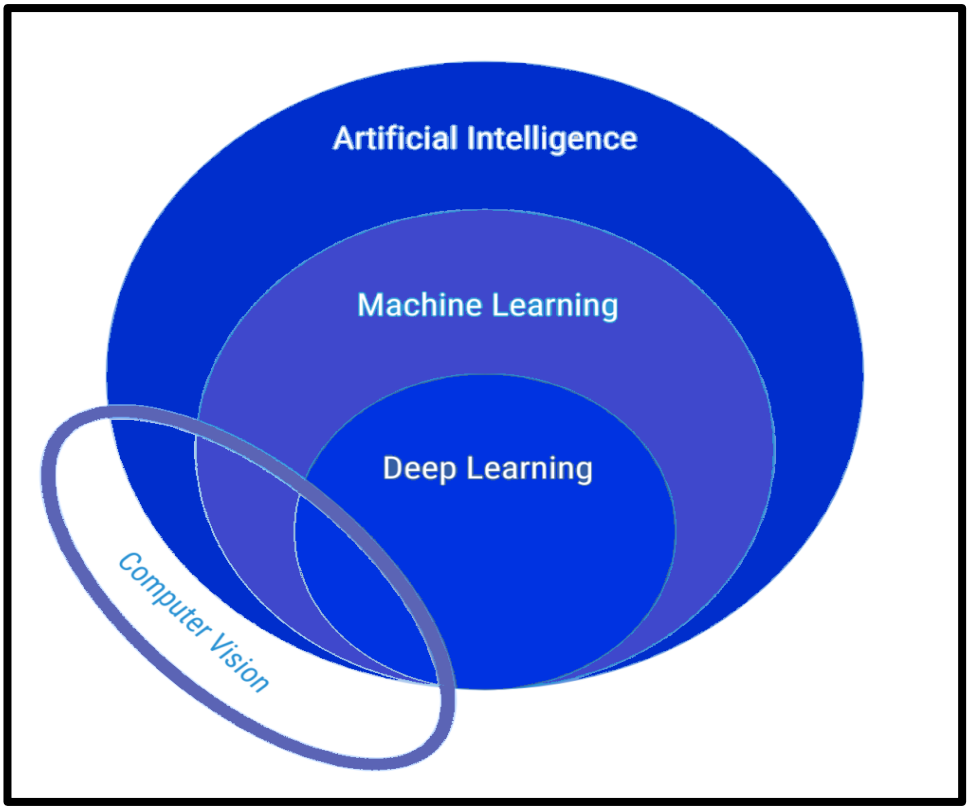

Figure 2.1 Machine Learning and Deep Learning are artificial intelligence subsets.

2.3 AI in COVID-19 detection methods importance

(AI) has become more prevalent in various fields, particularly in medical detection [41]. AI is frequently employed to improve detection outcomes and ease the strain on the healthcare system [42]. It can speed up decision-making compared to conventional methods of detection [43]. The advancement of the prediction, prevention, and detection of future global health risks is thought to be significantly aided by the development of AI methods to recognize the dangers of epidemic diseases [44]. Several researchers have reported various kinds of AI classifiers using actual COVID-19 datasets with various case studies and goals [45]. Choosing the right AI technique that can yield high accuracy is difficult, despite the fact that they can be helpful in the diagnosis and classification of COVID-19 [46, 47]. The detection of images aims at localization and classification of interest areas by illuminating and labeling the bounding boxes around various areas of interest. This increases the accuracy of locating the different organs and their orientations. Mathematically, let I be a picture with n regions or objects of interest. Following that, the detection function $D(I)$computes$(h_i, w_i, y_i, x_i, c_i)$ these are the class label, centroid x and y coordinates, and the proportion of the bounding box relation to the image's width and height, respectively.as given in (2.1).

$$\bigcup_{i=1}^{n} c_i, x_i, y_i, w_i, h_i = D(I) \qquad 2.1$$

COVID-19 diagnosis and classification, it can be challenging to choose between the many different AI techniques that are currently available, especially when

there isn't a single, clearly superior AI technique. Additionally, the majority of these techniques have poor computational efficiency [48].On the other hand, the evaluation and comparison processes are challenging because there are numerous evaluation criteria and conflicts between them [49]. The main importance of AI methods to detect the COVID-19 pandemic are:

2.3.1 Early infection identification and diagnosis

AI can fast detect unusual symptoms and other "special flags," alerting both patients and healthcare officials [50]. Faster, more economical decision-making is facilitated by it. It aids in creating a new method of diagnosis and process improvement for COVID 19 cases, using efficient algorithms. Infected cases can be diagnosed using AI with the aid of medical imaging technologies like Magnetic resonance imaging (MRI), CT scan, and CXR of human body sections as shown in Figure (2.2).

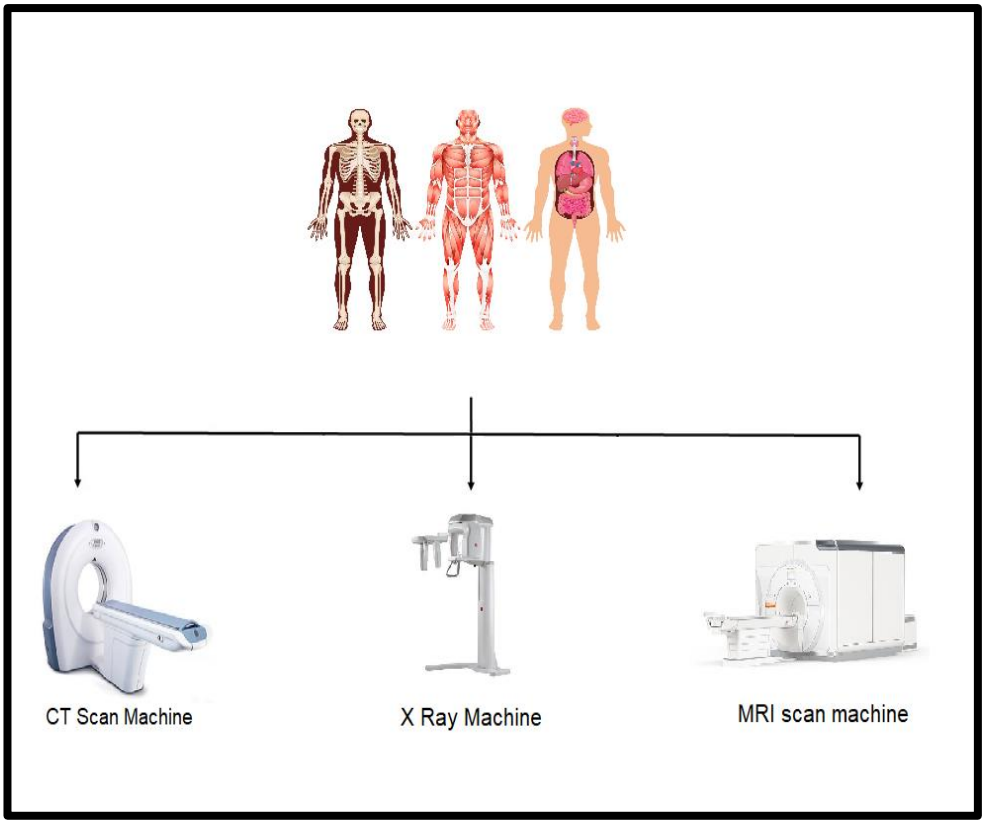

Figure 2.2 Human body diagnostic machine

2.3.2 Treatment monitoring

AI can create a smart system for the automatic pursuit and forecasting of this virus spread. It is also possible to create a neural network to extract the visual disease features, which would aid in the care of those who are afflicted [51-53]. It is able to provide daily updates on the patient's conditions as well as guidelines for dealing with the COVID-19 pandemic. Figure (2.3) shows the mechanism for extracting the advantages by entering the data after fetching it from the dataset sites that have been recommended on ML, where they are subject to training.

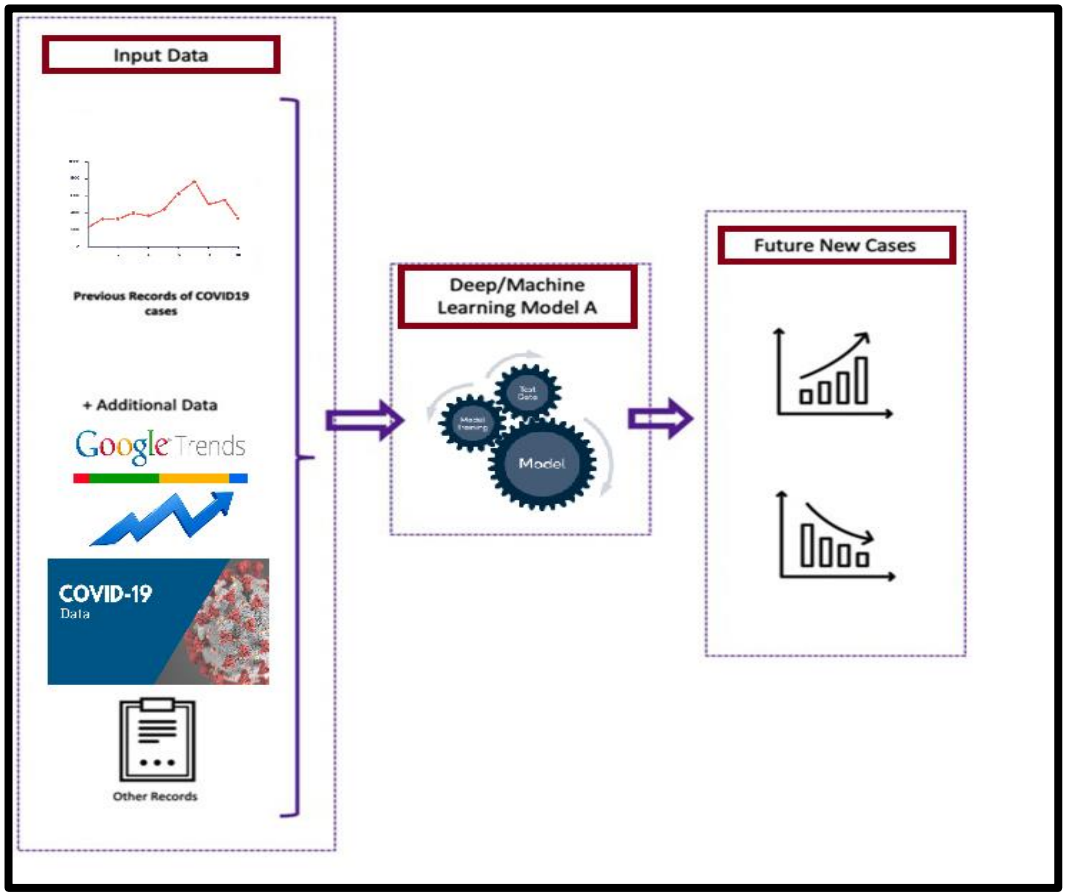

Figure 2.3 COVID-19 prediction using artificial intelligence

2.3.3 Digital contact tracing

By locating clusters and analyzing the virus's level of infection, AI can successfully track down contacts for individuals and keep an eye on them. It can forecast the progression of this illness and its likelihood of recurrence.

2.3.4 Case and mortality projections

Using information about the risks of infection and its probable disperse from social media and other media platforms, this technique can monitor and predict the

virus's characteristics. Additionally, it has the ability to forecast the number of positive cases and fatalities in any area. In order to take appropriate action, AI can assist in identifying the most sensitive nations, populations, and areas.

2.3.5 Drugs and vaccines Development

By examining the COVID-19 data that is currently available, AI is used for drug research. Designing and developing drug delivery systems can benefit from it. When compared to standard testing, which takes a long time, this technology enables us to considerably speed up the process, which may not be possible by humans [51, 52]. It has developed into a potent tool for developing diagnostic test designs and vaccines [53, 54]. AI supports clinical studies during the progress of the vaccine and speeds up the process of developing immunizations and treatments.

2.3.6 Disease prevention

AI can provide up-to-date information that is useful in preventing of covid-19 disease with the implementation of real-time data analysis. During this crisis, it can be used to forecast the likely sites of disease, the spread of the virus, and the demand for beds and medical personnel. With the aid of historical supervised data over data prevalent over time, AI is useful for the prevention of future viruses and diseases. It pinpoints characteristics, root causes, and mechanisms underlying infection spread. This technology will be crucial in the future in the fight against pandemics. It can

fight many other diseases and act as a preventive measure. More predictive and preventive healthcare will be made possible by AI. In order to improve clinical outcome, hospitals and research facilities will use AI to program computers to process and analyze rapidly and correctly.

2.4 Advantages and Disadvantages of AI disease detection

AI can provide methods for detecting the presence of diseases. Using algorithms and data, these technologies can identify patterns and provide automated insights that aid in common applications such as disease prediction, patient state diagnoses, and Assessment of the percentage of inflammation in the affected parts of the body [55]. The advantages and disadvantages of AI detection methods techniques are explained in the following two subsections.

2.4.1Advantages of AI disease detection

- Speed up diagnosis and discovery by building up auto predictions using ML with large data sets [56].
- Models driven by ML can examine and analyze massive amounts of data, examine specifics, evaluate, and deliver the findings to physicians. [48].
- ML aids in creating a system that learns automatically and generates outcomes with minimal effort and time enabling automated discovery [57].
- Effectiveness in resolving complicated problems [58].

- AI with the help of a machine vision approach can get accurate, perfect, and very fast results as compared to human vision [59].
- AI in detecting covid-19 can be useful in eliminating drawbacks such as the insufficient number of RT-PCR test kits available, the time it takes to get results, and the costs of testing. [15].

2.4.2 Disadvantages of AI disease detection

- Requires human verification despite the progress AI has made in medicine, human oversight is still crucial.
- Inexactness is still possible, medical AI mainly relies on diagnosis information gleaned from millions of instances that have been cataloged. A mistake is conceivable when there is limited information on certain illnesses.
- Subject to risk to information security.
- There are instances when it can be abused and cause extensive destruction.
- Software mismatch may lead to counterproductive results.

2.5 Working principle of Deep learning covid-19 detection

Deep learning is one of the most important current trends in dealing with images related to medicine. Its primary purpose is to aid radiologists by providing

them with a high-accuracy diagnosis, by giving quantitative analysis of epidemics of concern and allowing for a faster clinical workflow than traditional methods. Deep learning has shown a high-precision performance in identifying the tasks assigned to it and computer vision that significantly overcomes the capabilities of humans [60].AI, backed by the massive development of advanced computing and the amount of big data and modern algorithms, is becoming more and more popular. AI has been applied in various fields such as manufacturing, healthcare, and in various aspects of life. Artificial intelligence is divided into three categories. The first is an approach that elicits answers based on search engines. Another is based on Bayes' theorem approach, the other is based on deep neural networks (DNNs) [61].

While each of these approaches has weaknesses and strengths, the deep learning approach is of interest to solve the most complex problems. The current biggest challenge is the creation and development of some technologies for non-invasive detection of patients with COVID-19 through AI such as DL. Another challenge is to choose the data set that fits the model to be trained. To achieve accurate prediction without overfitting, the data should go through a number of steps including segmentation, augmentation, normalization, sampling, and sifting. The majority of the DL techniques and datasets that were used to create COVID-19 detection are shown in Figure (2.4) [62].

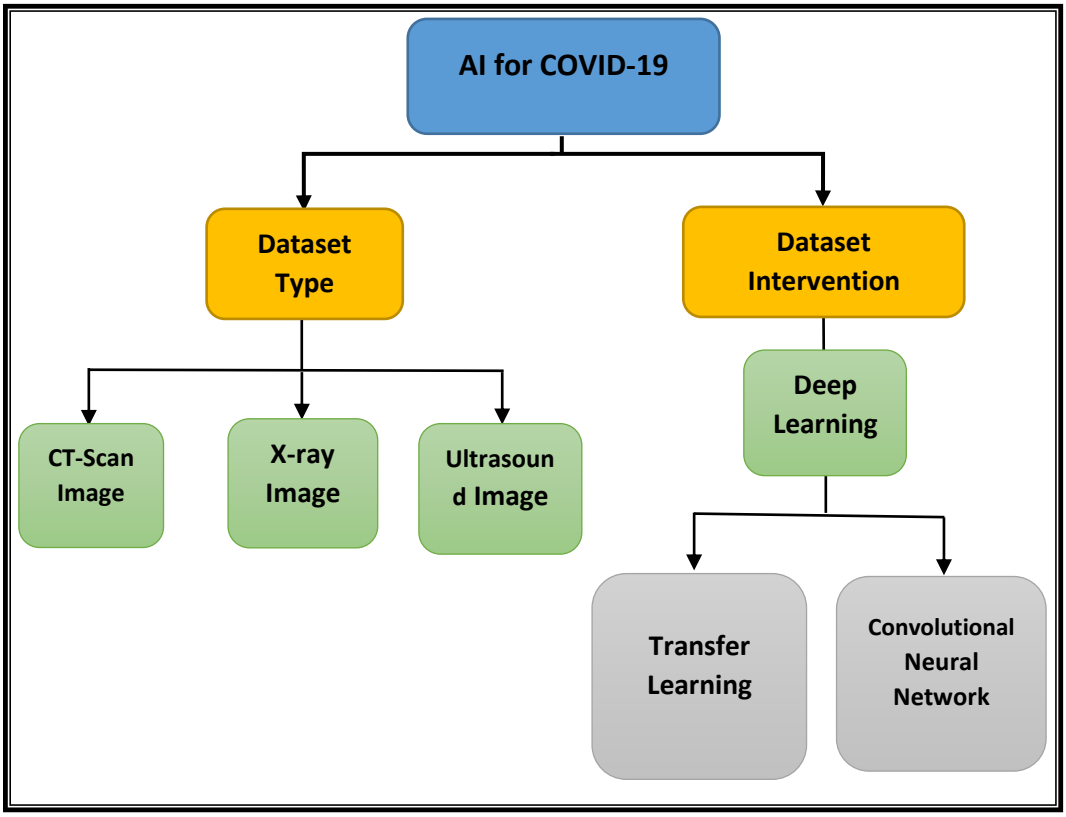

Figure 2.4 DL methods and datasets used against COVID-19.

The structure of the DL algorithm is more complex compared to the traditional ML algorithm. The DL structure consists of three processing steps; the first step is to pre-process data understanding, DL model building extraction of these entries' benefits is the second stage, the third and last phase has to do with the many classifiers that are used to classify each item (training, and validation and interpretation). As depicted in Figure (2.5).The DL greatly reduces human intervention and is concerned with processing complex data which has become a challenge. It is not underestimated in ML as it produces very accurate results in a short period [63]. Many studies relied on the convolutional neural network and

transfer learning to detect COVID-19 because they represent the most important current methods for dealing with images in deep learning [64].

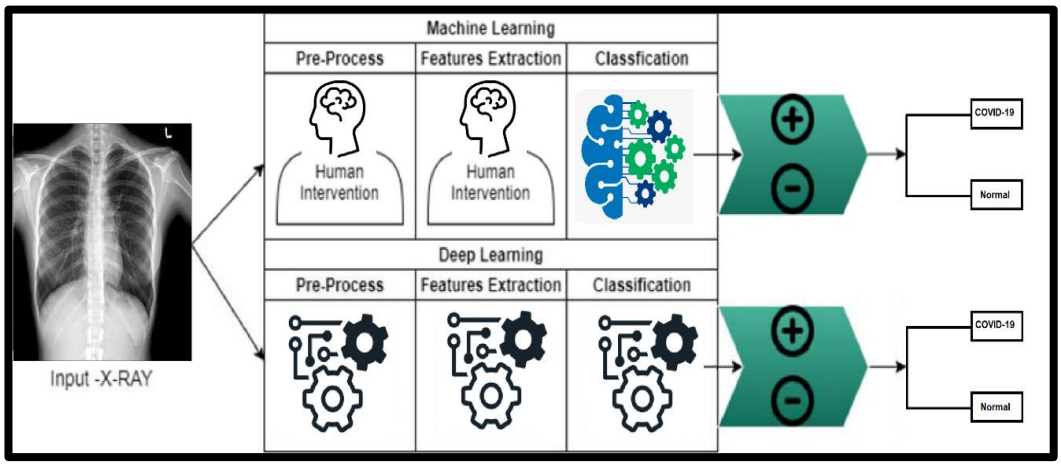

Figure 2.5 Deep learning and machine learning Explaining.

2.5.1 Convolutional neural networks (CNNs)

CNN is an artificial neural network consisting of a set of layers, and each of these layers is a multi-input neuron that works in a similar way to neurons in the human brain. CNN has proven itself in the field of medical image classification [65]. CNN is the backbone of all proposed models that are used to detect and diagnose the presence of COVID-19, for three different types of images: CXR, CT scan, and ultrasound (ULS) [66]. CNN has recently been highlighted in computer vision in both supervised and unsupervised learning tasks [67]. The main role and strength of a CNN lies in identifying edges, lines, and patterns in so on an image. Each hidden layer of a CNN consists of convolutional layers that convolute the input matrix with a convolution kernel with weight parameters. Multiple cores produce multiple distinct images and are successful in various vision tasks such as classification and

segmentation. Between convolutional layers [68, 69]. The basic building blocks of CNNs can be arranged as convolutional layers, activation functions, pooling, and fully-connected layers [70]. As shown in the Figure (2.6).

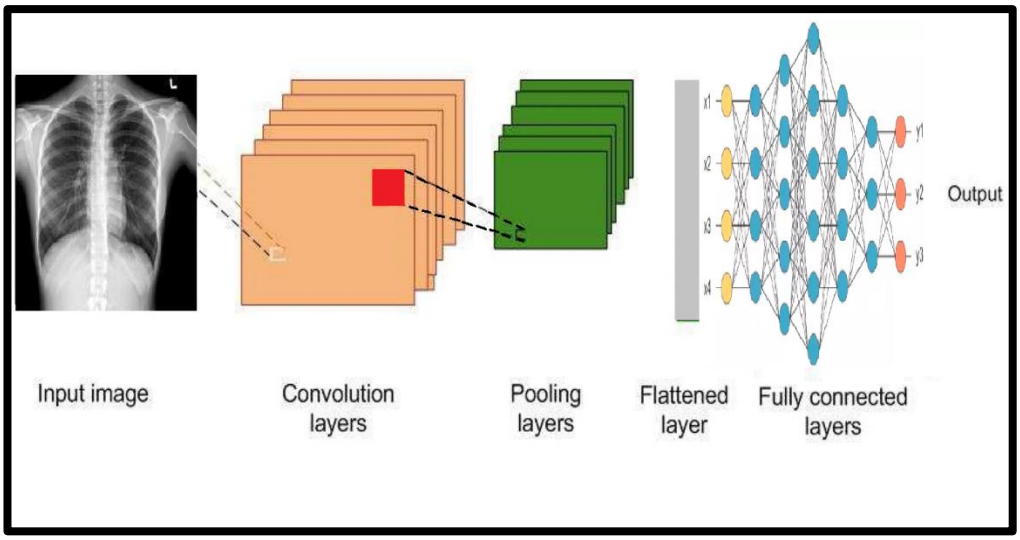

Figure 2.6 the basic building blocks of CNNs.

- **Convolution layers (Conv layers):** Various features are extracted by neurons for the purpose of understanding the image. Extracting the features represented by color, edges, lines, gradient direction, and texture. It is carried out by the transformation layer above the neurons. The transformation layers consist of learnable filters called convolutional filters of size m × n × d, where the dot product is calculated intuitively between the input and the filter input by wrapping the kernel across the height and width of the input size during the forward pass process. The CNN learns which filters are

activated by the features it encounters. Inside the activation function layer the output of the transformation layer is fed.

- **Activation functions:** Mostly real-world data is nonlinear, so activation functions are used for nonlinear transformations of data. Activation functions are used to ensure that the representation is that the inputs are mapped to different outputs according to the requirements.
  - **Sigmoid:** Represent a real-valued number, x, into the range between 0 and 1.

$$f(x) = \frac{1}{1 + e^{-x}} \qquad 2.2$$

  - **Tan hyperbolic:** Represents a real-valued number, x, represents range between 1 to 1.

$$f(x) = \frac{1 - e^{-2x}}{1 + e^{-2x}} \qquad 2.3$$

  - **Rectified linear unit (ReLU):** ReLU is the nonlinear function that CNN uses the most frequently. It takes less time to computation. If real value x is a negative number, it is converted to 0.

$$f(x) = max(0, x) \qquad 2.4$$

- **Pooling:** Performs a linear and nonlinear sampling of the convolved feature. Through dimensionality reduction, the amount of computing power needed to process the data is reduced. Combining data from various sources, reduces the spatial size depending on feature type or space, prevents overfitting, and

eliminates image rotational and translational variance. Results in the input being divided into a number of rectangular patches. Depending on the type of pooling chosen, each patch is replaced by a single value. There are other various kinds like average pooling and maximum pooling.

- **Fully connected (FC) layer:** pretty like an artificial neural network, where each node has incoming connections from all the inputs and all the connections have weights associated with them. The output is the sum of all the inputs multiplied by the corresponding weights. The sigmoid activation function, which serves as a classifier, comes after the FC layer.

2.5.2 Transfer Learning

Is a technique used mostly in DL for solving new tasks with minimal training time and high accuracy by applying previously acquired model knowledge. Compared to conventional machine learning methods [67]. It is possible to take advantage of the knowledge resulting from the previous training of a particular dataset and apply it to the new training data set as shown in Figure (3.7). this technique was developed based on the CNN model and it is called the pre-training model. Using a predefined cost function, the ideal convolution coefficient values are found during the learning process, and then the characteristics are automatically determined. Because the DL takes a large amount of data for training purposes. As a result, the need for a large volume of data represents a difficult barrier to addressing some essential tasks, especially, in the medical sector, where it is difficult

and expensive to produce large, high-quality annotated medical or health datasets. Additionally, even though researchers are making great efforts to improve it, the standard DL model still necessitates a lot of computational resources, such as a server with GPU support. Transfer Learning, a transfer learning approach based on DL, might therefore be useful to address this problem [71].

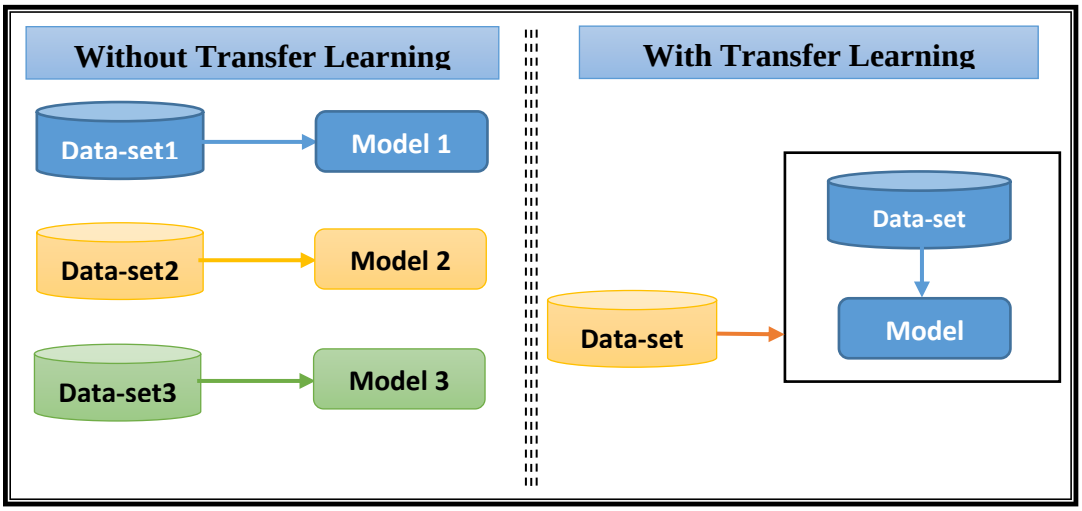

Figure 2.7 Deep learning (Transfer Learning)

2.6 Data preprocessing and augmentation

Before sending the images to the CNN, the images obtained from the imaging methods must pass through several stages, including the stage of primary processing and augmentation [72]. Image data may be skewed with severe inhomogeneity during image sampling, so it must be fed onto the preprocessing unit. There are many ways to pre-process the data, and the recommended methods are normalization and subtraction. Training the data on CNN directly without increasing

the amount of dataset may not achieve better performance, so is important to increase the training data set to get better performance results. Via vertical and horizontal fluctuations, density changes, scaling, transformations, random clipping, and color jitter. Then the data is ready to be fed into the CNN.

The Data preprocessing and augmentation of Deep learning are explained in the following two subsections:

2.6.1 Data Preprocessing

Is the process used to enhance the data's quality before mining is applied, ensuring that the data will produce high-quality mining results. The common data preprocessing tasks for creating operational data analyses are summarized in Figure (2.8). Preprocessing building operational data typically entails five main tasks [73, 74].

- **Data cleaning:** Data cleaning is the process of removing inaccurate, incomplete, and misleading data from datasets and replacing the values that are missing. It can be used to remove noise and fix inconsistencies in the data [75].
- **Data Reduction:** Used for reducing the data size by reducing the amount of data, this process makes analysis simpler yet produces the same or almost the same result. This technique reduction also helps to reduce storage space. It can be achieved in several ways. Dimensionality reduction, data compression, and, Numerosity reduction [76].

- **Data scaling:** Is an important technique in AI, data scaling makes it simple for a model to learn and comprehend the issue. When applying machine learning algorithms to the data set, scaling the data is one of a set of data pre-processing steps. The majority of supervised and unsupervised learning techniques base their conclusions on the data sets that have been applied to them, and frequently the algorithms calculate the space between the data points to draw more accurate conclusions from the data for example, the data scaling is used to prevent the problem of converging to zero or diverging to infinity during the classification model training process because maybe specific feature values in the dataset are too large or too small [77].

- **Data transformation:** The purpose of data transformation is to prepare the original data in formats that different data mining algorithms will find useful. The complexity of this step depends on the requirements. There are some methods in data transformation. Can be used to convert categorical variables into numerical ones to make the process of creating prediction models easier [78].

- **Partitioning:** The aim of data partitioning is to separate the entire set of data into various groups for in-depth analysis .There are several methods to accomplish this technique, the most important of which are: clustering analysis, the decision tree methods [73].

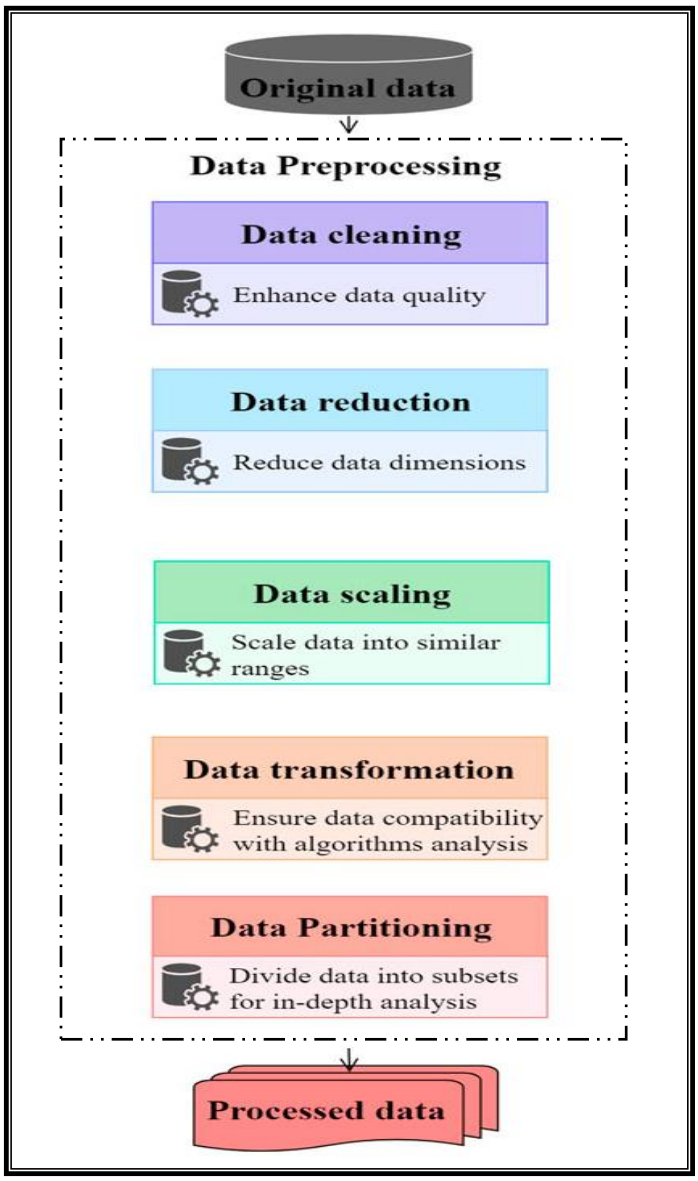

Figure 2.8 The basic Building Operational for Data Preprocessing [73].

2.6.2 Data Augmentation

Through the technique of data augmentation, it's possible to address the potential data shortage problem as a quick and lightweight solution as shown in Figure (2.9), the main goal of data augmentation is to create artificial data with data distributions that are similar to those of the original data. The performance of data-driven prediction models can then be improved by combining the synthetic data with real data. The field of computer visions has made extensive use of ta augmentation techniques [79]. Methods based on transformations such as rotation, scaling, flipping, and jittering are time series data augmented using conventional methods, by introducing additional variability into preexisting time series data, such techniques can generate new data samples.

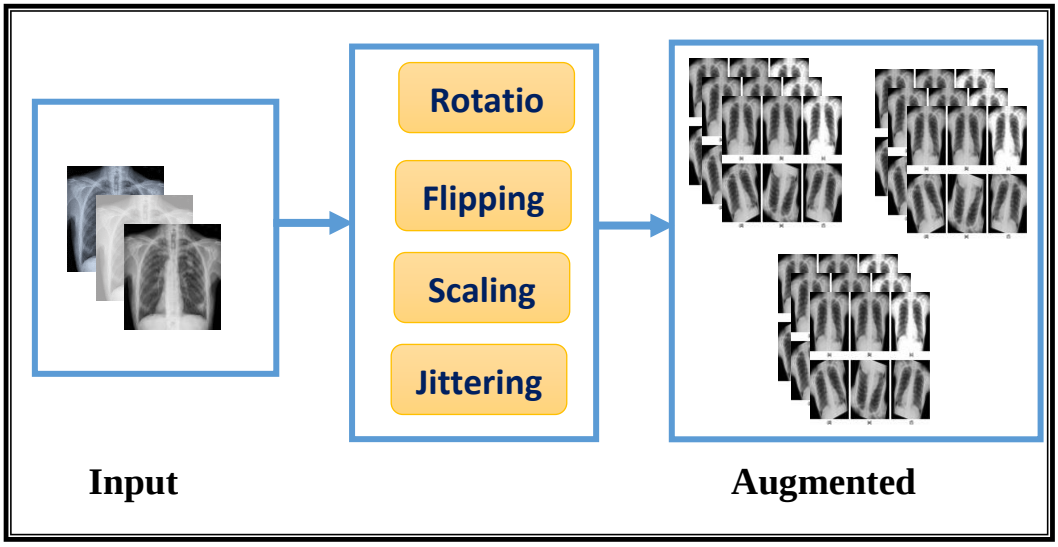

Figure 2.9 the data augmentation techniques

2.7 Deep-learning techniques for COVID-19 detection

Deep learning and artificial intelligence methods that mimic how humans learn are similar to machine learning methods. Deep learning is a crucial part of data science, which also includes statistics and predictive modeling. An example of a deep neural network used to analyze visual imagery is a CNN ,which is a deep learning technique that takes an input image and gives weights to different objects to help it distinguish between them, wherefore used to categorize and identify images due to its high degree of accuracy [79]. Usually deep learning architectures are used, the most popular being, VGG16, Xception, DenseNet, EfficientNet, and MobileNet, to classify data. A thorough explanation is given below.

2.7.1 VGG16

One of the most important CNN models, developed by the Visual Geometry Group (VGG) at Oxford University, is the successor to AlexNet as it was replaced by it. VGG16 is 16 layers, three fully connected layers, five max pooling layers, and one softmax layer, as shown in Figure (2.10). On the basis of and as part of a specific ImageNet competition, the architecture was designed. A small integer is used to specify the convolution blocks' width. The width parameter is increased twice until it reaches 512 after each max-pooling operation. The VGG16 has an image size of pixels. Spatial padding preserved the image's spatial resolution [80]. The stride is set to one pixel with five max-pooling layers use a determined stride of 2 and (2 x

2) pixel filter. A padding of 1 pixel is done for the (3 x 3) convolutional layers all the layers of the network use ReLU as the activation function [81].

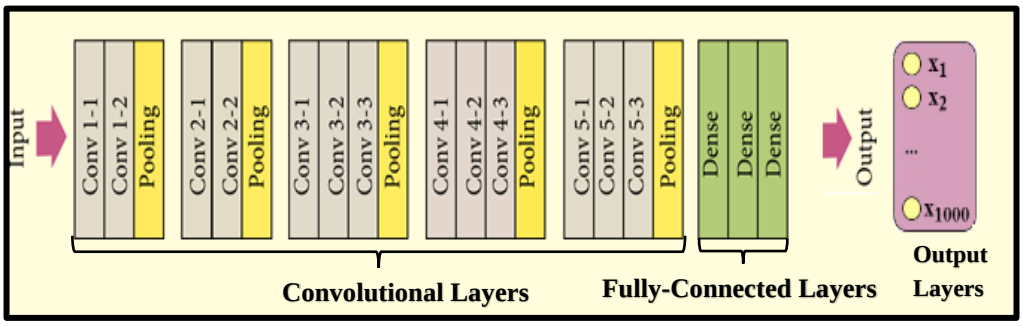

Figure 2.10 VGG16 architecture.

2.7.2 Xception

The inception network has been replaced by the Xception network. The Inception V3 from Google is a variation of the DL Architectures series. It was trained with 1000 classes using the initial ImageNet dataset, which contains more than 1 million images [82]. "eXtreme Inception" is the meaning behind the name Xception. Convolution layers that are depth-wise separable are used in the Xception network. Figure (2.11) shows the schematic illustration of a block in Xception. Spatial and cross-channel correlations, which can be completely dissociated in CNN feature maps, are mapped in Xception. Xception performed better than the Inception architecture it was built on (Inception). Convolution layers make up the 36 layers of the Xception model, which can be further broken down into 14 different modules [83]. By omitting the first and last layers, each layer has a linear residual connection all the way around it. Xception, in a nutshell, is the linear stacking of depth-wise separable convolution layers made up of residual connections. Instead of being

viewed as a 3D mapping, the correlations can be thought of as a 2D + 1D mapping. In Xception, 1D space correlation comes after 2D space correlation at first [80].

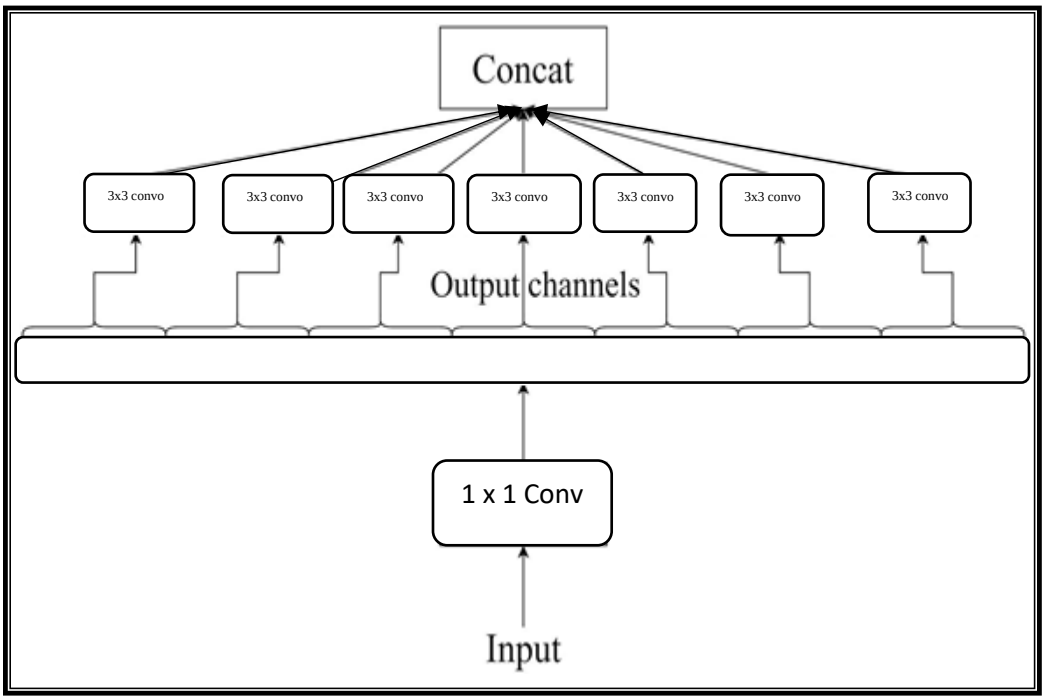

Figure 2.11 Xception architecture.

2.7.3 DenseNet121

A densely connected neural network is called DenseNet. It is alternative method to extend deep convolutional networks without running into issues with expanding and disappearing gradients. These problems are resolved by directly coupling every layer to every other layer, allowing maximum information transfer and gradient flow. Instead of obtaining representational strength from extensive

deep or wide CNN architectures, the main strategy in this case is to investigate feature reuse. DenseNets require fewer or an equal number of nodes than traditional CNN. Because DenseNets do not learn feature maps, parameters are not required. There are also ResNets versions that have made only a small contribution; those layers can be removed. DenseNet layers are narrow, i.e., there are very few filters, and they only add a small number of new feature-maps as shown in Figure (2.12). Given that any level can provide input to the width layer, the DenseNet is a network that can be used in any situation. Deep neural networks have an issue when training the input because of the information flow and gradients stated before. By directly accessing the gradients and transfer functions of the input itself, DenseNets resolve these problems. As the feature maps from the $(k-1)^{th}$ layer are added, the network structure of the DenseNet becomes increasingly hierarchical. Layer is the (k^{th}) layer's input. As the input of the i^{th} layer can be of $(i-1)^{th}$ order, it be can say that the DenseNet is a network that is generalizable. As the input of the i^{th} layer can be of $(k-1)^{th}$, $(k-2)^{th}$ or even $(k-n)^{th}$ order, the DenseNet can be said to be a generalizable network. Where n has to be lower than the number of layers overall. The fact that the feature maps' sizes must be uniform when concatenating them necessitates that the output of the convolutional layer be the same size as the input. To demonstrate how densely concatenated convolutions function, use the following Eq2.5 [84].

$$X_i = R_i\left(\left[X_0, X_1, \ldots X_{(i-1)}\right]\right) \qquad 2.5$$

Where R_i represents the i^{th} layer, X_i demonstrates the result of the i^{th} layer. The output of all the frontal levels in the equation above is fed by the input of each layer.

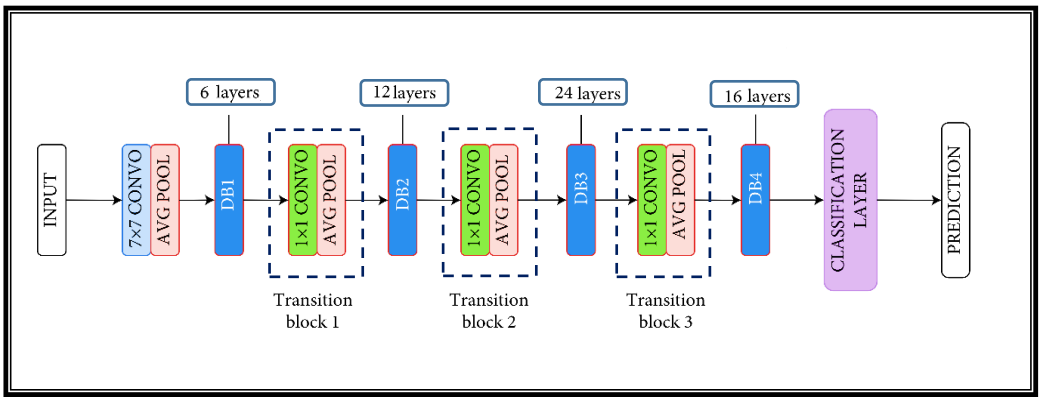

Figure 2.12 DenseNet121 architecture [83].

2.7.4 EfficientNet

Scaling the model is one of the key problems with using CNNs. We are aware that the system performs better as the model's depth increases. However, choosing the model's depth requires using a manual hit-and-trial method in order to select a model that performs better. Therefore, the Google research group introduced "EfficientNets" to address this problem [84]. MBConv serves as the EfficientNet models' foundation. Squeeze-and-excitation optimization is now part of this block. The MBConv block works similarly to the MobileNet v2 inverted residual blocks. A shortcut connection is made between the start and finish of a convolution block. 3x3 reductions are carried out in the output feature maps' channels using depth- and point-wise convolutions. The narrow layers are connected using shortcut connections. But between the skip connections, the wider layers are preserved.

According to Figure (2.13) (a) and (b), respectively, this architecture leads to a decrease in the model's size and the total number of operations in the structure.

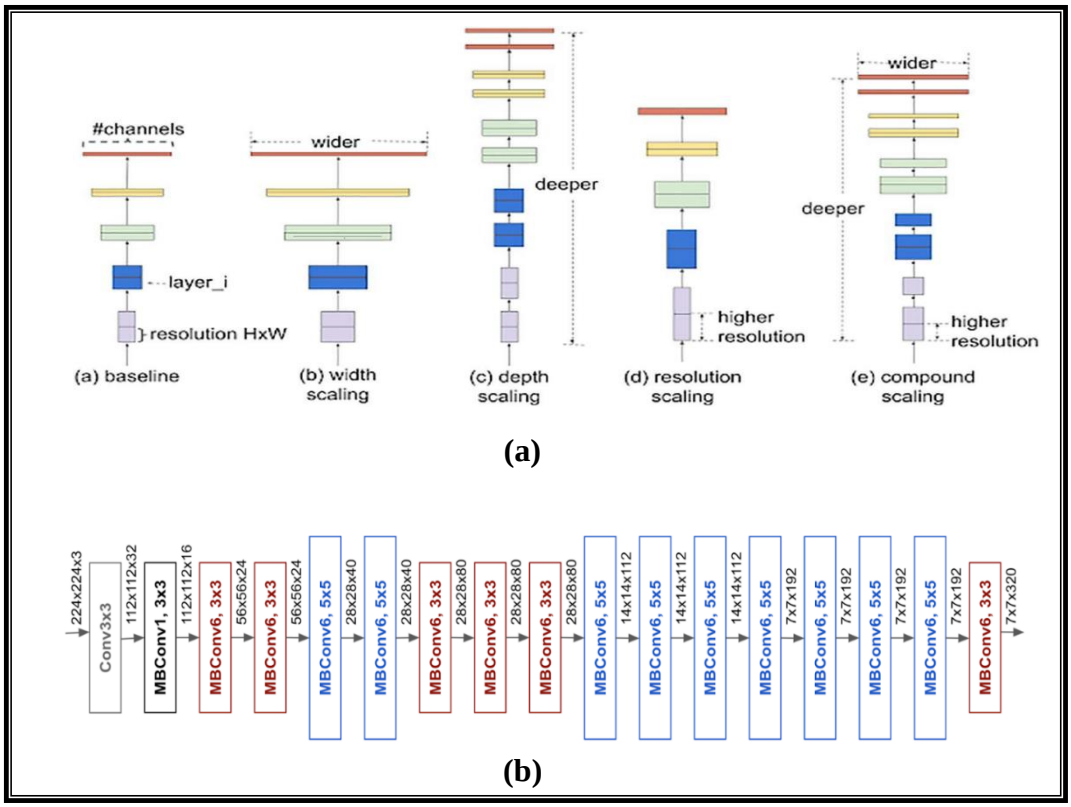

Figure 2.13 (a) A diagram that shows the EfficientNet general architecture and (b) Example of a network infrastructure for EfficientNet-B0 [85].

2.8 Fuzzy Logic technique

The development of AI as a tool to enhance health care offers enormous opportunities to enhance clinical outcomes and patient outcomes, lower costs, and affect community health. Fuzzy logic is a type of logic theory, and the truth value of logic can be thought of as a real number with values ranging from 0 to 1. It is also

a form of artificial intelligence. However, in the field of artificial neural networks (ANN), neuro fuzzy combines artificial intelligence and fuzzy logic [88]. Fuzzy logic is a type of computational archetype that provided us with a simple mathematical tool for human logic to handle different types of uncertainty as shown in Figure (2.14).

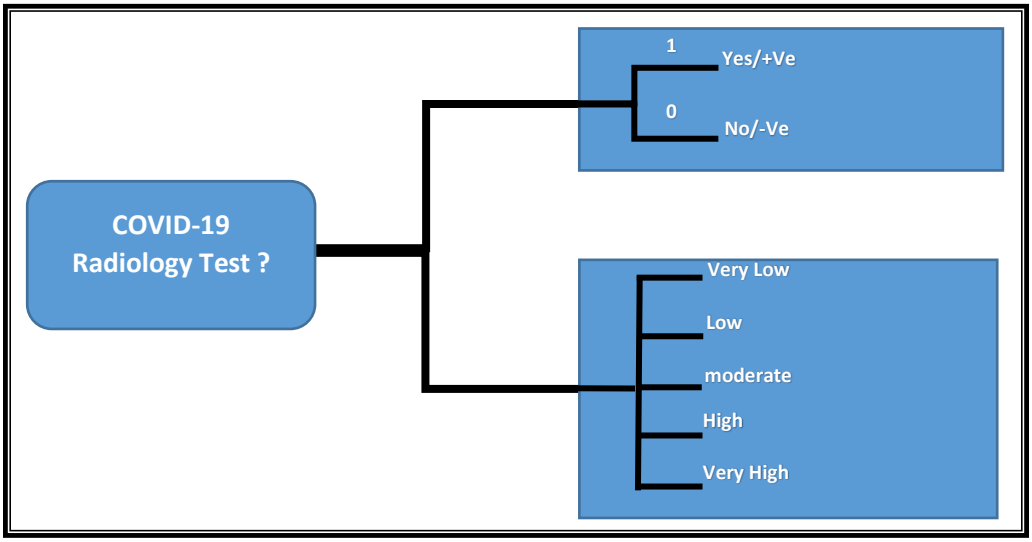

Figure 2.14 Systems of fuzzy and Boolean logic comparison.

The power of fuzzy logic lies in the linguistic expression of human knowledge. Therefore, it is important to develop the use of this technique in diagnosing diseases, by using it as a representation of doctors and experts to express the severity of diseases and symptoms [89, 90]. By relying solely on the membership function, L. A. Zadeh's 1965 fuzzy logic proposal deals with uncertainty [91]. The fuzzy models have the capacity for data and information recognition, manipulation, representation, interpretation, and use. These Mamdani rule-based systems form the foundation for fuzzy models [92, 93].

1. All input values should be fuzzified into fuzzy membership functions.
2. Determine the fuzzy output functions by putting all applicable rules in the rule-based system to use.
3. Defuzzify the values that have been fuzzified.

To represent certain situations or decisions in a manner that is similar to how humans make decisions, Fuzzy Inference Systems (FIS) employ fuzzy reasoning as shown in Figure (2.15).

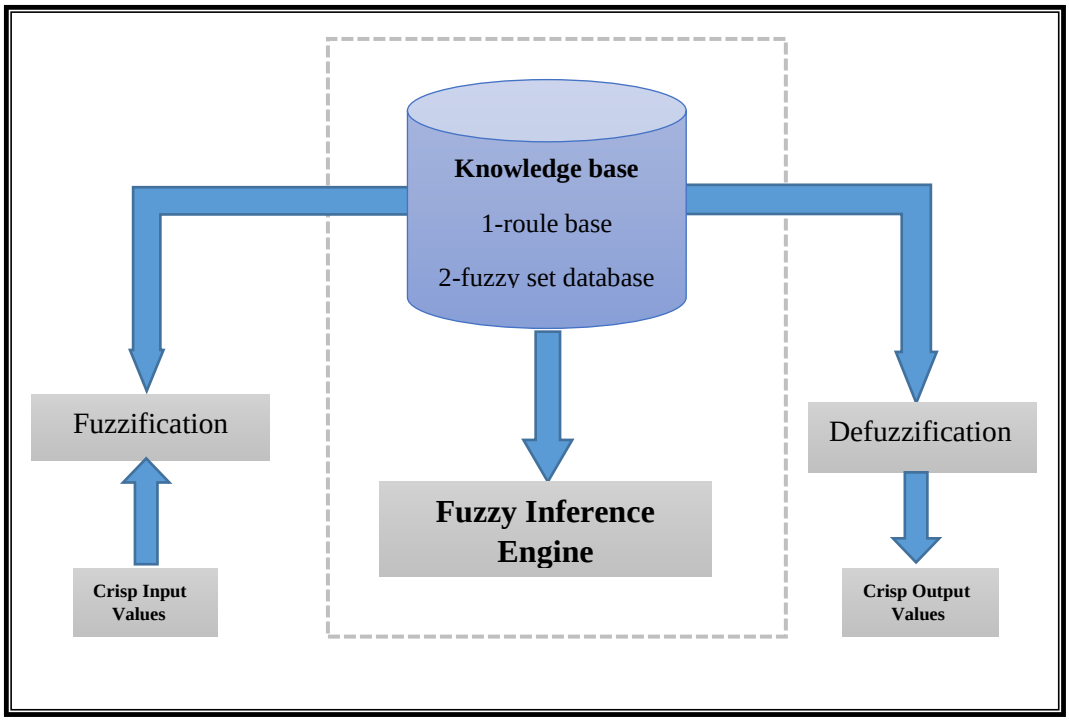

Figure 2.15 Block Diagram of the Fuzzy Inference System.

2.8.1 Fuzzy theory

The fuzzy logic method relies heavily on the axioms of judgment for the decision maker to obtain assessments of things to be evaluated that cannot be measured physically. Taking into account the knowledge and experience related to the decision maker. Probability theory and fuzzy set theory are not interchangeable, but they do complement one another. Despite the (degrees of freedom) that fuzzy set theory possesses in the processes of union and intersection, different types of fuzzy sets (organic functions), probability theory is no less sophisticated and uniquely defined in structure and process. Fuzzy sets of the probability, Linguistic variables, and trapezoidal membership functions are selected. Therefore, the fuzzy set seems to have adaptability. With different contexts Experts evaluate using the linguistic variable of probability, translate the values into fuzzy numbers, and then perform defuzzification [94-96].

2.8.2 Fuzzy logic design and mathematical representation

Intuitionistic Fuzzy Sets $\tilde{A}$ in a universe of discourse a membership function defines X.

$$\mu_{\tilde{A}}: X \rightarrow [0,1] \qquad 2.6$$

Such that it associates a real number with each element x in the $[0,1]$ range that gives a membership degree. Fuzzy numbers are particular fuzzy sets that meet the conditions shown in Figure (2.16);

- The convex fuzzy set ($if\ \mu_{\tilde{A}}(\lambda, x_{1+}(1-\lambda)\ x_2) \geq \mu_{\tilde{A}}(x_1) \wedge \mu_{\tilde{A}}(x_2)$for each $\lambda \in (0,1]$ and $x_1, x_2 \in X$, subsequently, $\tilde{A}$ is a convex fuzzy set).
- Fuzzy set normalized (if $Core(\tilde{A}) = \{x \in X: \mu_{\tilde{A}}(x) = 1 \neq \emptyset$, subsequently, $\tilde{A}$ is a normalized),
- It has a piecewise continuous membership function.
- It has a real number definition.

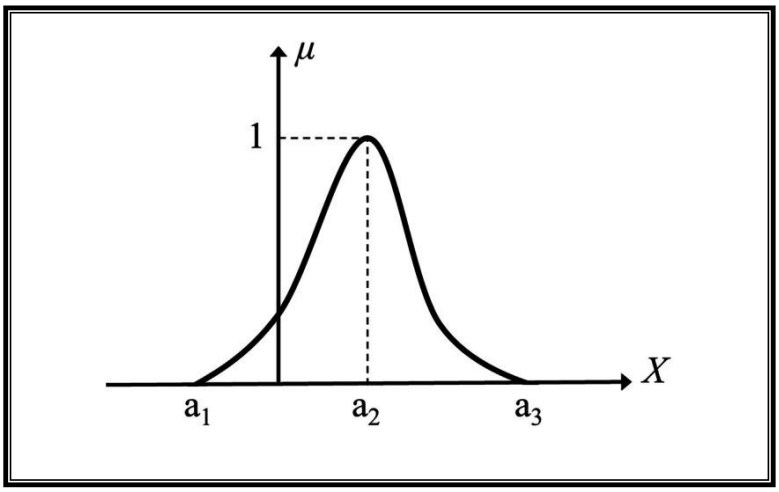

Figure 2.16. Fuzzy number.

There are numerous types of fuzzy numbers, including Gaussian, Triangular, S-shaped, G-bell, Trapezoidal, Sigmoidal, and Z-shaped fuzzy numbers. Fuzzy numbers are used in an inference system's fuzzification interface, which means that the inputs to the system are described by fuzzy numbers.

A set of fuzzy IF-THEN rules make up a fuzzy rule base. Which are the main theme of the fuzzy inference system. These rules are implemented in a reasonable manner using all other components, such as membership functions. In a practical and effective way, a fuzzy (IF-THEN) rule typically takes on the form:

$$\mathbf{R}: \text{ If } \mathbf{x}_1 \text{ is } \tilde{A}_1 \text{AND (OR) } \mathbf{x}_2 \text{ is } \tilde{A}_2, \text{ THEN } \mathbf{y} \text{ is } \tilde{B}, \qquad 2.7$$

Where, $\tilde{A}_1$, $\tilde{A}_2$, and $\tilde{B}$, are FIS linguistic variables that are defined, on the input and output worlds, by fuzzy numbers, respectively. Following are definitions of the logical operators AND and OR's fuzzy intersection or conjunction (AND) and fuzzy union or disjunction (OR):

$$\begin{aligned} \tilde{A}_1 \text{ OR } \tilde{A}_2 &: \max\{\mu_{\widetilde{A_1}}, \mu_{\widetilde{A_2}}\}, \\ \tilde{A}_1 \; AND \; \tilde{A}_2 &: min\{\mu_{\widetilde{A_1}}, , \mu_{\widetilde{A_2}}\}. \end{aligned} \qquad 2.8$$

After establishing the rule base, we use the method for combining the fuzzy sets that represent each rule's outputs into a single fuzzy number (set), which is referred to as rule aggregation. Different operators, such as Max, Sum, or Prober, can aggregate data. In general, when compensation between input variables is desired, the Max operator is preferred. The Max operator can be found in:

$$\mu_{output} = \max\{\mu_{rule^1}, \mu_{rule^2}, \ldots. \; \mu_{rule^r}\} \qquad 2.9$$

The defuzzification interface is the final step, which converts the output fuzzy set obtained after the aggregation step into a crisp number. Center of area or centroid defuzzification techniques are frequently employed in Mamdani-based FIS, Area-based bisector, Mean of maxima, Small of maxima, and Largest of maxima (LoM). gives an element with the highest membership values a defuzzified crisp value x^* so that when multiple elements have the highest membership values, the mean value of the maxima is taken, as shown in Figure (2.17).

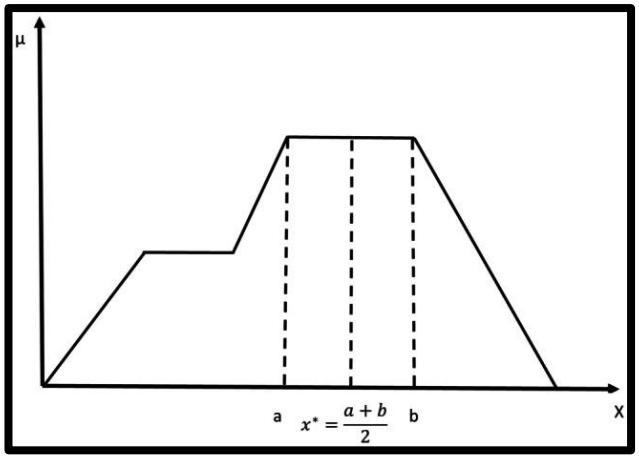

Figure 2.17 The mean of maxima defuzzification

The Python Fuzzy Logic Toolbox can be used to perform all of the mathematical operations described above.

2.8.3 Fuzzy logic application

Fuzzy logic systems can be applied in various fields as follows [97]:

- Medical diagnostic systems FIS for chronic diseases.
- Pattern recognition and image analysis.
- Satellite spacecraft control.
- Intelligent traffic control systems.
- Control theory in AI decision making support system.
- Banknote transfer control system stock market prediction.

2.9 Independent Component Analysis (ICA) technique

A statistical method for resolving the blind signal separation (BSS) problem, possibly the most popular one. It is a developed class of exploratory tools whose primary role lies in the analysis of both images and sound. It is called "blind" because it retrieves source signals from signals with unknown mixing coefficients. For example, if we had a set of microphones in a room and were recording signals from several speakers (source) each microphone would have a different texture range. ICA are methods whose task is to separate blind signals formed as a result of the assumed statistical independence of the source signal [98, 99]. The diverse nature of the signals in the field of X-ray images and other medical images indicates that blind signal separation techniques can be used to isolate these different sources [100-101]. For example, the separation of the rib bones from the lung, as well as in many image processing operations. It can be regarded as an algorithm to handle the blind source separation issue [102]. Additionally, ICA has applications in a wide range of fields, including econometrics, biomedical signal processing, image processing, and telecommunications [103].

2.9.1 The history of Independent Component Analysis

Was formulated by Herault and Jutten in 1986 [104].In an effort to address the signal processing BSS issue. Based on BSS research, Jutten and Herault hypothesized a square (number sensors = number sensors), linear and instantaneous

mixing, and using an artificial neural network (ANN) to calculate inverse mapping estimates.

2.9.2 ICA Mathematical Basic Definitions

A multichannel signal with an n-channel count is used by standard ICA, number of channels n being higher than the number of source signals *p* but not lower. Calculating statistically independent components is the basis of ICA (source signals) $s_1, \dots, s_p$ and a $p \times n$ mixing matrix *A* for $n \geq p$ solely on the basis of n values of observed signals (signals generated) $x_1, \dots, x_n$ Equation (2.9) describes a typical linear ICA model in the following:

$$x = As \qquad 2.10$$

Where $s = (s_1, \dots, s_p)^T$ is a signal source vector, $x = (x_1, \dots, x_n)^T$ is a vector of signals observed, A is an $p \times n$ mixing matrix Figure (2.18). Equation (2.10) shows how ICA resolves the separation problem.

$$\hat{s} = Wx = WAs \qquad 2.11$$

Where matrix W is a rough estimate of A inverse known as a filtration matrix and $\hat{s} = (\hat{s}_1, \dots, \hat{s}_n)^T$ is a prediction of s . When $p = n$, the filtration matrix W is a member of the general linear group $Gl(n)$ of non-singular matrices $\det(W) \neq 0$.

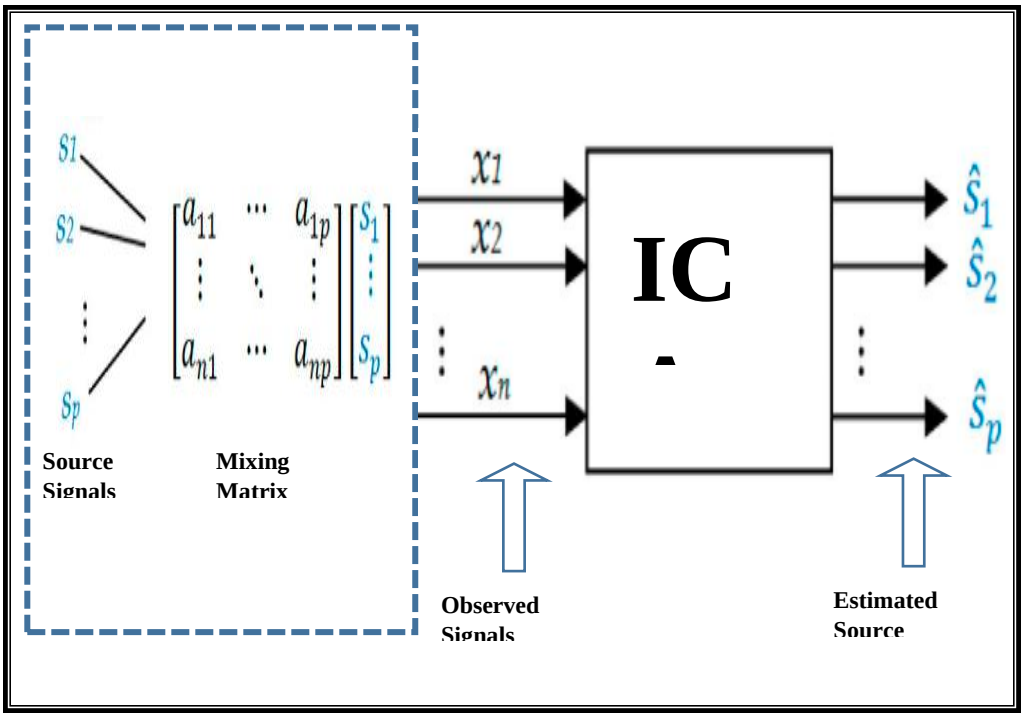

Figure 2.18 standard independent component analysis

2.9.3 ICA applications

BSS has attracted a lot of interest from both the business and academic worlds. BSS applications can be found in fields like medical signal processing, wireless communication systems, remote sensing, image recognition, and pattern analysis. The BSS technique is also applied to radio communication systems [105]. The BSS technique has been employed in a wide range of other fields. It also has another use in the fields of medicine, and it is used in the analysis of CXR images, and its usefulness lies in separating the rib bones from the lung [106].

CHAPTER THREE

The proposed COVID-19 detection system

3.1 Introduction

To achieve the objectives of the current study, in this chapter, both fuzzy logic, and ICA techniques will be presented in detail, it will also introduce the mechanism to know the role of each of these techniques in improving system performance by applying them to the datasets used in the proposed model. The suggested approach makes use of a multi-input network with three images type as input: a fuzzy image using a fuzzy trapezoidal membership function, ICA to reduce unnecessary features and original dataset images as shown in Figure (3.1). There are four stages to the proposal:

The first: Read the collection of the two different datasets for CXR images.

The second: Apply the enhancement technique (fuzzy logic as a filter and ICA as dimensionality reduction) on the dataset.

The third: Images treated with a fuzzy filter and ICA are used to train six networks (VGG16, ResNet152V2, InceptionV3, Xception, DenseNet121, EfficientNetB3) using transfer learning.

The fourth: The proposed work is practically tested by installing the best weight model on the mini-computer (Raspberry Pi), by creating graphical user interface (GUI) designed by (HTML and Python) programming language, in addition to uploading the diagnostic results to the cloud using Internet of Things (IoT) technologies.

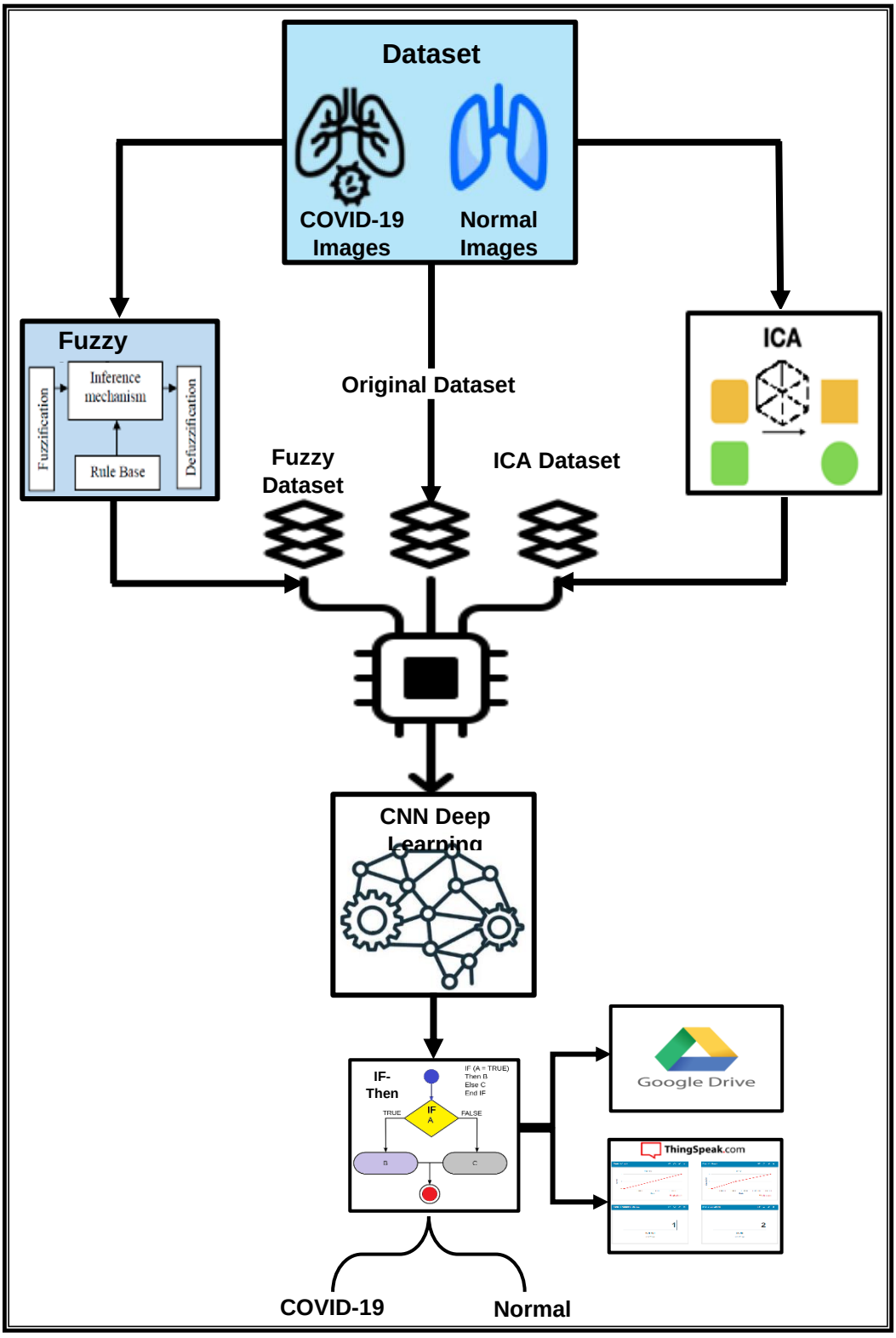

Figure 3.1 proposed method

3.2. Approaches to Fuzzy Edge images using trapezoidal membership functions

A discrete description of reality can be found in a digital image. And carries some implicit ambiguity. This ambiguity appears in two distinct facts: the color of the pixels (since there are a variety of tones available, but only a finite number), and the placement of the objects (because of the discrete number of pixels). There are a number of additional issues with information analysis, such as noise. The image is composed of the position of these objects and the color of the pixels [107]. The discretization issues with the image must be taken into consideration in any possible treatment. For instance, it can occasionally be difficult to tell which pixel belongs to which item. Even the human has some trouble determining where the edges of an image. For segmenting regions with distinct borders, traditional segmentation techniques like watershed, region growing, and thresholding are appropriate. These techniques, however, are unable to aid in the segmentation of the areas when there are boundaries and inhomogeneity. Fuzzy logic technique therefore seems like a good option. The traditional Boolean logic, which only has the two states of false or true, can be replaced by fuzzy systems. The membership values are indicated by either a 1 for full accuracy or a 0 for absolute falsehood [108].

In the proposed work applying a fuzzy filter on the CXR images analyze the effects of the fuzzy set's shape on the conversion of gradient magnitudes into curve degrees.

A curve known as the membership function defines how each input pixel is transformed into a membership value between 1 and 0. Two scalar parameters (b, a) determine the MF curve, which is a function of a vector named x any fuzzy logic system's central component is the fuzzy inference system. The first stage of a fuzzy inference system is fuzzification. On the universe of discourse$X$, a membership function for a fuzzy set A is defined formally is defined as $\mu_{\tilde{A}}: X \rightarrow [0,1]$, where every X component is assigned a value between 0 and 1. This value, called degree of membership or membership value, quantifies the grade of membership of the element in X to the fuzzy set$A$. Here, X is the universal set and A is the fuzzy set derived from X [109] as shown in Figure (3.2).

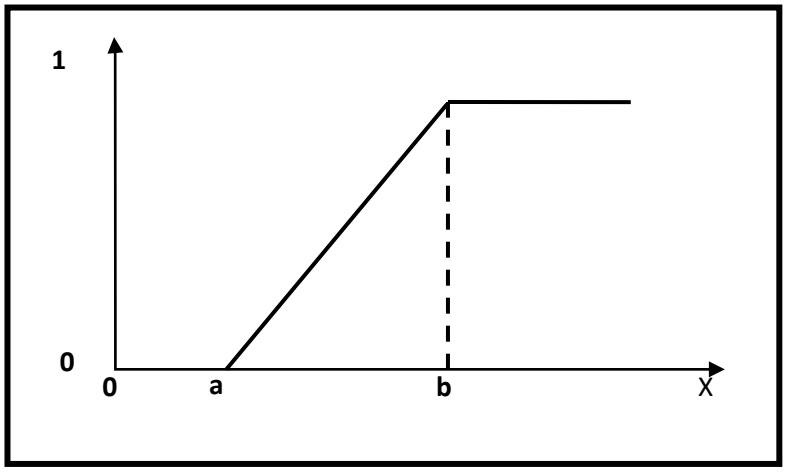

Figure 3.2 Gradient magnitude Proposed membership function

3.2.1 Fuzzy filter experimental procedure

-Input: CXR Medical image.

-Output: New dataset with fuzzy logic filter.

Step1: Read CXR medical image from the dataset.

Step2: Make a loop to read the pixels in a CXR medical image.

Step3: Define the parameters for fuzzy Trapezoidal membership functions

Step4: Determine the lower and upper limits based on the best parameters [a, b] for the fuzzy filter.

Step5: New dataset with fuzzy logic filter.

Step6: End.

3.3. Approaches to Image dimensionality reduction Using ICA

The ICA dimensionality reduction (ICA-DR) method is use to transforms a set of variables (pixels) to a new set of components (features); it does so such that that the statistical independence between the new components is maximized. This is similar to Principle Component Analysis (PCA), Where the primary distinction between (principle component analysis) PCA and ICA is that PCA seeks components that are uncorrelated, whereas ICA seeks out independent factors [110] as shown in Figure (3.3). Similar to other dimensionality reduction techniques, ICA aims to minimize the number of variables in a set of data while preserving important information.

In the proposed work, an image's pixels are represented by the variables. Utilizing ICA on images is one of the reasons for performing image compression, meaning that much less memory is used to store the independent components of an image rather than thousands or even millions of pixels. With preserving the features of the original image. By create a new dataset with low-dimensional very similar to the original version as shown in Figure (3.4). Additionally, ICA extracts the independent components of images by nature; as a result, it will locate the curves and edges in an image. For example, in CXR images, ICA will identify the ribs, the lung, the sternum etc. as independent components. The main functionality of proposed work get by using python language and use the FastICA library available from sklearn.decomposition.

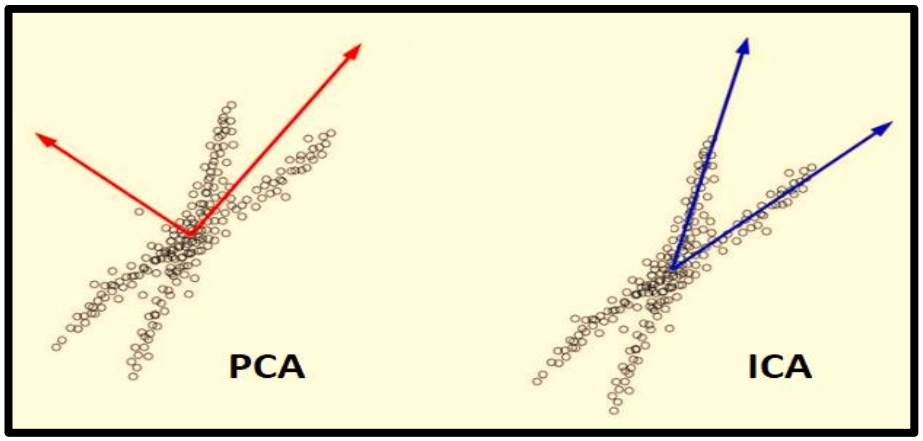

Figure 3.3 PCA vs ICA transforms with feature space

3.3.1 ICA-DR experimental procedure

-Input: CXR Medical image.

-Output: A new dataset with low-dimensional.

Step1: Read CXR medical image from the dataset.

Step2: Set the parameter, as_grey and make a loop to read the pixels in a CXR medical image.

Step3: Create a FastICA object.

Step4: Define the parameters (choose a number of components)

Step5: A new dataset with low-dimensional very similar to the original version.

Step6: End.

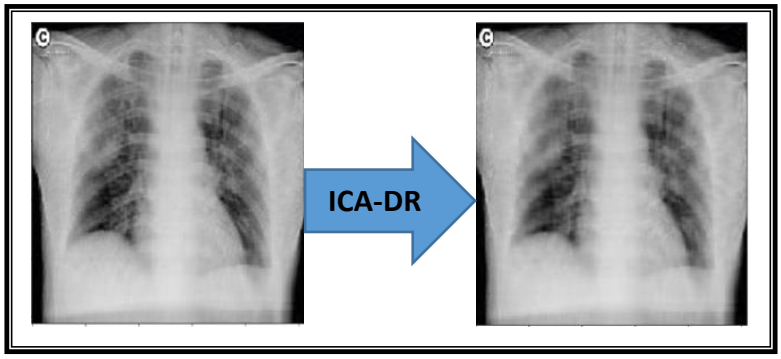

Figure 3.4 New CXR image with reduced-dimension similar to the original.

3.4. Methodology of Enhancement COVID-19 detection

The final proposed method involves feeding two inputs of CXR dataset into a multi-input network: a fuzzy images using a fuzzy trapezoidal membership function then pass it on the ICA for reducing unnecessary features by using the proposed approach ICA-DR and the second with original images. There are four stages to the proposal. The first one data shuffle and reads the images from the two datasets that were previously exhibited. The second is to compare which one obtains the maximum level of accuracy by using the fuzzy logic filter and the dimensionality reduction. The fuzzy trapezoidal number generated by the fuzzy logic filter is displayed as:

$$Trapezoidal: f(x,a,b,c,d) = \begin{cases} 0, x \leqslant a & \\ x - \dfrac{a}{b} - a & a \leqslant x \leqslant b \\ 1, & b \leqslant x \leqslant c \\ d - \dfrac{x}{d} - c, & c \leqslant x \leqslant d \\ 0, & d \leqslant x \end{cases} \quad 3.1$$

Every pixel of CXR images from the input is directed to a membership value between 1 and 0 according to a membership function curve that specifies. The membership function curve is a function of a vector x and is determined by four scalar parameters b, a, c, and d. This study uses the computationally efficient Blind/reference less image spatial quality evaluator (BRISQUE) technique to assess an image's quality score. The spatial approach was used by the BRISQUE model. First, the following equation is used to determine a localized luminance, commonly known as Mean Subtracted Contrast Normalized (MSCN) [111]:

$$I(m,n) = \frac{I(m,n) - \mu(m,n)}{\sigma(m,n) + c} \quad 3.2$$

Where $I(m,n)$is the intensity image, normalizes using local variance $\sigma\ (m,n)$, and $\mu(m,n)$ is the local mean, N is spatial indices, M and N are the image width and height, respectively, to avoid a zero variance. The local mean $\mu(m,n)$ and local variance $\delta(m,n)$ are calculated using the following equations:

$$\mu(m,n) = \sum_{k=-K}^{K} \sum_{l=-L}^{L} w_{k,l} I_{k,l}(m,n) \quad 3.3$$

$$\sigma(m,n) = \sqrt{\sum_{k=-K}^{K} \sum_{l=-L}^{L} w_{k,l}(I_{k,l}(m,n) - \mu(m,n))^2} \quad 3.4$$

Where $w = \{w_{k,l} | k = -K, \dots, K, l = -L, \dots, L\}$

Use the Brisque score to select the best parameters $(\mathrm{a}, \mathrm{b}, \mathrm{c}, \mathrm{d})$ for the fuzzy logic filter. In first , using transfer of learning, four networks are trained using diffuse-filtered and clustered images. Called VGG16,ResNet152V2, EfficientNetB3, VGG16, and InceptionV3. The purpose of this test is to assess how well the cluster averages and the diffuse filter under test perform. Where evaluating the tests using the accuracy, AUC recall metrics and precision. Applying tests to a multi-input network with two pre-trained networks makes up the third stage. A fully connected layer was substituted for the last layer to change the networks, divided into a second fully connected sigmoid layer with 20 nodes and one node. The criteria are applied in various combinations: InceptionV3, EfficientNetB3, ResNet152V2, DenseNet121, Xception and VGG16. 25 epochs were used to run these tests. The

combination that had a higher AUC score was picked for tuning and assessment. Tuning the best model selected is the fourth step of the process. Was trained using the best model in 25 epochs, and metrics including the receiver operating characteristic curve (ROC) curve, and recall are shown. The final step compares explainable ML practice with and without the fuzzy logic filter using class activation maps.

3.5. Dataset

In this work, three data sets were used to train the proposed model. The website https://github.com/ieee8023/covid-chestxray-dataset based on the first data set, as this set of data is characterized by its reliability and approved by the University of Montreal's Ethics Committee as shown in Figure (3.5).

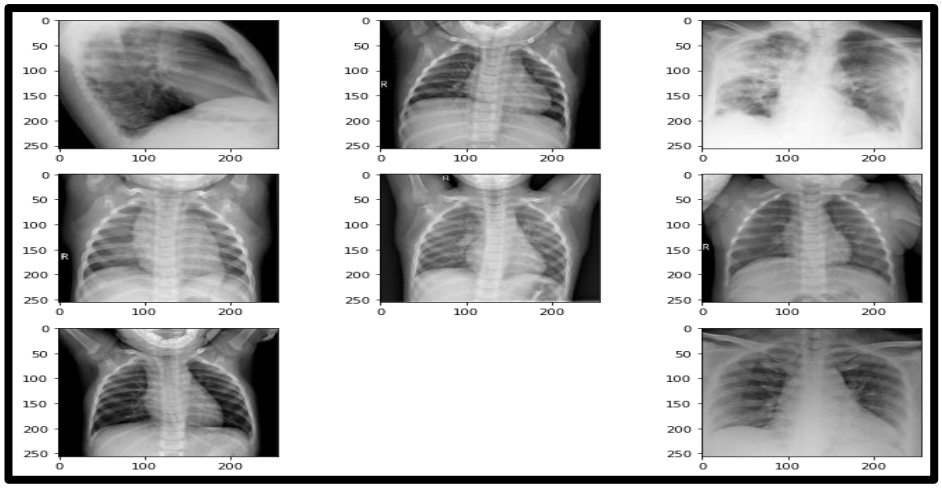

Figure 3.5 selected dataset's image samples.

The dataset is made up of CXRs from patients with healthy vs. affected by pneumonia (Corona), infected patients, and a few other categories like SARS (severe acute respiratory syndrome), streptococcus, and ARDS (acute respiratory distress syndrome), as shown in Figure (3.6). The Kaggle platform hosts the second dataset on https://www.kaggle.com/nabeelsajid917/covid-9-X-ray-10000-images and was employed to test the model. The variety of patient cases from the dataset is depicted in Figure (3.7) .The initial dataset includes 5903 images. Where 4.265 have pneumonia of unknown reasons, 1.576 Normal, 4 SARS images, and 58 cases of COVID-19. Third dataset offered by https://www.kaggle.com/alifrahman/covid19-chest-xray-image-Dataset to enhance test outcomes.

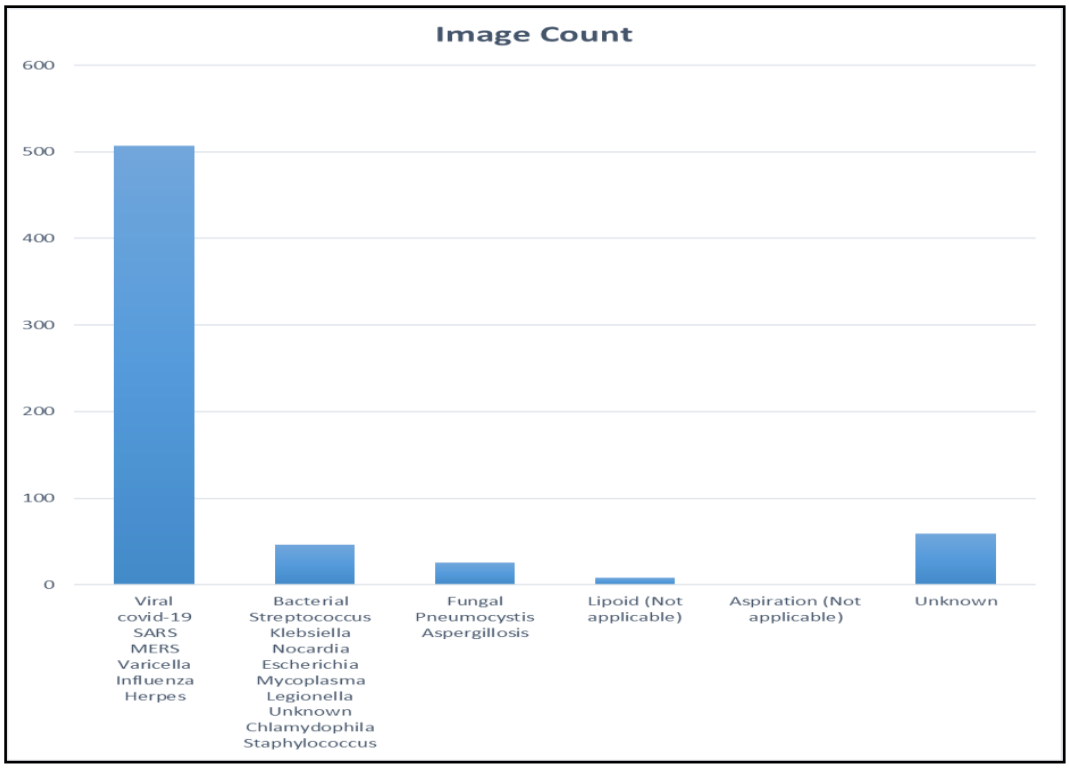

Figure 3.6 Distribution of Virus types among ieee8023 dataset.

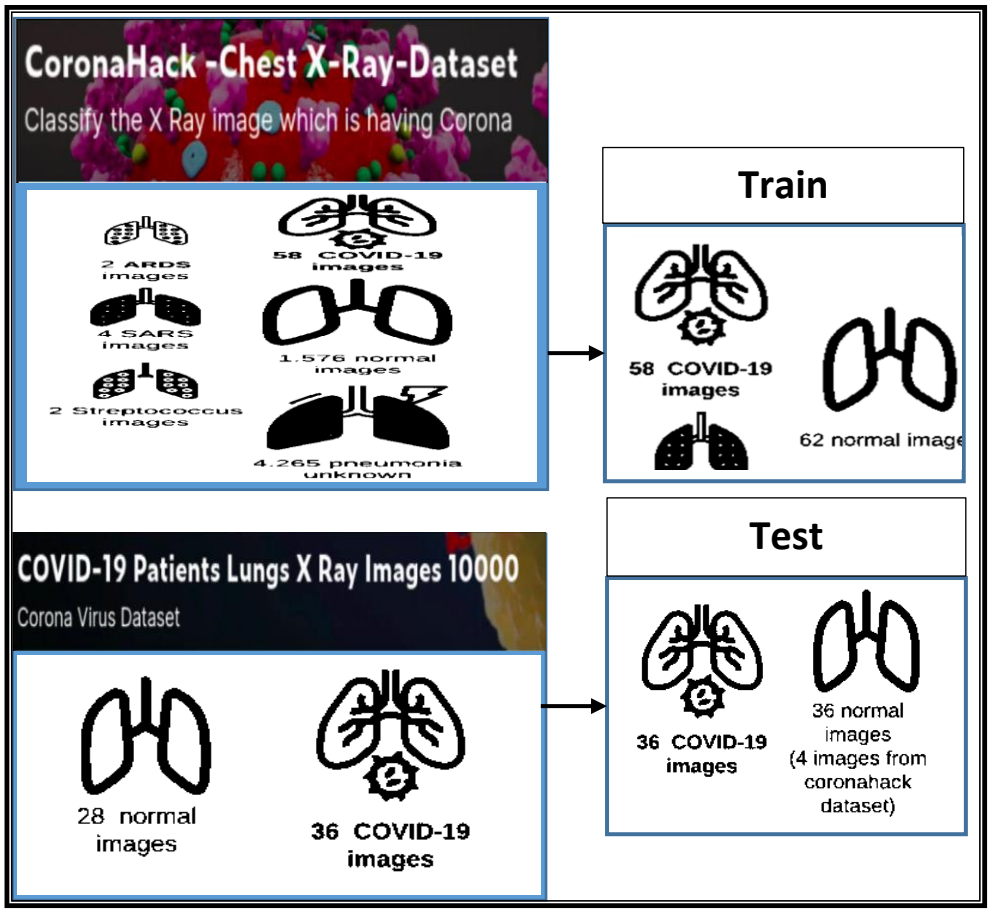

Figure 3.7 An explanation of the dataset used in this study.

3.6. Practical IOT application for proposed Covid-19 detection

In this proposed practical work shown in Figure (3.8), small computer (Raspberry pi) was used as a server. It runs an operating system called (Raspbian). This operating system is one of Linux distributions operating system, where proposed model was trained using artificial intelligence algorithms (deep learning) using the Python programming language environment. Where a local (Webserver) was created that contains a page called (webpage) that was built through Hypertext

Markup Language (HTML), which is a user interface that is used while entering the browser through a tablet or mobile device.

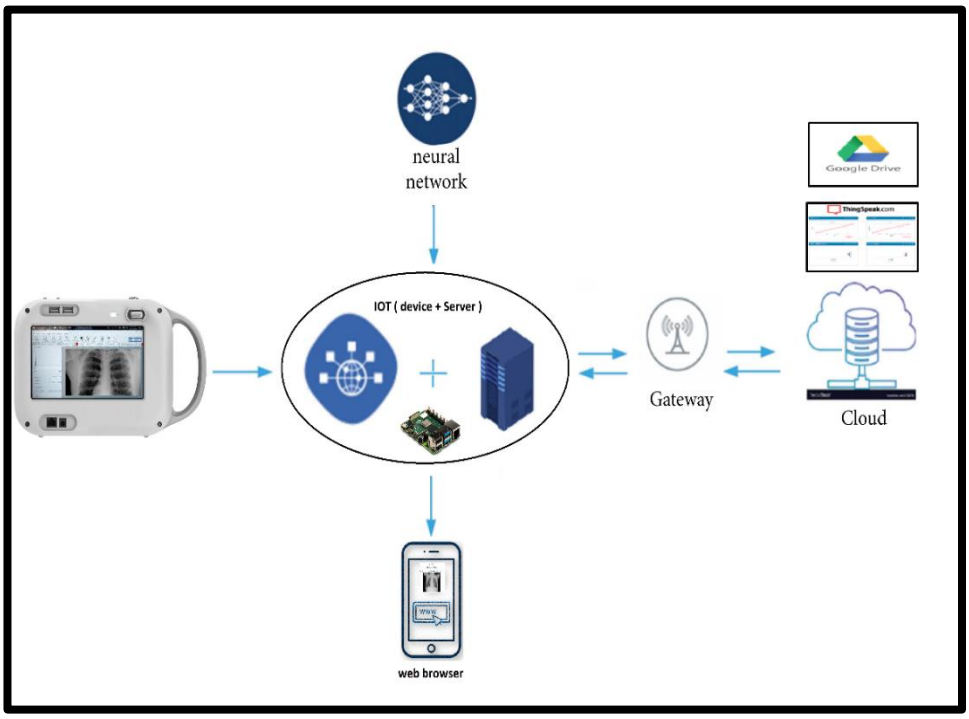

Figure 3.8 Practical application for Covid-19 detection.

When the server starts up, connect the Raspberry Pi to a local network called an Access Point. Make sure it has the latest version of the Raspbian operating system. To access the Graphical User Interface (GUI), when typing the IP address into the browser, an interface appears in Figure (3.9). asking the user to enter the CXR image to be examined, to predict it by the stored model. The system gives the result of predicting whether the owner of the image is infected or not infected with the possibility of displaying the rate of injury through the proposed fuzzy logic technology model with the (IF-then) rule. Then the result of the image is sent to the

cloud (Google Drive) after predict process, to be confirmed by the specialist when available.

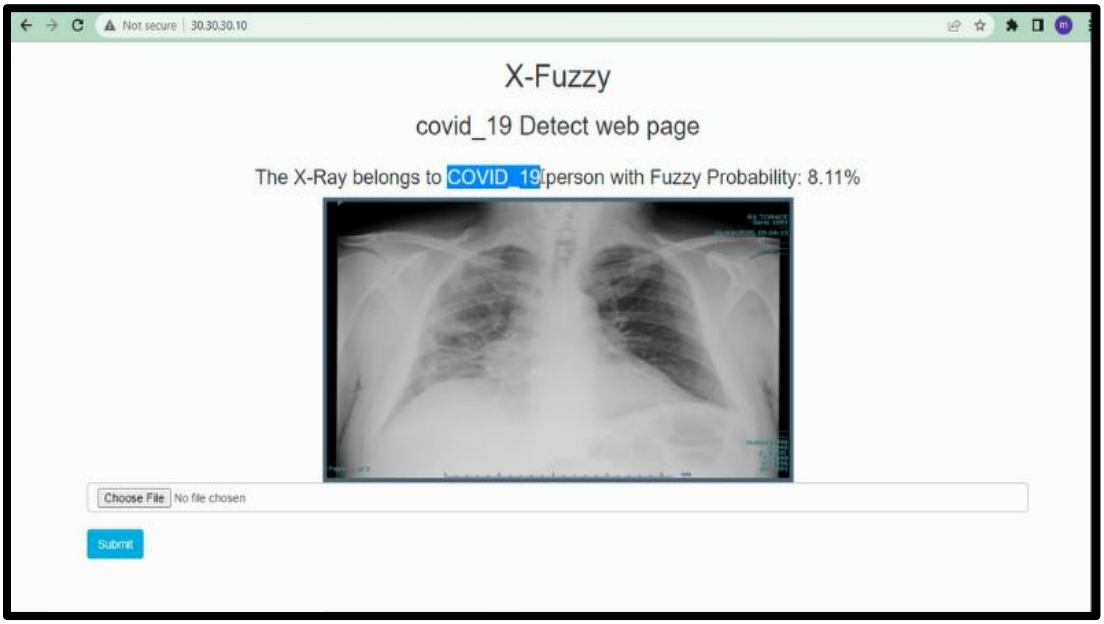

Figure 3.9 Graphical User Interface (GUI) Webpage.

In addition, the total number of patients and healthy people is sent to a special server called (ThingSpeak) for statistical purposes called the Internet of Things (IoT) as shown in Figure (3.10).

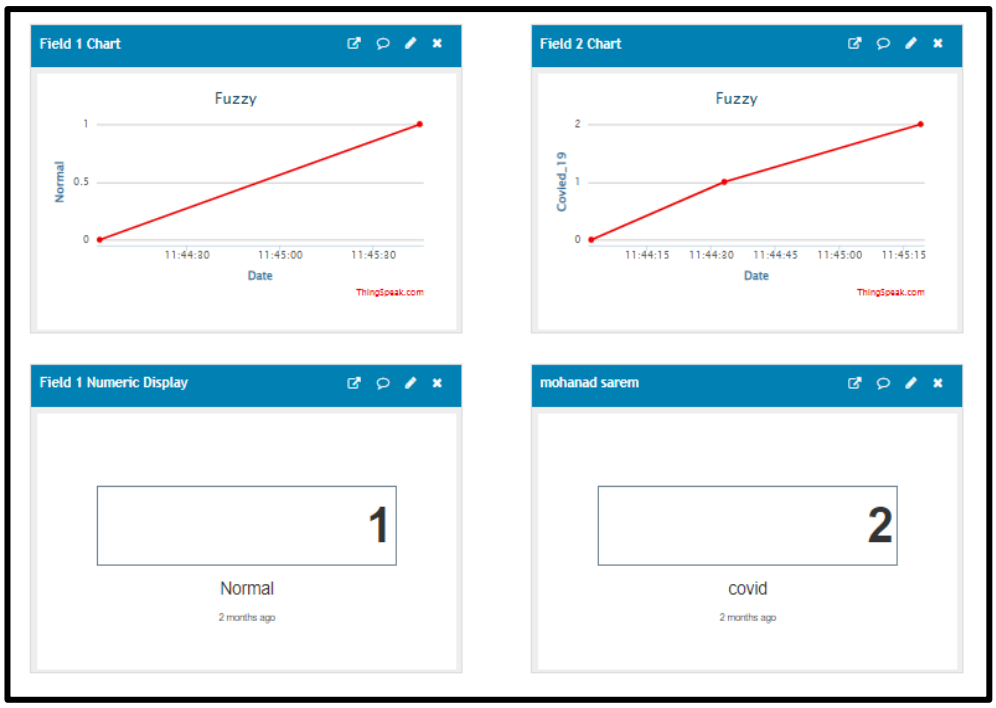

Figure 3.10 Data collection (Covid-19, Normal) in the cloud and statistical analysis.

• Software libraries used in this work:

- ✓ **TensorFlow**: It is a Google open-source artificial intelligence library that creates models using data flow diagrams. It enables the development of multilayered, large-scale neural networks. The main purposes of TensorFlow are to categorize, perceive, comprehend, find, predict, and create [112].
- ✓ **Flask**: Provides tools, libraries, and technique that allow creating a web application. A web application can be webpage, Flask is used to develop web applications using Python, and implemented on a. Advantages of using the

Flask framework: It runs as an embedded development server and a fast debugger [113].

- ✓ **CNN library**: A particular kind of artificial neural network used for image recognition and processing, convolutional neural network libraries are built to process data through pixels. Convolutional neural networks (CNN/ConvNet) are a subset of deep neural networks used most frequently for visual image analysis [114].

3.6.1 Hardware component

The goal of this research is to ascertain whether a COVID-19 detection model on a cheap mobile device can be applied to practical tasks. Employed a Raspberry Pi 4 Model B as a mobile platform. The Raspberry Pi is a single-board computer that low cost . One circuit board houses the microprocessor, memory, wireless radios, and ports. Since the Raspberry Pi is a Linux machine, it can theoretically carry out all operations that a Linux machine is capable of, including hosting email and web servers, acting as network storage, and carrying out object detection [114]. Since the Raspberry Pi board doesn't have any built-in storage like most computers do, the operating system is installed on a micro SD card, which is also where you'll store all of your files (you can always add a USB hard drive). This structure, as shown in figure (3.11). makes it simple to increase storage and switch between different operating systems by exchanging micro-SD cards.

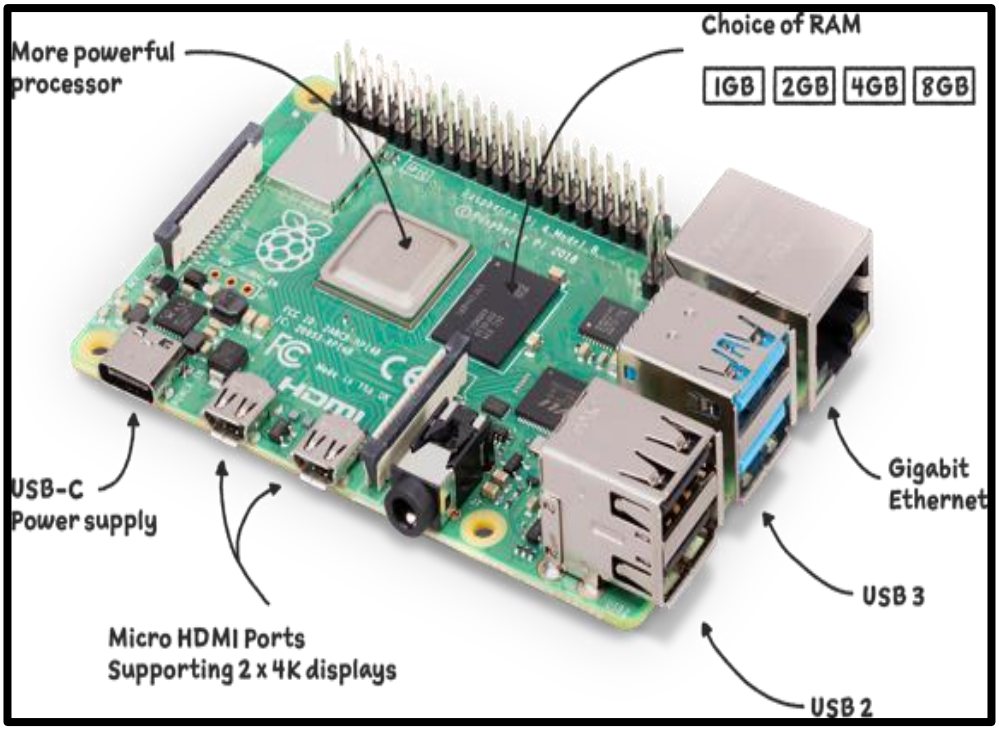

Figure 3.11 Suggested hardware device (Raspberry Pi 4)

As the hardware part of COVID-19 detector, used the Raspberry Pi 4 Model B. Need to the Raspbian operating system installed since TensorFlow 2.0.0 + Keras 2.3.1 officially supports the Raspberry P. Also need a microSD card, with at least 32 Gb of memory.

3.6.2 Software Implementation

In this research, part of the practical device was simple Web Server development to control the input of images. For this project here, where used FLASK [115], a very simple and free micro framework for Python. With Flask, will be very simple to control Raspberry pi over the internet. Flask is referred to as a micro framework

because it doesn't need specific tools or libraries. It doesn't have a form validation layer, database abstraction layer, or any other component where pre-existing third-party libraries already perform common functions. Flask does, however, support extensions that can be used to add application features as if they were built directly into the framework. On this project, The Raspberry Pi was used as a local Web server, where we will control via a simple webpage as shown in Figure (3.12).

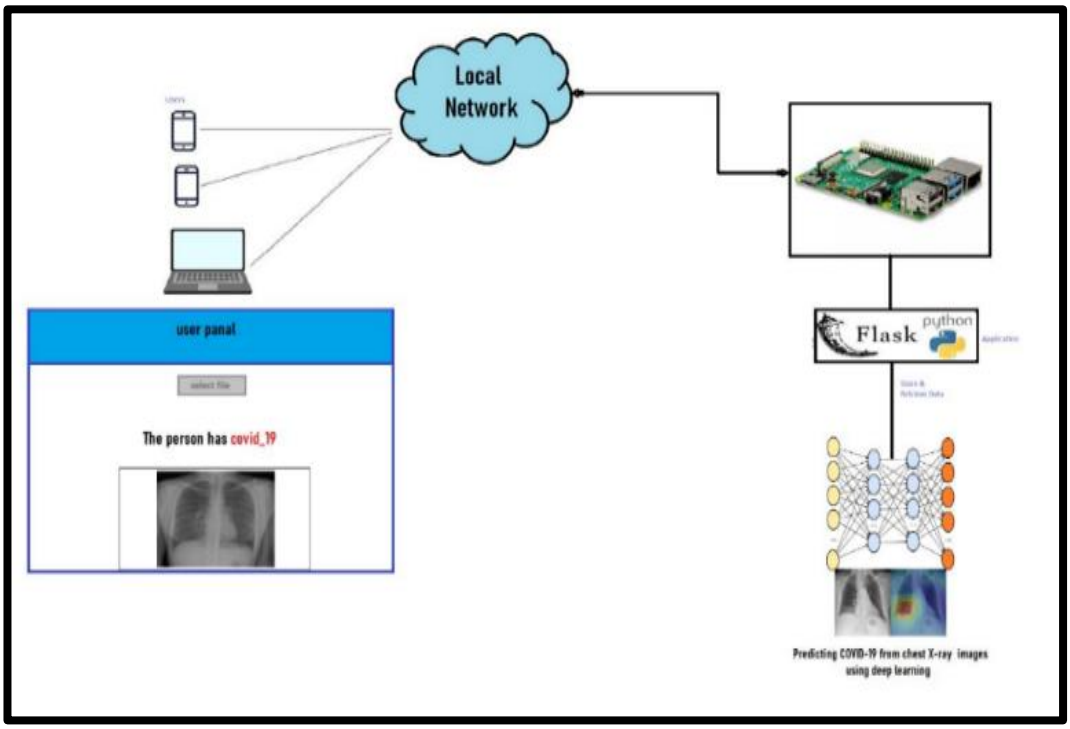

Figure 3.12 Software FLASK Implementation.

In the figure (3.13) below is a picture showing the mechanism of action of the raspberry Pi and how to upload the image and predict the presence of Covid-19 and show the results using the fuzzy method (IF-then rule).

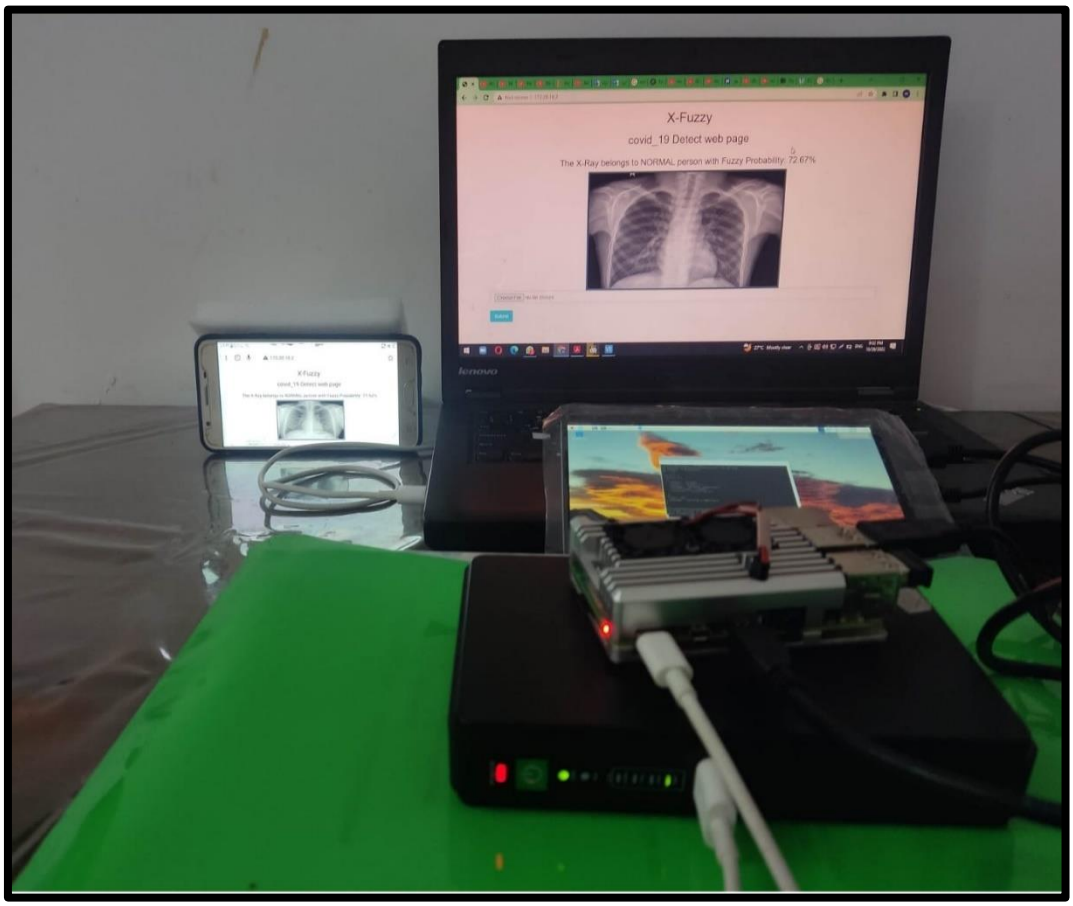

Figure 3.13 Implementation of Practical device

CHAPTER FOUR

Results and Discussion

4.1 Introduction

The main objective of this study is to present a monitoring model and lessen human error in the diagnosis of COVID-19. It is characterized by rapid diagnostic results and is also considered one of the necessary social distancing methods to prevent infection between people, so artificial intelligence techniques are necessary for this type of epidemic, as it is an important type of quick and temporary diagnosis until a specialist doctor becomes available. So, the results in this study consist of demonstrating the calculated results by using the fuzzy logic technique only and demonstrating the calculated results using the ICA technique. Then compare the results with and without these techniques. The results are based on model analysis techniques accuracy, AUC, recall, and precision. Real CXRs image data for both normal and COVID-19 patients are taken from Kaggle and GitHub databases.

4.2. Mathematical Model Analysis

Training performance and validation performance for the proposed model are verified based on the graphs of accuracy, precision, AUC, and recall. Then comparing the result for each technique of the proposed model.

4.2.1. Model Accuracy

The models' performance in classifying positive and negative classes is measured by accuracy. The rating is determined by evaluating all detailed data with all data. It is given by eq (4.1):

$$Accuracy = \frac{TP + TN}{TP + TN + FP + FN} \qquad 4.1$$

Where: FP the number of False Positives, TP is the number of true positives, TN is the number of true negatives, and FN is the number of false negatives.

4.2.2. Model Precision

The degree of precision indicates how closely the measurements match. There is a random error component in every measurement in a series. It's given by eq (4.2):

$$P = \frac{TP}{FP+TP} \qquad 4.2$$

Where: FP the number of False Positives, TP is the number of true positives, and P is Precision.

4.2.3. Model AUC

The AUC is calculated using the trapezoidal rule. This Mann-Whitney U statistic divided by $N1 * N2$ gives the resulting area [118]. Where $N1$ and $N2$ are the number of instances in C1 andC2, respectively. So The likelihood of properly

identifying the C1 example when presented with a randomly chosen case from each class is known as the AUC.

4.2.4. Model Recall

Percentage of a certain class correctly identified (from all of the given examples of that class),is the classifier's capacity to locate each sample. The ideal number is 1, while the worst number is 0. The recall is given by eq (4.3):

$$R = \frac{TP}{TP+FN} \qquad 4.3$$

Where: FN the number of false negatives, TP is the number of true positives, and R is Recall.

4.2.5. Confusion matrix

Is a table that's used to describe how well a classification method performs. Let $\mathrm{I(x,y)}: \mathbb{R}^2 \to \mathbb{R}$ be a medical image and $S(\mathrm{I(x,y)}): \mathbb{R}^2 \to \Omega, \Omega = 0,1$ a binary decision of picture$\mathrm{I(x,y)}$. Using the gold standard as G and the outcome as R, according to [121], Each fold can be categorized as: False Positive: $G(x,y) = 0\text{^}R(x,y) = 1$,False Negative: $G(x,y) = 1\text{^}R(x,y) = 0$, True Positive: $G(x,y) = 1\text{^}R(x,y) = 1$, True Negative:: $G(x,y) = 0\text{^}R(x,y) = 0$.

4.2.6. ROC curve

Is a graph illustrating the behavior of a classification model at all classification thresholds. It can be represented with curve plots of two parameters [119]:

-True Positive Rate (TPR)

-False Positive Rate (FPR)

4.3 Applying a Fuzzy Logic Filter

In Figure (4.1) (a) below is a histogram showing the effect of applying a fuzzy edge on the CXRs image of a person with a healthy lung to be compared to an image of an infected lung in Figure (4.1) (b), where this type of proposed fuzzy filter helps clarify the affected areas of the lung.

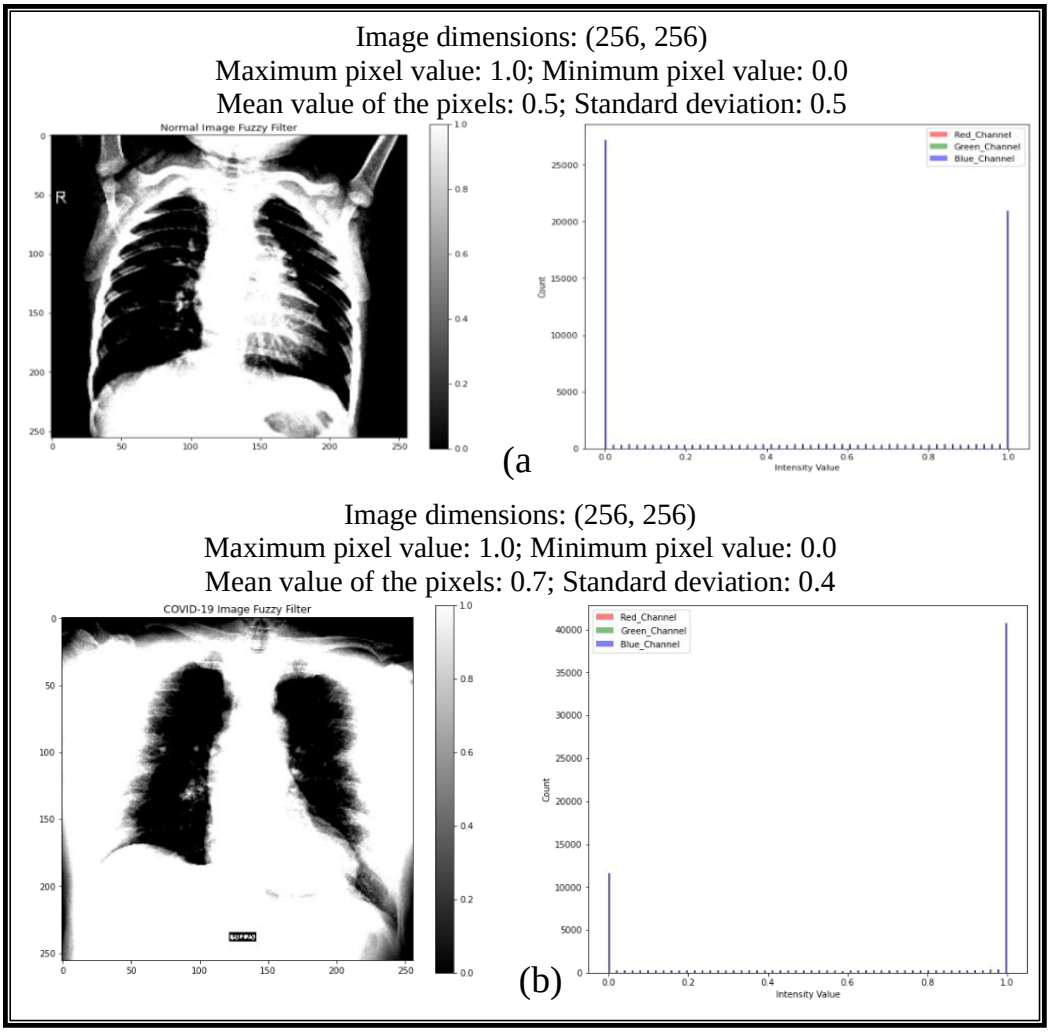

Figure. 4.1 (a) Normal image fuzzy filter and (b) COVID-19 image fuzzy filter.

Table (4.1) demonstrates below presents results without using the fuzzy logic technique, where AUC of 94.4%, Precision of 90%, and accuracy rate up to 94.9%, for ResNet152V2. Achieving AUC of 99.4%, a Precision of 87.8%, and an accuracy rate up to 93%, for DenseNet121, while the use of the fuzzy logic technique proposed contributed to an increase in AUC of 96.7 %, a precision of 99 %, and an accuracy rate of 97.2 % was attained for ResNet152V2 using this training method. DenseNet121 has an AUC of 96.1 %, a precision of 94.5%, and an accuracy rate of

up to 95.8 % as illustrated in table (4.2) below. Figure (4.2) (a) and (b) present the AUC and the loss by 25 epochs of the best single input models with fuzzy technique.

Table 4.1 Result without Fuzzy logic technique

No.	Model	Accuracy	AUC	Precision
1	ResNet152V2	0.96	0.95	0.91
2	DenseNet121	0.93	0.99	0.88

Table 4.2 Result with Fuzzy logic technique

No.	Model	Accuracy	AUC	Precision
1	ResNet152V2	0. 98	0.97	0.99
2	DenseNet121	0. 96	0.96	0.95

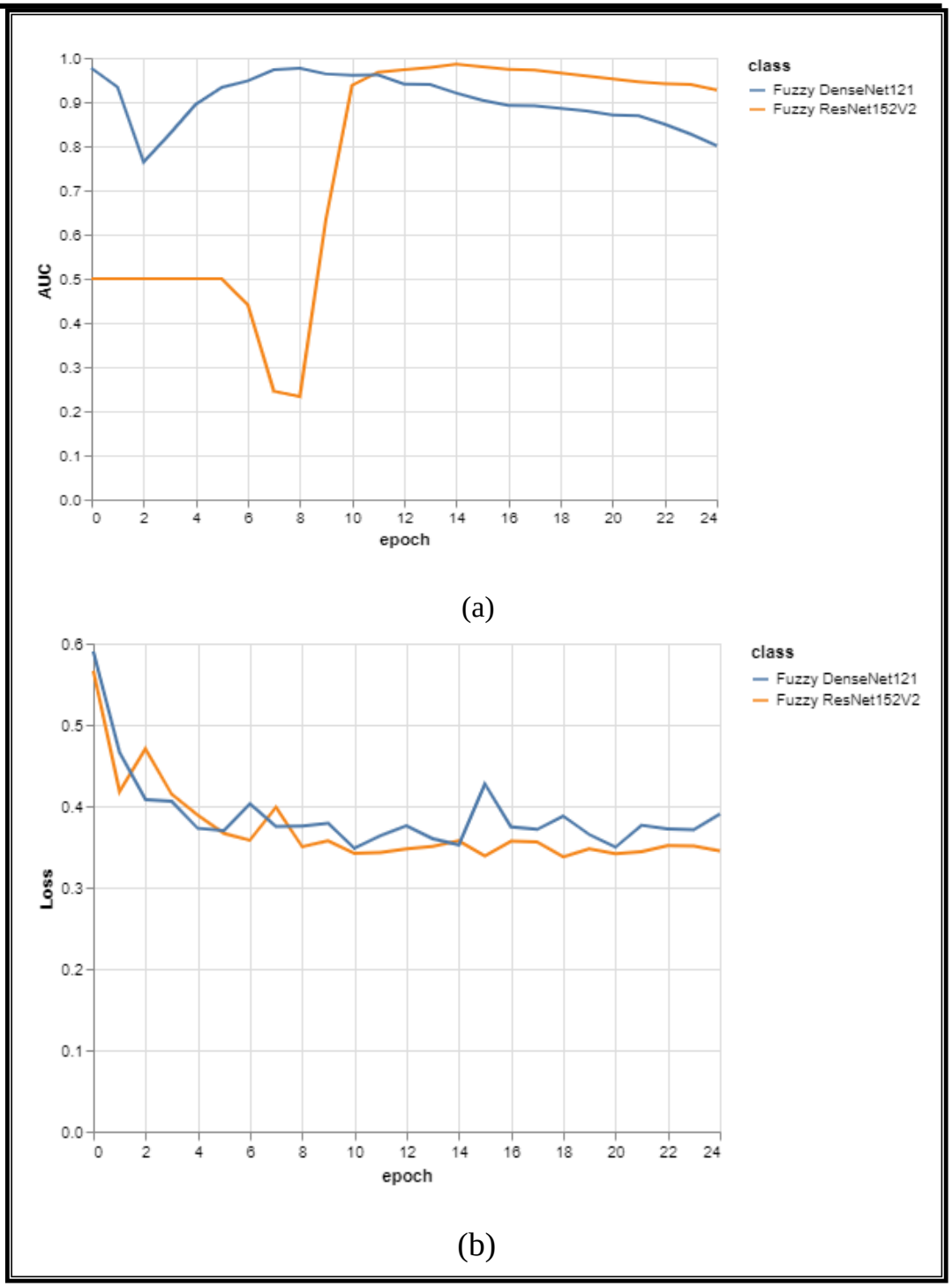

Figure 4.2 (a) AUC by the epoch of the fuzzy models. And (b) Loss by the epoch of the fuzzy models

4.4 Applying ICA-DR

The dimensionality reduction for Gaussian signals is a difficult problem in image processing, and the ICA requires non-Gaussian signals. Gaussian signals are incompatible with ICA because it is impossible to identify the original sources from the components that are acquired, which might also have been formed by other arbitrary mixing of the sources. For this matter, the ICA-DR is introduced into image Dimensionality reduction. The fastICA algorithm has its own advantages in image Dimensionality reduction. However, it is difficult to achieve the perfect effect as reduction is incomplete. In order to best reduce dimension, the dataset images were entered into the ICA algorithm, to produce CXR images with less dimension than before. A new image Dimensionality reduction method based on ICA is proposed. As shown in Figure (4.3) (a-f), the histogram and the method of the color intensity distribution in both the normal and covid-19 image with eight component ICA.

In order to measure the performance of noise reduction algorithm objectively, was verified based on the graphs of accuracy, AUC, and precision. Where the model was trained on both DenseNet121 and ResNet152V2 algorithms, table (4.3) shows that among these two deep learning models with best ICA in five components ResNet152V2 outperforms the others with the highest test accuracy of 95%. It attains a precision of 94%, while the AUC is 99%. On the other hand, DenseNet121 provided an accuracy of 87% and a precision of 80%. The AUC is recorded as 98%.

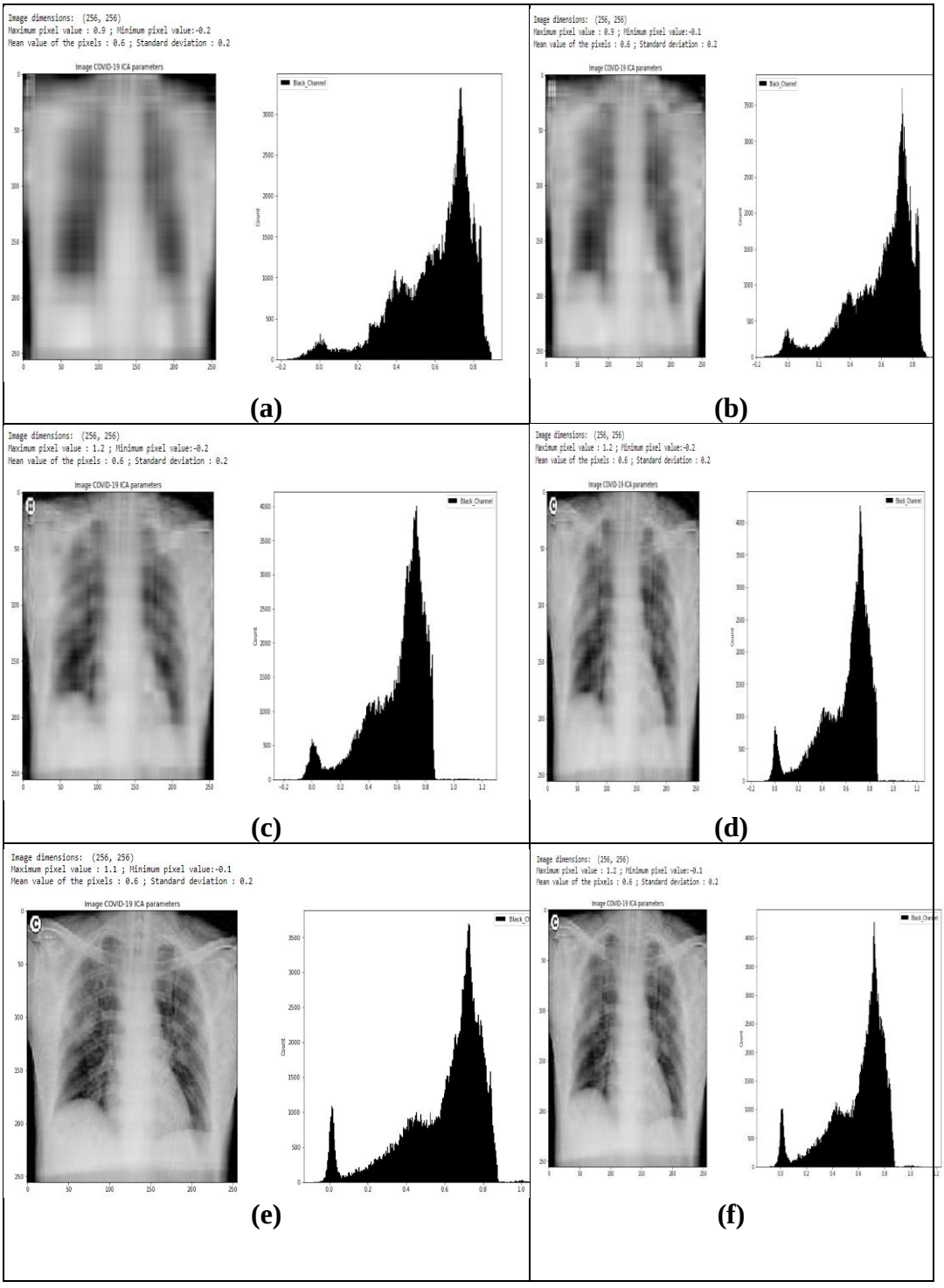

Figure 4.3 Histogram of X-ray image with ICA parameters. (a) 3- components. (b) 5- components. (c) 10- components. (d) 15- components. (e) 5-components. (f) 35-components.

Table 4.3 Result with ICA technique

No.	Component	Model	Accuracy	AUC	Precision
1	**3**	ResNet152V2	0. 94	0.97	0.92
		DenseNet121	0. 86	0.98	0.78
2	**5**	ResNet152V2	0. 95	0.99	0.94
		DenseNet121	0. 87	0.98	0.80
3	**7**	ResNet152V2	0. 77	0.89	0.81
		DenseNet121	0. 88	0.95	0.81
4	**9**	ResNet152V2	0. 98	0.97	0.99
		ResNet152V2	0. 77	0.89	0.81
5	**15**	ResNet152V2	0. 91	0.89	0.89
		DenseNet121	0. 97	0.97	0.94
6	**25**	ResNet152V2	0.81	0.87	0.75
		DenseNet121	0.95	0.98	1.00

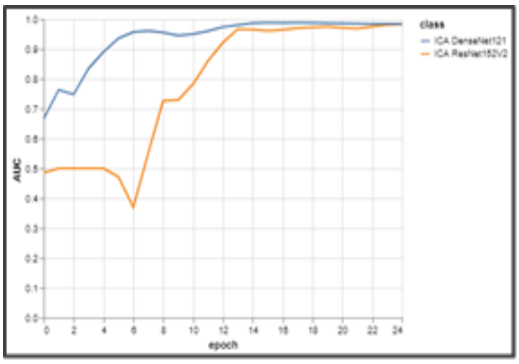

(A) AUC for 3-component ICA

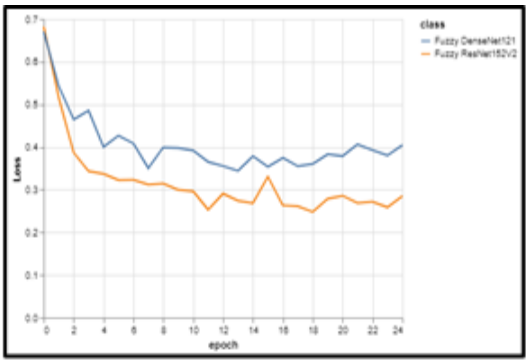

(B) Loss for 3-component ICA

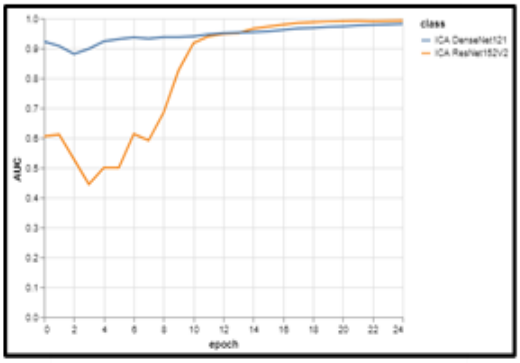

(C) AUC for 5-component ICA

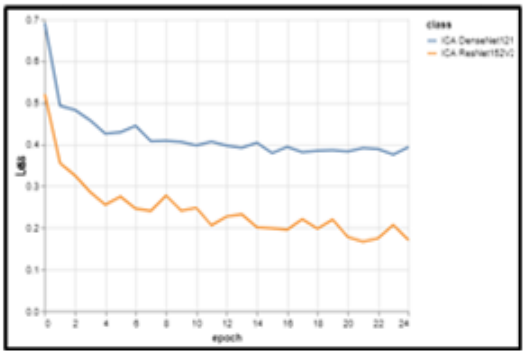

(D) Loss for 5-component ICA

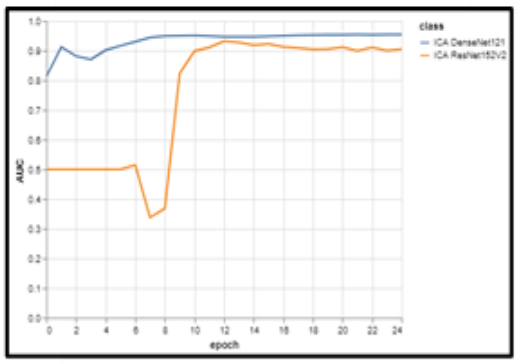

(E) AUC for 7-component ICA

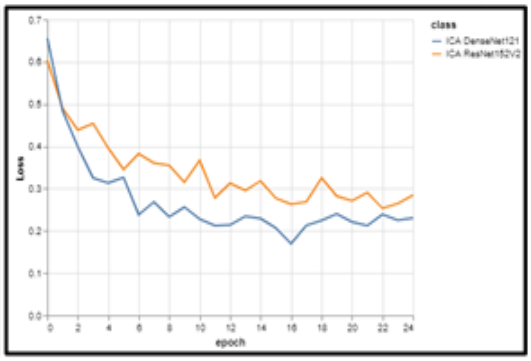

(F) Loss for 7-component ICA

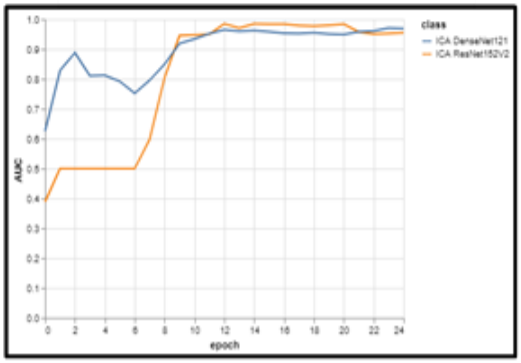

(G) AUC for 9-component ICA

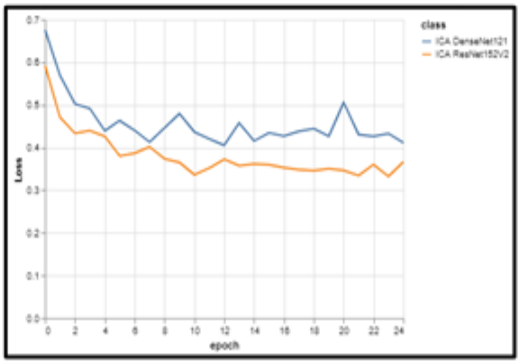

(H) Loss for 9-component ICA

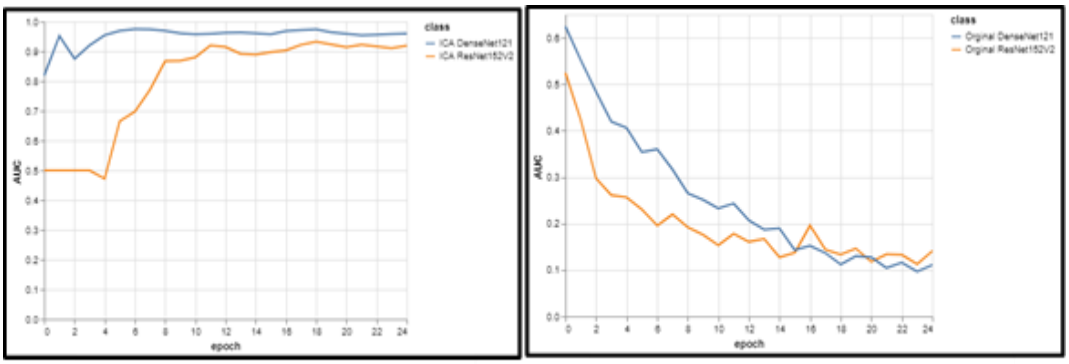

(G) AUC for 15-component ICA (H) Loss for 15-component ICA

Figure 4.4 ICA Model Analysis

4.5 Evaluate the proposed model performance

Figure. (4.5) these results are also validated using a confusion matrix of the proposed model it is important to note that no normal patients were misclassified. Where these findings demonstrate that the model can successfully differentiate between and correctly identify the two classes, i.e., Normal versus COVID-19.

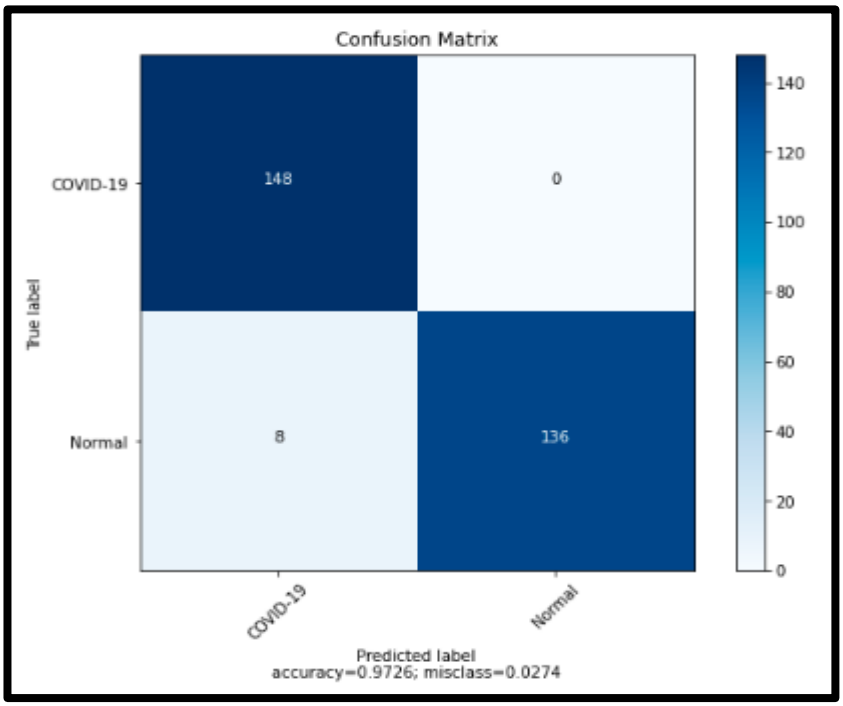

Figure 4.5 Confusion Matrix of Normal positive and Covid-19 patients

Table (4.4) below shows the ResNet152V2 results have significantly improved thanks to the fuzzy logic filter. As opposed to that, fuzzy logic filters reduce the AUC of DenseNet121. The use of the ICA filter surpassed the use of the fuzzy filter in all experiments.

Table (4.4) Comparison results between the uses of images with each technique separately

Model1	Analysis	ResNet152V2	DenseNet121
Fuzzy Logic	Accuracy	0.84	0.95
	AUC	0.92	0.99
	Precision	0.77	0.94
	Loss	0.41	0.25
ICA	Accuracy	0.91	0.97
	AUC	0.91	0.97
	Precision	0.89	0.94
	Loss	0.24	0.24
Original Dataset	Accuracy	0.90	0.96
	AUC	0.90	0.96
	Precision	0.97	0.97
	Loss	0.14	0.17

A higher AUC in each cases of the (fuzzy logic and ICA) filter was obtained. Therefore, it is simple to draw the conclusion that (the fuzzy logic and ICA) technique helps predict whether COVID-19 will be positive or negative. Figure (4.6) (a) and (b) present the AUC and loss by an epoch of the best input models.

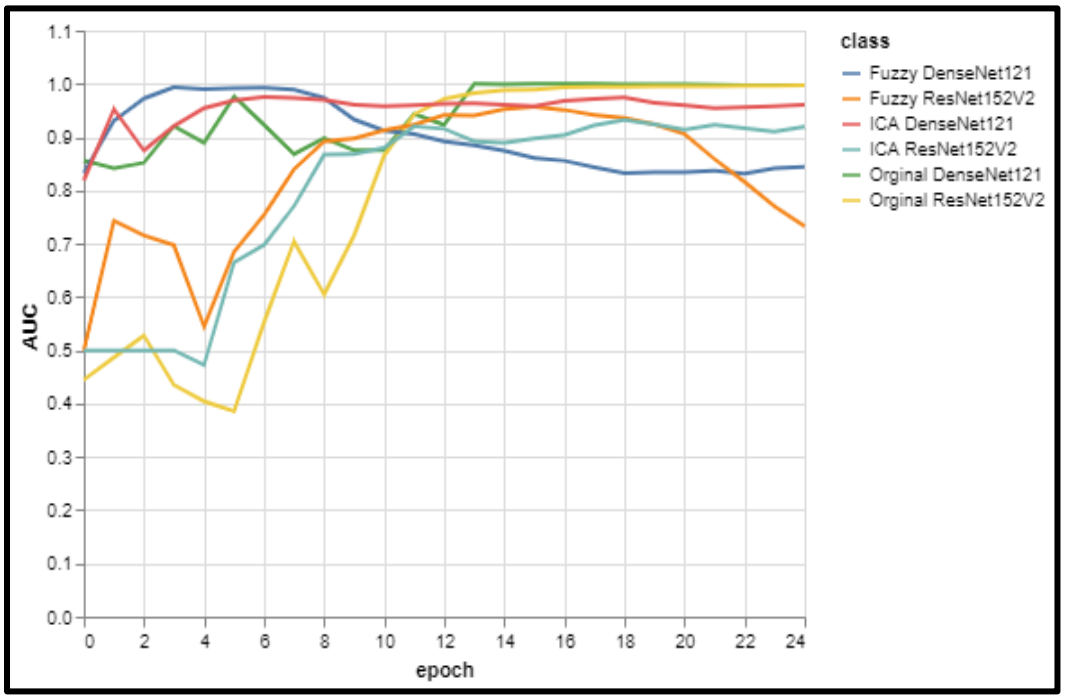

(a)

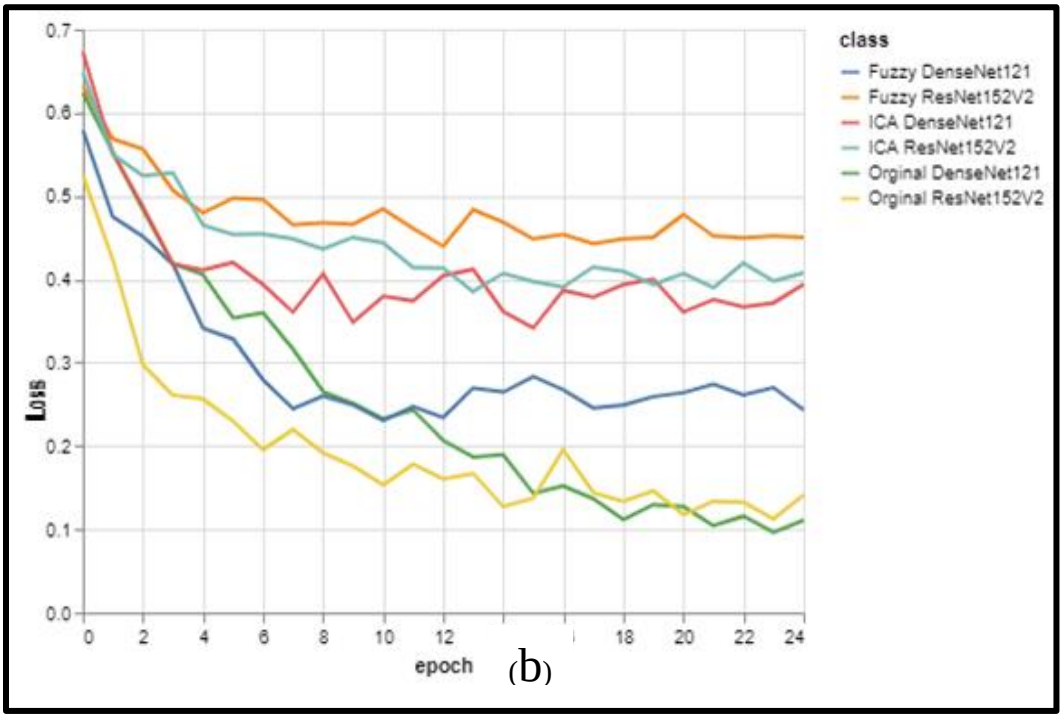

(b)

Figure 4.6 Comparative of AUC and Loss by epoch results

Table 4.5 shows that among these six deep learning CNN, InceptionV3, EfficientNetB3, ResNet152V2, DenseNet121, Xception, and VGG16 models with enhancing techniques for the combination of (Fuzzy logic and ICA-DR) InceptionV3 outperforms the others with the highest test accuracy of 97%. It attains precision and recall at 92% and 92.75%, respectively, while the AUC is 99%. On the other hand, EfficientNetB3 provided an accuracy of 93%, a precision of 91%, a recall of 94%, and the AUC is recorded as 98%.25 epochs were used to run these tests.

Table 4.5 Results of experiment input classification with the combination of (Fuzzy logic and ICA-DR).

Exp	Model	Accuracy	AUC	Precision	Recall
0	VGG16	0.88	0.96	1.00	0.77
1	ResNet152V2	0.84	0.94	0.76	1.00
2	InceptionV3	0.97	0.99	0.97	0.97
3	Xception	0.93	0.97	0.89	0.97
4	DenseNet121	0.90	0.95	0.93	0.86
5	EfficientNetB3	0.93	0.99	0.91	0.94

Figure (4.7) (a) Shows the AUC results of experiment input classification models with the combination of (Fuzzy logic and ICA-DR) technique. Figure (4.7) (b) presents the Loss Results of these experiments for each model.

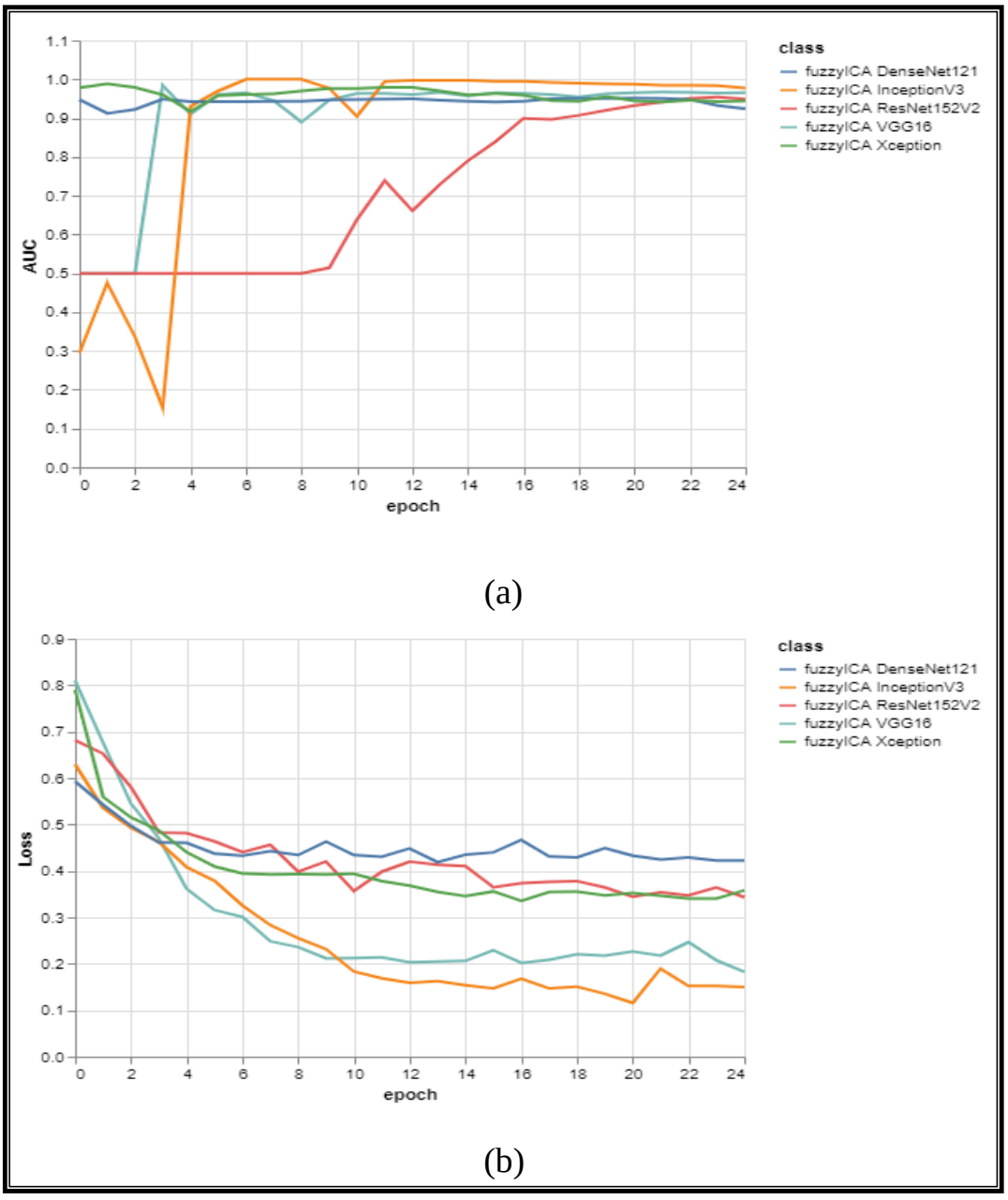

Figure 4.7 Fuzzy_ICA classification model

Table 4.6 shows the comparison of the results of proposed enhancing techniques between CNN networks. Except for the VGG16 and DenseNet121 models. Results of the proposed technique using the proposed combination enhancing techniques

between CNN networks. Are presented in Table 4.6. This proposed technique significantly improves the results of these two models. According to Table 4.6, InceptionV3 attains the highest test AUC of 97%, while the precision, accuracy, and recall are 97%, and spend less than 25 seconds for training. Among the other models, EfficientNetB3 performs better than VGG16, ResNet152V2, Xception, and DenseNet121 and attains an accuracy of 93%, a value of precision is 91%, 25 seconds for training, and an AUC is 99%. The use of the fuzzy logic and ICA surpassed the use of the original dataset directly in some experiments Figure (4.10) (a) presents the AUC by an epoch of the better model results. Figure (4.10) (b) presents the loss by an epoch of the better model results. And it shows the comparison with and without the proposed enhancing technique. Based on which best results are AUC and loss for both methods.

Table 4.6 Results of experiment input classification with and without enhancing technique

		With enhancing technique				Without enhancing technique (Original Dataset)			
No.	**Model (DL)**	**Acc**	**AUC**	**Prec**	**Recall**	**Acc**	**AUC**	**Prec**	**Recall**
1	**VGG16**	0.88	0.96	1.00	0.77	0.95	0.98	0.94	0.97
2	**ResNet152V2**	0.84	0.94	0.76	1.00	0.95	1.00	0.92	1.00
3	**InceptionV3**	0.97	0.99	0.97	0.97	0.94	0.99	0.90	1.00
4	**Xception**	0.93	0.97	0.89	0.97	0.94	0.98	0.92	0.97
5	**DenseNet121**	0.90	0.95	0.93	0.86	0.97	0.98	0.97	0.97
6	**EfficientNetB3**	0.93	0.99	0.91	0.94	0.87	0.96	0.88	0.86

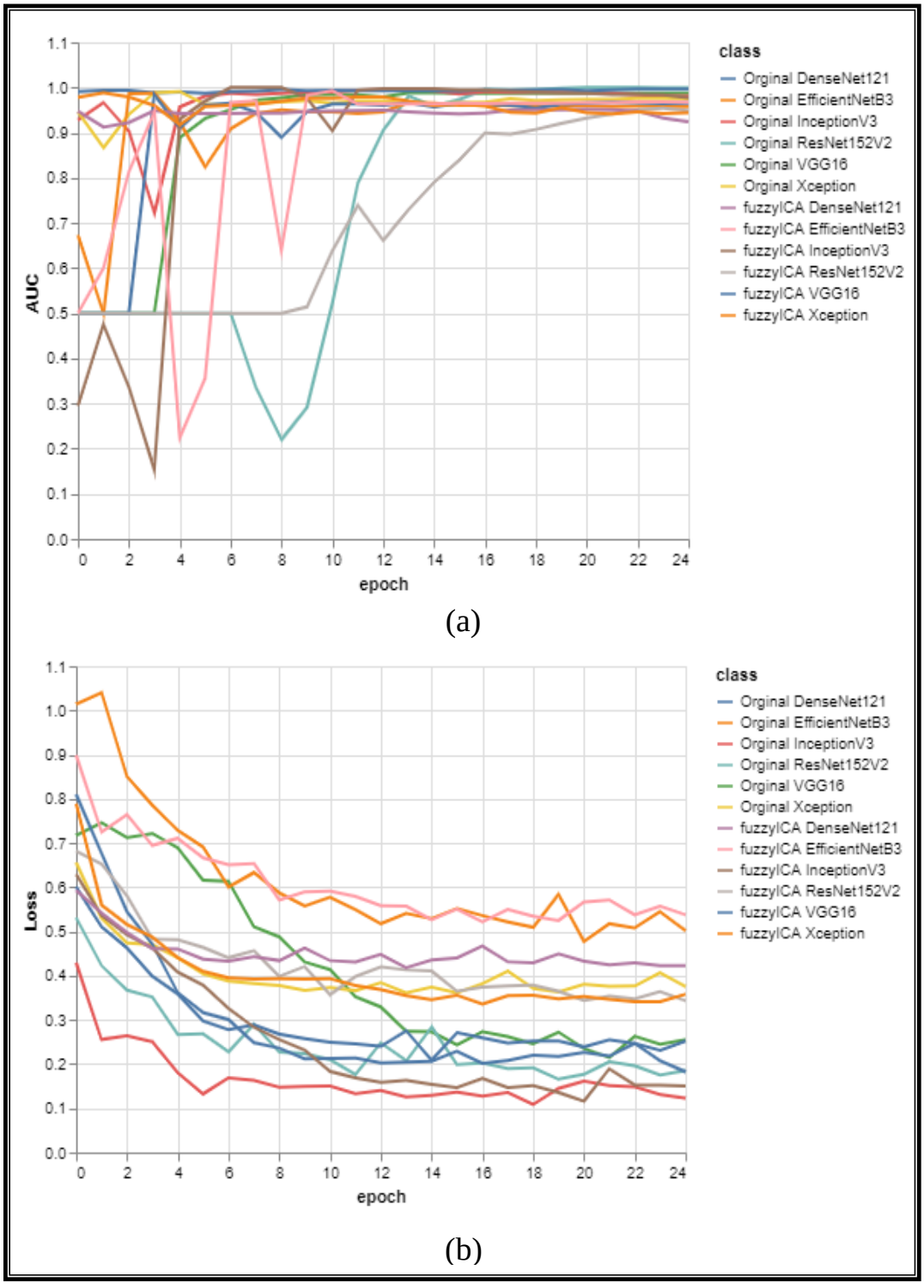

Figure 4.8 AUC and Loss by epoch results with and without use of (Fuzzy logic and ICA-DR) technique

Figure 4.10 shows the performance of a classification proposed model for all classification thresholds.

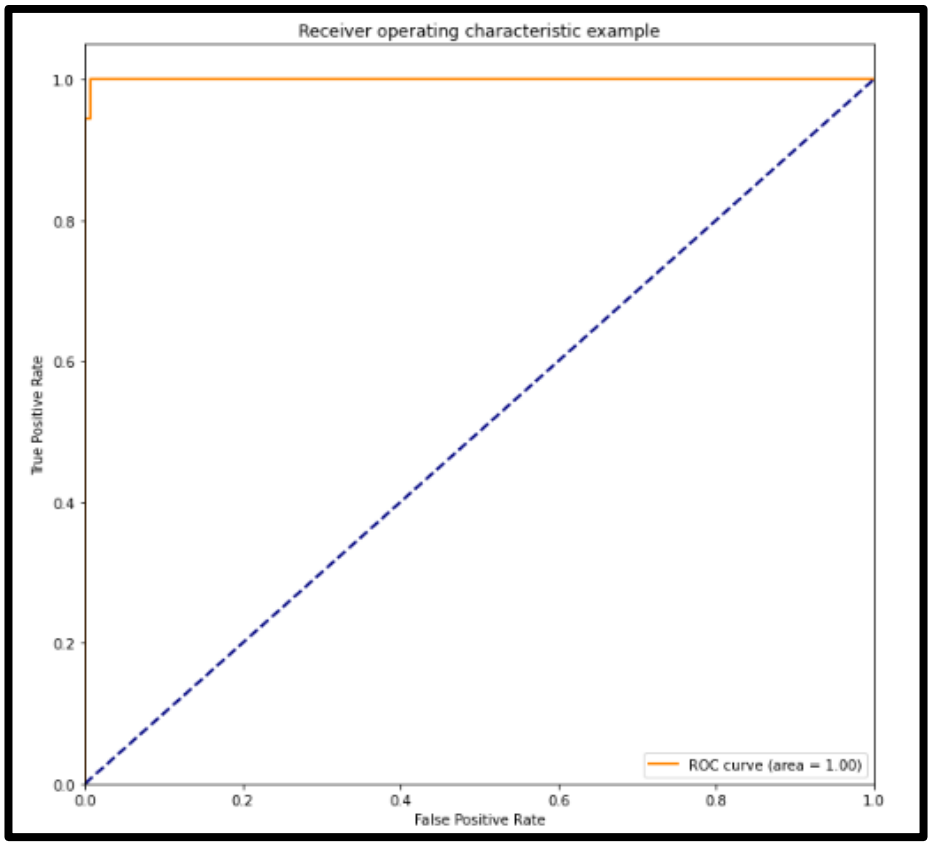

Figure. 4.9 ROC curve of a classification model

In this study has a more significant AUC value than the research presented in the literature review. A practical diagnostic mechanism was introduced, through the use of mni-computers that work as low cost server. In contrast to the rest of the other research, which was limited to theoretical performance. Wang et al. show an AUC value of 93%. Babu Karthik et al. obtained a high degree of accuracy (98.8 %). (98.8%). Ozturlet et al. 98.1 % and 87.0 % accuracy in binary classification.

However, the given solution must be validated in a more extensive sample set and clinical tests before using it in the clinical environment. The AUC and precision outcomes are enhanced by fuzzy logic and ICA.

CHAPTER FIVE

Conclusions and Future Works

5.1 Conclusion

The Coronavirus infection has spread quickly and continues to pose a threat to the lives of a lot of people. This prompted researchers to rush towards developing solutions for early diagnosis of Covid-19 patients because early detection of this type of epidemic is vital to treat and control the disease. In this research:

1- A fast and precise diagnosis strategy based on the patient's CXR images results was presented.

2- Prove that the technique for each of fuzzy logic and ICA, helps achieve very high accuracy for enhancing COVID-19 detection.

3- Using transfer learning and benefiting from pre-trained models.

4- The ability of Raspberry Pi work as a low cost server with high performance in diagnostics through a graphic user interface that is easy to use by the patient.

5- Using IOT technique for uploading the images to the cloud for the verification purpose then sent confirmation state to the patient .With the possibility record of counting the number of people infected with Coronavirus disease periodically for statistical purposes.

6- The aim of this project is to provide assistance to the radiologist during the epidemic period, as it helps in the early important initial diagnosis of the Coronavirus.

7- Despite the high results obtained, this does not mean that the project is ready for production, especially in light of the limited number of COVID-19 case photos that are currently available.

5.2 Future works

Regarding future work, the obtained results by fuzzy logic and ICA are very encouraging to design and implement a network of servers in the future distributed in health places within cities and villages, to help in the diagnosis while maintaining the property of social distancing as shown in Figure (5.1).

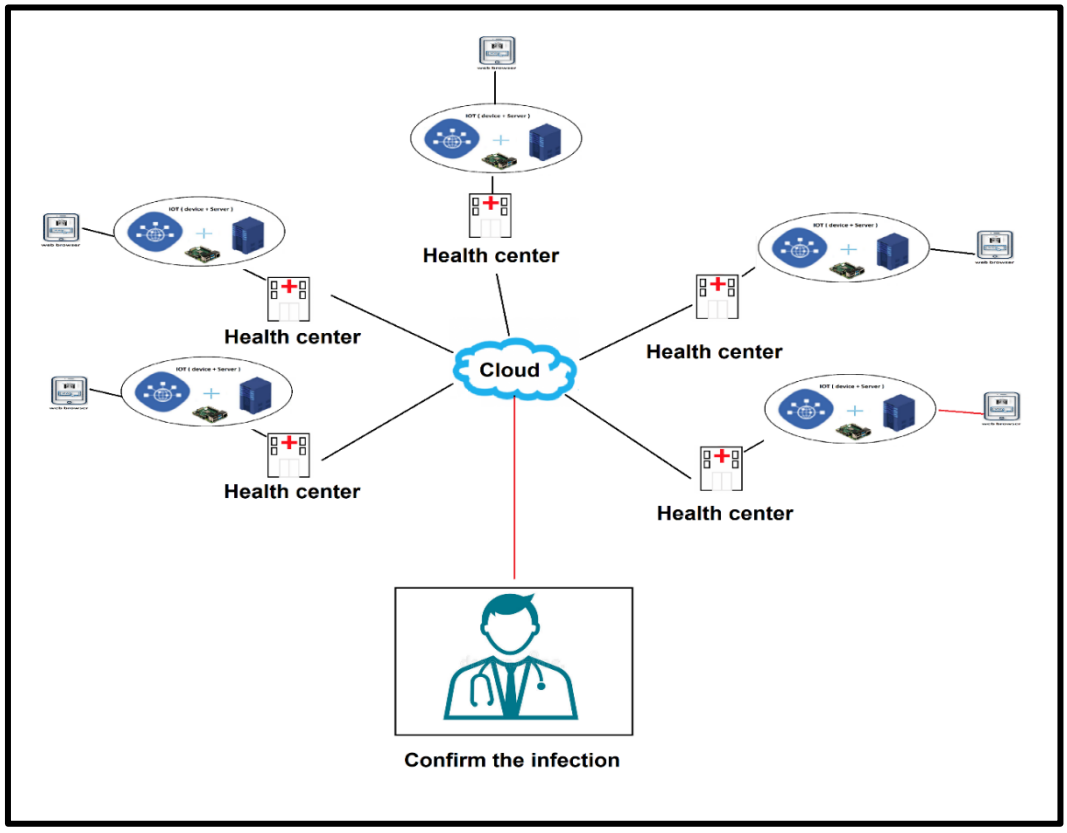

Figure 5.1 Future work of Covid-19 Early Diagnostic System.

In the future, designing an ICA algorithm that works for Rib Suppression in Chest Radiographs to get a more accurate covid-19 diagnosis system as shown in Figure (5.2). After it showed that the purpose of the ICA in this research is to reduce noise in the chest x-ray image.

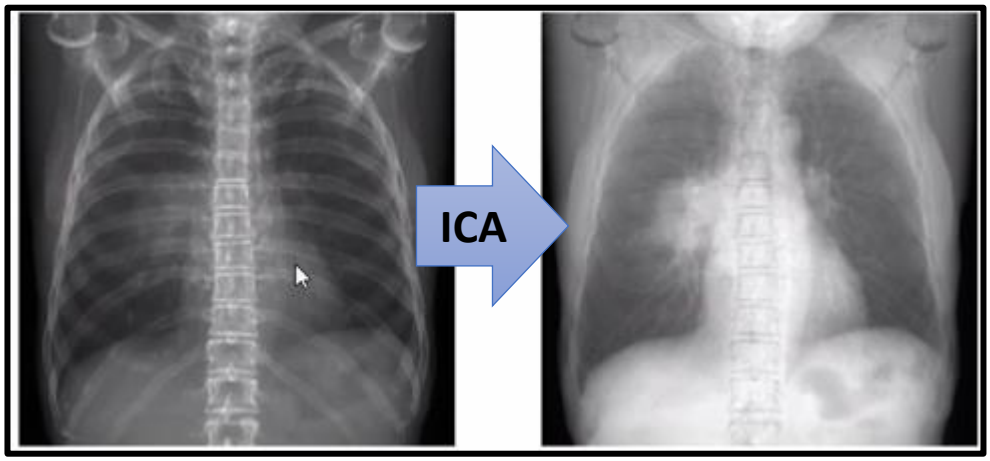

Figure 5.2 Future work of Rib bone Suppression using ICA.

5.3 Drawbacks

From the obtained results and specially ICA (FastICA) algorithm is not the most suitable algorithm to deal with the (Gaussian) signals. The algorithms are limited to deal with the problem of linear mixed signals only and not suitable for nonlinear mixed signal.

References

[1] Cozzi, D., Cavigli, E., Moroni, C., Smorchkova, O., Zantonelli, G., Pradella, S., & Miele, V. (2021). Ground-glass opacity (GGO): a review of the differential diagnosis in the era of COVID-19. Japanese journal of radiology, 39(8), 721-732.

[2] Waheed, A., Goyal, M., Gupta, D., Khanna, A., Al-Turjman, F., & Pinheiro, P. R. (2020). Covidgan: data augmentation using auxiliary classifier gan for improved covid-19 detection. Ieee Access, 8, 91916-91923.

[3] Abdel-Basset, M., Mohamed, R., Elhoseny, M., Chakrabortty, R. K., & Ryan, M. (2020). A hybrid COVID-19 detection model using an improved marine predators algorithm and a ranking-based diversity reduction strategy. IEEE access, 8, 79521-79540.

[4] Mohammedqasim, H., & Ata, O. (2022). Real-time data of COVID-19 detection with IoT sensor tracking using artificial neural network. Computers and Electrical Engineering, 100, 107971.

[5] Ng, H. P., Ong, S. H., Foong, K. W. C., Goh, P. S., & Nowinski, W. L. (2006, March). Medical image segmentation using k-means clustering and improved watershed algorithm. In 2006 IEEE southwest symposium on image analysis and interpretation (pp. 61-65). IEEE.

[6] Chouhan, V., Singh, S. K., Khamparia, A., Gupta, D., Tiwari, P., Moreira, C., ... & De Albuquerque, V. H. C. (2020). A novel transfer learning based approach for pneumonia detection in chest X-ray images. Applied Sciences, 10(2), 559.

[7] Ohata, E. F., Bezerra, G. M., das Chagas, J. V. S., Neto, A. V. L., Albuquerque, A. B., de Albuquerque, V. H. C., & Reboucas Filho, P. P. (2020). Automatic detection of COVID-19 infection using chest X-ray images through transfer learning. IEEE/CAA Journal of Automatica Sinica, 8(1), 239-248.

[8] Dourado, C. M., da Silva, S. P. P., da Nobrega, R. V. M., Reboucas Filho, P. P., Muhammad, K., & de Albuquerque, V. H. C. (2020). An open IoHT-based deep learning framework for online medical image recognition. IEEE Journal on Selected Areas in Communications, 39(2), 541-548.

[9] Ding, W., Abdel-Basset, M., Eldrandaly, K. A., Abdel-Fatah, L., & De Albuquerque, V. H. C. (2020). Smart supervision of cardiomyopathy based on fuzzy Harris Hawks optimizer and wearable sensing data optimization: a new model. IEEE Transactions on Cybernetics, 51(10), 4944-4958.

[10] de Souza, R. W. R., De Oliveira, J. V. C., Passos, L. A., Ding, W., Papa, J. P., & de Albuquerque, V. H. C. (2019). A novel approach for optimum-path forest classification using fuzzy logic. IEEE Transactions on Fuzzy Systems, 28(12), 3076-3086.

[11] Singh, H., Gupta, M. M., Meitzler, T., Hou, Z. G., Garg, K. K., Solo, A. M., & Zadeh, L. A. (2013). Real-life applications of fuzzy logic. Advances in Fuzzy Systems, 2013.

[12] Li, D., Zhao, J., Liu, H., & Hao, D. (2014). The application of FastICA combined with related function in blind signal separation. Mathematical Problems in Engineering, 2014.

[13] Ashtiyani, M., Asadi, S., & Birgani, P. M. (2008, April). ICA-based EEG classification using fuzzy c-mean algorithm. In 2008 3rd International Conference on Information and Communication Technologies: From Theory to Applications (pp. 1-5). IEEE.

[14] Boudrioua, M. S. (2020). COVID-19 detection from chest X-ray images using CNNs models: Further evidence from Deep Transfer Learning. Boudrioua, Mohamed Samir (2020)" COVID-19 Detection from Chest X-ray Images using CNNs Models: Further Evidence from Deep Transfer Learning," The University of Louisville Journal of Respiratory Infections, 4(1).

[15] Ozturk, T., Talo, M., Yildirim, E. A., Baloglu, U. B., Yildirim, O., & Acharya, U. R. (2020). Automated detection of COVID-19 cases using deep neural networks with X-ray images. Computers in biology and medicine, 121, 103792.

[16] Khan, A. I., Shah, J. L., & Bhat, M. M. (2020). CoroNet: A deep neural network for detection and diagnosis of COVID-19 from chest x-ray images. Computer methods and programs in biomedicine, 196, 105581.

[17] Wang, L., Lin, Z. Q., & Wong, A. (2020). Covid-net: A tailored deep convolutional neural network design for detection of covid-19 cases from chest x-ray images. Scientific Reports, 10(1), 1-12.

[18] Marques, G., Agarwal, D., & de la Torre Díez, I. (2020). Automated medical diagnosis of COVID-19 through EfficientNet convolutional neural network. Applied soft computing, 96, 106691.

[19] Ezzat, D., Hassanien, A. E., & Ella, H. A. (2021). An optimized deep learning architecture for the diagnosis of COVID-19 disease based on gravitational search optimization. Applied Soft Computing, 98, 106742.

[20] Babukarthik, R. G., Adiga, V. A. K., Sambasivam, G., Chandramohan, D., & Amudhavel, J. (2020). Prediction of COVID-19 using genetic deep learning convolutional neural network (GDCNN). Ieee Access, 8, 177647-177666.

[21] Minaee, S., Kafieh, R., Sonka, M., Yazdani, S., & Soufi, G. J. (2020). Deep-COVID: Predicting COVID-19 from chest X-ray images using deep transfer learning. Medical image analysis, 65, 101794.

[22] Umer, M., Ashraf, I., Ullah, S., Mehmood, A., & Choi, G. S. (2022). COVINet: A convolutional neural network approach for predicting COVID-19 from chest X-ray images. Journal of Ambient Intelligence and Humanized Computing, 13(1), 535-547.

[23] Keles, A., Keles, M. B., & Keles, A. (2021). COV19-CNNet and COV19-ResNet: diagnostic inference Engines for early detection of COVID-19. Cognitive Computation, 1-11.

[24] Li, K., Fang, Y., Li, W., Pan, C., Qin, P., Zhong, Y., ... & Li, S. (2020). CT image visual quantitative evaluation and clinical classification of coronavirus disease (COVID-19). European radiology, 30(8), 4407-4416.

[25] Cucinotta, D., & Vanelli, M. (2020). WHO declares COVID-19 a pandemic. Acta Bio Medica: Atenei Parmensis, 91(1), 157.

[26] Ieracitano, C., Mammone, N., Versaci, M., Varone, G., Ali, A. R., Armentano, A., ... & Morabito, F. C. (2022). A fuzzy-enhanced deep learning approach for early detection of Covid-19 pneumonia from portable chest X-ray images. Neurocomputing, 481, 202-215.

[27] Lauer, S. A., Grantz, K. H., Bi, Q., Jones, F. K., Zheng, Q., Meredith, H. R., ... & Lessler, J. (2020). The incubation period of coronavirus disease 2019 (COVID-19) from publicly reported confirmed cases: estimation and application. Annals of internal medicine, 172(9), 577-582.

[28] Phua, J., Weng, L., Ling, L., Egi, M., Lim, C. M., Divatia, J. V., ... & Asian Critical Care Clinical Trials Group. (2020). Intensive care management of coronavirus disease 2019 (COVID-19): challenges and recommendations. The lancet respiratory medicine, 8(5), 506-517.

[29] Wong, H. Y. F., Lam, H. Y. S., Fong, A. H. T., Leung, S. T., Chin, T. W. Y., Lo, C. S. Y., ... & Ng, M. Y. (2020). Frequency and distribution of chest radiographic findings in COVID-19 positive patients. Radiology.

[30] Varela-Santos, S., & Melin, P. (2021). A new approach for classifying coronavirus COVID-19 based on its manifestation on chest X-rays using texture features and neural networks. Information sciences, 545, 403-414.

[31] Bertone, E., Luna Juncal, M. J., Prado Umeno, R. K., Peixoto, D. A., Nguyen, K., & Sahin, O. (2020). Effectiveness of the early response to COVID-19: Data analysis and modelling. Systems, 8(2), 21.

[32] Aydin, N., & Yurdakul, G. (2020). Assessing countries' performances against COVID-19 via WSIDEA and machine learning algorithms. Applied Soft Computing, 97, 106792.

[33] Gayathri, G. V., & Satapathy, S. C. (2020). A Survey on techniques for prediction of asthma. In Smart Intelligent Computing and Applications (pp. 751-758). Springer, Singapore.

[34] Pegoraro, F., Santos, E. A. P., Loures, E. D. F. R., & Laus, F. W. (2020). A hybrid model to support decision making in emergency department management. Knowledge-based systems, 203, 106148.

[35] Holmes, J., Sacchi, L., & Bellazzi, R. (2004). Artificial intelligence in medicine. Ann R Coll Surg Engl, 86, 334-8.

[36] Greenhill AE, B. . A Primer of AI in Medicine. Techniques in Gastrointestinal Endoscopy. Epub 2019

[37] Malik, P., Pathania, M., & Rathaur, V. K. (2019). Overview of artificial intelligence in medicine. Journal of family medicine and primary care, 8(7), 2328.

[38] Hamet, P., & Tremblay, J. (2017). Artificial intelligence in medicine. Metabolism, 69, S36-S40.

[39] Hoogenboom, S. A., Bagci, U., & Wallace, M. B. (2020). Artificial intelligence in gastroenterology. The current state of play and the potential. How will it affect our practice and when?. Techniques and Innovations in Gastrointestinal Endoscopy, 22(2), 42-47.

[40] Le Berre, C., Sandborn, W. J., Aridhi, S., Devignes, M. D., Fournier, L., Smail-Tabbone, M., ... & Peyrin-Biroulet, L. (2020). Application of artificial intelligence to gastroenterology and hepatology. Gastroenterology, 158(1), 76-94.

[41] Miller, D. D., & Brown, E. W. (2018). Artificial intelligence in medical practice: the question to the answer?. The American journal of medicine, 131(2), 129-133.

[42] Yu, K. H., Beam, A. L., & Kohane, I. S. (2018). Artificial intelligence in healthcare. Nature biomedical engineering, 2(10), 719-731.

[43] Albahri, A. S., Hamid, R. A., Al-qays, Z. T., Zaidan, A. A., Zaidan, B. B., Albahri, A. O., ... & Madhloom, H. T. (2020). Role of biological data mining and machine learning techniques in detecting and diagnosing the novel coronavirus (COVID-19): a systematic review. Journal of medical systems, 44(7), 1-11.

[44] Yang, Z., Zeng, Z., Wang, K., Wong, S. S., Liang, W., Zanin, M., ... & He, J. (2020). Modified SEIR and AI prediction of the epidemics trend of COVID-19 in China under public health interventions. Journal of thoracic disease, 12(3), 165.

[45] Shi, F., Wang, J., Shi, J., Wu, Z., Wang, Q., Tang, Z., ... & Shen, D. (2020). Review of artificial intelligence techniques in imaging data acquisition, segmentation, and diagnosis for COVID-19. IEEE reviews in biomedical engineering, 14, 4-15.

[46] Alsalem, M. A., Zaidan, A. A., Zaidan, B. B., Hashim, M., Albahri, O. S., Albahri, A. S., ... & Mohammed, K. I. (2018). Systematic review of an automated multiclass detection and classification system for acute Leukaemia in terms of evaluation and benchmarking, open challenges, issues and methodological aspects. Journal of medical systems, 42(11), 1-36.

[47] Alsalem, M. A., Zaidan, A. A., Zaidan, B. B., Albahri, O. S., Alamoodi, A. H., Albahri, A. S., ... & Mohammed, K. I. (2019). Multiclass benchmarking framework for automated acute Leukaemia detection and classification based on BWM and group-VIKOR. Journal of medical systems, 43(7), 1-32.

[48] Zaidan, A. A., Zaidan, B. B., Alsalem, M. A., Albahri, O. S., Albahri, A. S., & Qahtan, M. Y. (2020). Multi-agent learning neural network and Bayesian model for real-time IoT skin detectors: a new evaluation and benchmarking methodology. Neural Computing and Applications, 32(12), 8315-8366.

[49] Zaidan, A. A., Zaidan, B. B., Albahri, O. S., Alsalem, M. A., Albahri, A. S., Yas, Q. M., & Hashim, M. (2018). A review on smartphone skin cancer diagnosis apps in evaluation and benchmarking: coherent taxonomy, open issues and recommendation pathway solution. Health and Technology, 8(4), 223-238.

[50] Aminian, A., Safari, S., Razeghian-Jahromi, A., Ghorbani, M., & Delaney, C. P. (2020). COVID-19 outbreak and surgical practice: unexpected fatality in perioperative period. Annals of surgery.

[51] Haleem, A., Vaishya, R., Javaid, M., & Khan, I. H. (2020). Artificial Intelligence (AI) applications in orthopaedics: an innovative technology to embrace. Journal of clinical orthopaedics and trauma, 11(Suppl 1), S80.

[52] Biswas, K., & Sen, P. (2020). Space-time dependence of corona virus (COVID-19) outbreak. arXiv preprint arXiv:2003.03149.

[53] Stebbing, J., Phelan, A., Griffin, I., Tucker, C., Oechsle, O., Smith, D., & Richardson, P. (2020). COVID-19: combining antiviral and anti-inflammatory treatments. The Lancet Infectious Diseases, 20(4), 400-402.

[54] Sohrabi, C., Alsafi, Z., O'neill, N., Khan, M., Kerwan, A., Al-Jabir, A., ... & Agha, R. (2020). World Health Organization declares global emergency: A review of the 2019 novel coronavirus (COVID-19). International journal of surgery, 76, 71-76.

[55] Chen, S., Yang, J., Yang, W., Wang, C., & Bärnighausen, T. (2020). COVID-19 control in China during mass population movements at New Year. The Lancet, 395(10226), 764-766.

[56] Panesar, A. (2019). Machine learning and AI for healthcare (pp. 1-73). Coventry, UK: Apress.

[57] Kumar, Y., Koul, A., Singla, R., & Ijaz, M. F. (2022). Artificial intelligence in disease diagnosis: a systematic literature review, synthesizing framework and future research agenda. Journal of Ambient Intelligence and Humanized Computing, 1-28.

[58] Vamathevan, J., Clark, D., Czodrowski, P., Dunham, I., Ferran, E., Lee, G., ... & Zhao, S. (2019). Applicationsof machine learning in drug discovery and development. Nature reviews Drug discovery, 18(6), 463-477.

[59] Cammarota, G., Ianiro, G., Ahern, A., Carbone, C., Temko, A., Claesson, M. J., ... & Tortora, G. (2020). Gut microbiome, big data and machine learning to promote precision medicine for cancer. Nature reviews gastroenterology & hepatology, 17(10), 635-648.

[60] Sanil, H. S., Singh, D., Raj, K. B., Choubey, S., Bhasin, N. K. K., Yadav, R., & Gulati, K. (2021). Role of machine learning in changing social and

business eco-system–a qualitative study to explore the factors contributing to competitive advantage during COVID pandemic. World Journal of Engineering.

[61] Rustam, F., Reshi, A. A., Mehmood, A., Ullah, S., On, B. W., Aslam, W., & Choi, G. S. (2020). COVID-19 future forecasting using supervised machine learning models. IEEE access, 8, 101489-101499.

[62] Dey, A. K., Sharma, M., & Meshram, M. R. (2016). Image processing based leaf rot disease, detection of betel vine (Piper BetleL.). Procedia Computer Science, 85, 748-754.

[63] Kim, M., Yun, J., Cho, Y., Shin, K., Jang, R., Bae, H. J., & Kim, N. (2019). Deep learning in medical imaging. Neurospine, 16(4), 657.

[64] Nguyen, T. T. (2022). Detection of Arterial Occlusion on MRI Angiography of the Lower Limbs using Deep Learning.

[65] Santosh, K. C. (2020). AI-driven tools for coronavirus outbreak: need of active learning and cross-population train/test models on multitudinal/multimodal data. Journal of medical systems, 44(5), 1-5.

[66] Qjidaa, M., Ben-Fares, A., Mechbal, Y., Amakdouf, H., Maaroufi, M., Alami, B., & Qjidaa, H. (2020, June). Development of a clinical decision support system for the early detection of COVID-19 using deep learning based on chest radiographic images. In 2020 International Conference on Intelligent Systems and Computer Vision (ISCV) (pp. 1-6). IEEE.

[67] Phankokkruad, M. (2020, July). COVID-19 pneumonia detection in chest X-ray images using transfer learning of convolutional neural networks. In Proceedings of the 3rd international conference on data science and information technology (pp. 147-152).

[68] Young, B. E., Ong, S. W. X., Kalimuddin, S., Low, J. G., Tan, S. Y., Loh, J., ... & Singapore 2019 Novel Coronavirus Outbreak Research Team. (2020). Epidemiologic features and clinical course of patients infected with SARS-CoV-2 in Singapore. Jama, 323(15), 1488-1494.

[69] Cheung, K. S., Hung, I. F., Chan, P. P., Lung, K. C., Tso, E., Liu, R., ... & Leung, W. K. (2020). Gastrointestinal manifestations of SARS-CoV-2 infection and virus load in fecal samples from a Hong Kong cohort: systematic review and meta-analysis. Gastroenterology, 159(1), 81-95.

[70] Krizhevsky, A., Sutskever, I., & Hinton, G. E. (2012). Imagenet classification with deep convolutional neural networks. Advances in neural information processing systems, 25.

[71] Sarker, I. H. (2021). Machine learning: Algorithms, real-world applications and research directions. SN Computer Science, 2(3), 1-21.

[72] Pereira, S., Pinto, A., Alves, V., & Silva, C. A. (2016). Brain tumor segmentation using convolutional neural networks in MRI images. IEEE transactions on medical imaging, 35(5), 1240-1251.

[73] Fan, C., Chen, M., Wang, X., Wang, J., & Huang, B. (2021). A review on data preprocessing techniques toward efficient and reliable knowledge discovery from building operational data. Frontiers in Energy Research, 9, 652801.

[74] Fan, C., Xiao, F., & Yan, C. (2015). A framework for knowledge discovery in massive building automation data and its application in building diagnostics. Automation in Construction, 50, 81-90.

[75] Fan, C., Xiao, F., Madsen, H., & Wang, D. (2015). Temporal knowledge discovery in big BAS data for building energy management. Energy and Buildings, 109, 75-89.

[76] Khorram, S., Nelson, S. A., Cakir, H., & van der Wiele, C. F. (2013). Digital image acquisition: preprocessing and data reduction. In Handbook of Satellite Applications (pp. 809-837). Springer, New York, NY.

[77] Cho, E., Chang, T. W., & Hwang, G. (2022). Data Preprocessing Combination to Improve the Performance of Quality Classification in the Manufacturing Process. Electronics, 11(3), 477.

[78] Fan, C., Sun, Y., Zhao, Y., Song, M., & Wang, J. (2019). Deep learning-based feature engineering methods for improved building energy prediction. Applied energy, 240, 35-45.

[79] Rashid, K. M., & Louis, J. (2019). Times-series data augmentation and deep learning for construction equipment activity recognition. Advanced Engineering Informatics, 42, 100944.

[80] Fouladi, S., Ebadi, M. J., Safaei, A. A., Bajuri, M. Y., & Ahmadian, A. (2021). Efficient deep neural networks for classification of COVID-19 based on CT images: Virtualization via software defined radio. Computer communications, 176, 234-248.

[81] Qu, Z., Mei, J., Liu, L., & Zhou, D. Y. (2020). Crack detection of concrete pavement with cross-entropy loss function and improved VGG16 network model. Ieee Access, 8, 54564-54573.

[82] Kristiani, E., Yang, C. T., & Huang, C. Y. (2020). iSEC: an optimized deep learning model for image classification on edge computing. IEEE Access, 8, 27267-27276.

[83] Kogilavani, S. V., Prabhu, J., Sandhiya, R., Kumar, M. S., Subramaniam, U., Karthick, A., ... & Imam, S. B. S. (2022). COVID-19 detection based on lung CTscan using deep learning techniques. Computational and Mathematical Methods in Medicine, 2022.

[84] Chollet, F. (2017). Xception: Deep learning with depthwise separable convolutions. In Proceedings of the IEEE conference on computer vision and pattern recognition (pp. 1251-1258).

[85] Huang, G., Sun, Y., Liu, Z., Sedra, D., & Weinberger, K. Q. (2016, October). Deep networks with stochastic depth. In European conference on computer vision (pp. 646-661). Springer, Cham.

[86] Tan, M., & Le, Q. (2019, May). Efficientnet: Rethinking model scaling for convolutional neural networks. In International conference on machine learning (pp. 6105-6114). PMLR.

[87] Singh, B., & Sharma, D. K. (2021). Predicting image credibility in fake news over social media using multi-modal approach. Neural Computing and Applications, 1-15.

[88] Mittal, K., Jain, A., Vaisla, K. S., Castillo, O., & Kacprzyk, J. (2020). A comprehensive review on type 2 fuzzy logic applications: Past, present and future. Engineering Applications of Artificial Intelligence, 95, 103916.

[89] Dhiman, N., & Sharma, M. K. (2019). Mediative Sugeno's-TSK fuzzy logic based screening analysis to diagnosis of heart disease. Applied Mathematics, 10(06), 448.

[90] Dhiman, N., & Sharma, M. K. (2019). Mediative multi-criteria decision support system for various alternatives based on fuzzy logic. International Journal of Recent Technology and Engineering (IJRTE), 8(4).

[91] Zadeh, L. A. (1996). Fuzzy sets. In Fuzzy sets, fuzzy logic, and fuzzy systems: selected papers by Lotfi A Zadeh (pp. 394-432).

[92] Mamdani, E. H., & Assilian, S. (1975). An experiment in linguistic synthesis with a fuzzy logic controller. International journal of man-machine studies, 7(1), 1-13.

[93] Mamdani, E. H. (1977). Application of fuzzy logic to approximate reasoning using linguistic synthesis. IEEE transactions on computers, 26(12), 1182-1191.

[94] Saaty, T. L. (2008). Decision making with the analytic hierarchy process. International journal of services sciences, 1(1), 83-98.

[95] Goddard, S. T. (1983). Ranking in tournaments and group decisionmaking. Management Science, 29(12), 1384-1392.

[96] Roy, B. (1971). Problems and methods with multiple objective functions. Mathematical programming, 1(1), 239-266.

[97] Vyas, S., Gupta, S., Bhargava, D., & Boddu, R. (2022). Fuzzy Logic System Implementation on the Performance Parameters of Health Data Management Frameworks. Journal of Healthcare Engineering, 2022.

[98] Brown, G. D., Yamada, S., & Sejnowski, T. J. (2001). Independent component analysis at the neural cocktail party. Trends in neurosciences, 24(1), 54-63.

[99] Stone, J. V. (2002). Independent component analysis: an introduction. Trends in cognitive sciences, 6(2), 59-64.

[100] Lee, T. W., Girolami, M., & Sejnowski, T. J. (1999). Independent component analysis using an extended infomax algorithm for mixed subgaussian and supergaussian sources. Neural computation, 11(2), 417-441.

[101] Jung, T. P., Makeig, S., McKeown, M. J., Bell, A. J., Lee, T. W., & Sejnowski, T. J. (2001). Imaging brain dynamics using independent component analysis. Proceedings of the IEEE, 89(7), 1107-1122.

[102] McKeown, M. J., Makeig, S., Brown, G. G., Jung, T. P., Kindermann, S. S., Bell, A. J., & Sejnowski, T. J. (1998). Analysis of fMRI data by blind separation into independent spatial components. Human brain mapping, 6(3), 160-188.

[103] Rasheed, T., Ahmed, B., Khan, M. A., Bettayeb, M., Lee, S., & Kim, T. S. (2007, February). Rib suppression in frontal chest radiographs: A blind source separation approach. In 2007 9th International Symposium on Signal Processing and Its Applications (pp. 1-4). IEEE.

[104] Hyvärinen, A., & Oja, E. (2000). Independent component analysis: algorithms and applications. Neural networks, 13(4-5), 411-430.

[105] Herault, J., & Jutten, C. (1986, August). Space or time adaptive signal processing by neural network models. In AIP conference proceedings (Vol. 151, No. 1, pp. 206-211). American Institute of Physics.

[106] Gao, B. (2011). Single channel blind source separation (Doctoral dissertation, Newcastle University).

[107] Lopez-Molina, C., Bustince, H., Fernandez, J., & De Baets, B. (2011, August). Generation of fuzzy edge images using trapezoidal membership functions. In Proceedings of the 7th conference of the European Society for Fuzzy Logic and Technology (pp. 327-333). Atlantis Press.

[108] Kumar, E. B., & Sundaresan, M. (2014, March). Edge detection using trapezoidal membership function based on fuzzy's mamdani inference system. In 2014 International Conference on Computing for Sustainable Global Development (INDIACom) (pp. 515-518). IEEE.

[109] Vatti, N. R., Vatti, P. L., Vatti, R., & Garde, C. (2018). 2018 International Conference on Current Trends towards Converging Technologies (ICCTCT).

[110] Wang, J., & Chang, C. I. (2006). Independent component analysis-based dimensionality reduction with applications in hyperspectral image analysis. IEEE transactions on geoscience and remote sensing, 44(6), 1586-1600.

[111] Chow, L. S., & Rajagopal, H. (2017). Modified-BRISQUE as no reference image quality assessment for structural MR images. Magnetic resonance imaging, 43, 74-87.

[112] Abadi, M., Barham, P., Chen, J., Chen, Z., Davis, A., Dean, J., ... & Zheng, X. (2016). {TensorFlow}: a system for {Large-Scale} machine learning. In 12th USENIX symposium on operating systems design and implementation (OSDI 16) (pp. 265-283).

[113] Grinberg, M. (2018). Flask web development: developing web applications with python. " O'Reilly Media, Inc.".

[114] Sewak, M., Karim, M. R., & Pujari, P. (2018). Practical convolutional neural networks: implement advanced deep learning models using Python. Packt Publishing Ltd.

[115] Norris, D. J. (2017). Beginning artificial intelligence with the Raspberry Pi (pp. 1-369). Apress.

[116] A. Holzinger Biomedical informatics: discovering knowledge in big data Springer (2014)

[117] Birnbaum, Z. W. (1956, January). On a use of the Mann-Whitney statistic. In Proceedings of the third Berkeley symposium on mathematical statistics and probability (Vol. 1, pp. 13-17). Berkeley, CA, USA: University of California Press.

[118] Popovic, A., De la Fuente, M., Engelhardt, M., & Radermacher, K. (2007). Statistical validation metric for accuracy assessment in medical image segmentation. International Journal of Computer Assisted Radiology and Surgery, 2(3), 169-181.

[119] Park, S. H., Goo, J. M., & Jo, C. H. (2004). Receiver operating characteristic (ROC) curve: practical review for radiologists. Korean journal of radiology, 5(1), 11-18.

Appendix A

Appendix A: Python Software Implementation

#Function to install library

```
def install(api):
    import sys
    import subprocess
    import pkg_resources

    required = {api}
    installed = {pkg.key for pkg in pkg_resources.working_set}
    missing = required - installed
    if missing:
        !pip install -U $api
```

#Read test images

```
## Read test images

test_images=[]

import glob, os
os.chdir("/kaggle/input/coronahack-chest-xraydataset/Coronahack-Chest-XRay-Dataset/Coronahack-Chest-XRay-Dataset/test/")
for file in glob.glob("*.jpeg"):
    test_images.append(file)


test_images2=[]
import glob, os
os.chdir("/kaggle/input/covid-19-x-ray-10000-images/dataset/covid")
for file in glob.glob("*.jpeg"):
    test_images2.append(file)

test_images_normal=[]
import glob, os
os.chdir("/kaggle/input/covid-19-x-ray-10000-images/dataset/normal")
for file in glob.glob("*.jpeg"):
    test_images_normal.append(file)
```

#Install Fuzzy Library

```
install('scikit-fuzzy')

import skfuzzy as fuzz
```

```
Collecting scikit-fuzzy
  Downloading scikit-fuzzy-0.4.2.tar.gz (993 kB)
     ━━━━━━━━━━━━━━━━━━━━━━━━━━━━━━━━━━━━━━━━ 994.0/994.0 kB 3.4 MB/s eta 0:00:0000:0100:01
  Preparing metadata (setup.py) ... done
Requirement already satisfied: numpy>=1.6.0 in /opt/conda/lib/python3.7/site-packages (from scikit-fuzzy) (1.21.6)
Requirement already satisfied: scipy>=0.9.0 in /opt/conda/lib/python3.7/site-packages (from scikit-fuzzy) (1.7.3)
Requirement already satisfied: networkx>=1.9.0 in /opt/conda/lib/python3.7/site-packages (from scikit-fuzzy) (2.5)
Requirement already satisfied: decorator>=4.3.0 in /opt/conda/lib/python3.7/site-packages (from networkx>=1.9.0->scikit-fuzzy) (5.1.1)
Building wheels for collected packages: scikit-fuzzy
  Building wheel for scikit-fuzzy (setup.py) ... done
  Created wheel for scikit-fuzzy: filename=scikit_fuzzy-0.4.2-py3-none-any.whl size=894089 sha256=f862477ebd0e75a32bd3ff8ee6d2c36fd61eb27e5f632d2772475566d3387a4b
  Stored in directory: /root/.cache/pip/wheels/d5/74/fc/38588a3d2e3f34f74588e6daa3aa5b0a322bd6f9420a707131
Successfully built scikit-fuzzy
Installing collected packages: scikit-fuzzy
Successfully installed scikit-fuzzy-0.4.2
WARNING: Running pip as the 'root' user can result in broken permissions and conflicting behaviour with the system package manager. It is recommended to use a virtual environment inste
ad: https://pip.pypa.io/warnings/venv class="ansi-yellow-fg">
```

+ Code + Markdown

#Read Dataset

```
#Read dataset metadataa
import pandas as pd
x_ray=pd.read_csv('/kaggle/input/coronahack-chest-xraydataset/Chest_xray_Corona_Metadata.csv')

x_ray
```

#Dataset type graph

```
import matplotlib.pyplot as plt
x_ray['Dataset_type'].hist()
plt.show()
```

#Show train image sample

```
import matplotlib.pyplot as plt
plt.figure(figsize=(10,8))
for i in range(9):

    plt.subplot(3, 3, i + 1,aspect = 'equal')
    plt.imshow(train_images[i])
    plt.tight_layout()
```

#Fuzzy, ICA function

```
def fuzzy(image,a,b,c,d):



    mfx = fuzz.trapmf(image.flatten(),  [0.4, 0.6,200,200])



    return mfx.reshape(256,256,3)



import skimage.segmentation as seg
import skimage.color as color

def seg_(image):



    image_aux= seg.slic(image,n_segments=3)
    img2 = np.zeros_like(image)
    img2[:,:,0]=image_aux
    img2[:,:,1]=image_aux
    img2[:,:,2]=image_aux

    return  img2

def ICA_(image,x):
    ica = FastICA(n_components = x)
    nsamples, nx, ny  = image.shape
    d2_train_dataset = image.reshape((nsamples,nx*ny))
    ica.fit(d2_train_dataset)
    image_ica = ica.fit_transform(d2_train_dataset)
    ICA_restored = ica.inverse_transform(image_ica)
    return  ICA_restored
```

#Apply Fuzzy logic for each image on dataset

```
images_fuzzy=[]
for image,name in zip(train_images,filenames):

            fuzzy_image=fuzzy(image,best_a,best_a+best_b,best_c,best_d)


            images_fuzzy.append(fuzzy_image)



images_valid_fuzzy=[]
for image in valid_images:

            fuzzy_image=fuzzy(image,best_a,best_a+best_b,best_c,best_d)




            images_valid_fuzzy.append(fuzzy_image)
io.imshow(fuzzy_image)
show()
```

Apply ICA dimensionality reduction for each image on dataset

```
images_ICA=[]
for image,name in zip(train_images,filenames):

            ICA_image=ICA_(image,15)


            images_ICA.append(ICA_image.reshape(256,256,3))



images_valid_ICA=[]
for image in valid_images:

            ICA_image=ICA_(image,15)




            images_valid_ICA.append(ICA_image.reshape(256,256,3))
io.imshow(ICA_image.reshape(256,256,3))
show()
```

Apply Fuzzy logic and ICA dimensionality reduction for each image on dataset

```
# Show (Fuzzy logic with ICA Image )
```

```
images_ICAFuzz=[]
for FuzzImg,name in zip(images_fuzzy,filenames):

            ICAFuzz_image=ICA_(FuzzImg,15)


            images_ICAFuzz.append(ICAFuzz_image.reshape(256,256,3))



images_valid_ICAFuzz=[]
for image in valid_images:

            ICAFuzz_image=ICA_(FuzzImg,15)




            images_valid_ICAFuzz.append(ICAFuzz_image.reshape(256,256,3))
io.imshow(ICAFuzz_image.reshape(256,256,3))
show()
```

Method to create Single Input Model ----------

```
import tensorflow as tf
from tensorflow.keras.applications.vgg16 import VGG16
from tensorflow.keras.applications import ResNet152V2
from tensorflow.keras.applications import InceptionV3
from tensorflow.keras.applications import Xception
from tensorflow.keras.applications import DenseNet121
from tensorflow.keras.models import Model
from tensorflow.keras.layers import Dense
from tensorflow.keras.layers import Input
from tensorflow.keras.layers import Flatten
from tensorflow.keras.layers import BatchNormalization
from tensorflow.keras.layers import Dropout
from tensorflow.keras.layers import concatenate
from tensorflow.keras.models import Sequential
from tensorflow.keras.layers import GlobalMaxPooling2D
from tensorflow.keras.optimizers import Adam
from tensorflow.keras.applications import DenseNet121

import sys
import subprocess
import pkg_resources
required = {'efficientnet'}
installed = {pkg.key for pkg in pkg_resources.working_set}
missing = required - installed
if missing:
    !pip install -U efficientnet
import efficientnet.keras as efn

from efficientnet.keras import EfficientNetB0 as Net
from efficientnet.keras import EfficientNetB3
def create_single_model(weights,dropout_var,network):

    input_shape=(256,256,3)

    model1 = VGG16(include_top=False, input_shape=(256, 256, 3))
    if network[0]=='VGG16':
        model1 = VGG16(include_top=False, input_shape=(256, 256, 3))

    if network[0]=='ResNet152V2':
        model1 = ResNet152V2(include_top=False, input_shape=(256, 256, 3))


    if network[0]=='InceptionV3':
        model1 = InceptionV3(include_top=False, input_shape=(256, 256, 3))

    if network[0]=='Xception':
        model1 = Xception(include_top=False, input_shape=(256, 256, 3))
```

#Train Model

```
    print('Testing with  {} and {}  '.format(network,weights))

    print('Creating model')
    model=create_single_model(weights,0.5,[network])
    opt = Adam(lr=1e-3, decay=1e-3 / 100)
    print('Model created')
    losses = tf.keras.losses.BinaryCrossentropy()
    model.compile(loss="binary_crossentropy" ,optimizer=opt,metrics=[tf.keras.metrics.Precision(name='precision_2'),
                                                                     tf.keras.metrics.Recall(name='recall_2'),tf.keras.metrics.AUC(name='auc'),'accuracy'])
    print('Model compiled')
    history=model.fit(
        x=[np.array(images_seg)], y=y,
        validation_data=([valid_images],y_valid),
        epochs=25, batch_size=16,callbacks=callbacks)
    auc=max(history.history['val_auc'])
    if auc>best_auc:
        best_auc=auc
        best_network=network
        best_weight=weights

    print('val_auc',auc)
    if (auc)>0.98:
        print('find')

    df_history=pd.DataFrame.from_dict(history.history)
    df_history.to_csv('/kaggle/working/seg_K-mean_History to {}  with weight of  {} '.format(network,weights)+'.csv')

    from matplotlib.pyplot import figure
    figure(num=None, figsize=(10, 10), dpi=80, facecolor='w', edgecolor='k')
    print('Loss to {}  with weight of  {} '.format(network,weights))
    plt.plot(history.history['loss'])
    plt.plot(history.history['val_loss'])
    plt.title('Loss to {}  with weight of  {} '.format(network,weights))
    plt.ylabel('loss')
```

Appendix B

Appendix B: Result of Python Software Implementation

#dataset sample

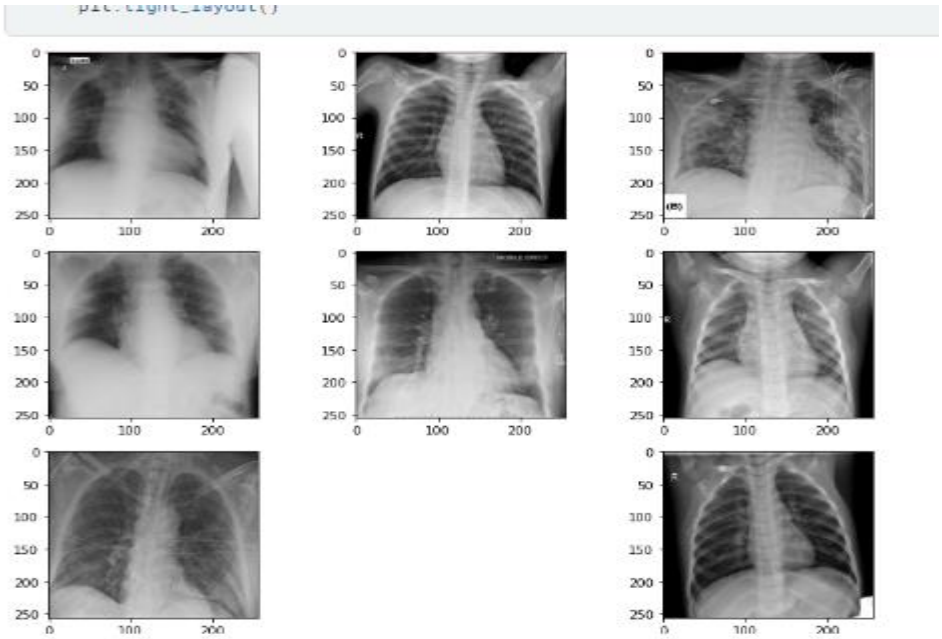

Result of Apply Fuzzy logic for each image on dataset

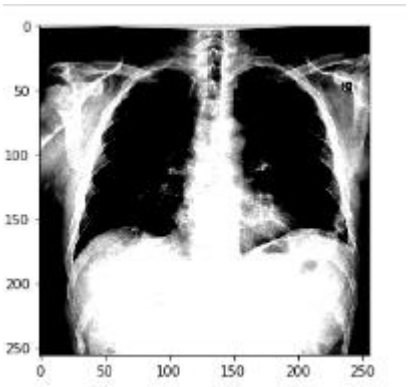

Apply ICA dimensionality reduction for each image on dataset

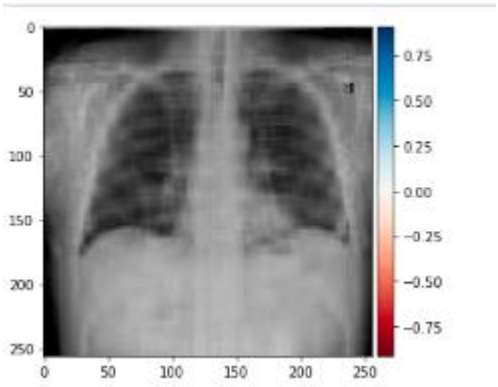

Apply Fuzzy logic and ICA dimensionality reduction

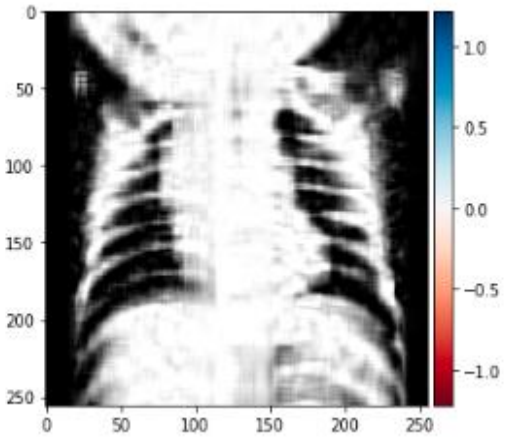

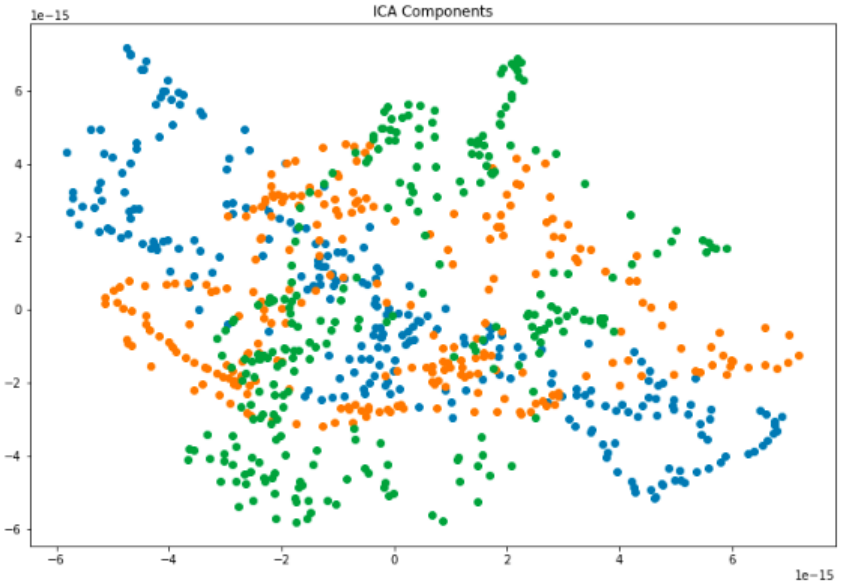

#Train for 25 epoch

```
Requirement already satisfied: efficientnet in /opt/conda/lib/python3.7/site-packages (1.1.1)
Requirement already satisfied: keras-applications<=1.0.8,>=1.0.7 in /opt/conda/lib/python3.7/site-packages (from efficientnet) (1.0.8)
Requirement already satisfied: scikit-image in /opt/conda/lib/python3.7/site-packages (from efficientnet) (0.19.3)
Requirement already satisfied: numpy>=1.9.1 in /opt/conda/lib/python3.7/site-packages (from keras-applications<=1.0.8,>=1.0.7->efficientnet) (1.21.6)
Requirement already satisfied: h5py in /opt/conda/lib/python3.7/site-packages (from keras-applications<=1.0.8,>=1.0.7->efficientnet) (3.7.0)
Requirement already satisfied: networkx>=2.2 in /opt/conda/lib/python3.7/site-packages (from scikit-image->efficientnet) (2.5)
Requirement already satisfied: scipy>=1.4.1 in /opt/conda/lib/python3.7/site-packages (from scikit-image->efficientnet) (1.7.3)
Requirement already satisfied: imageio>=2.4.1 in /opt/conda/lib/python3.7/site-packages (from scikit-image->efficientnet) (2.19.3)
Requirement already satisfied: pillow!=7.1.0,!=7.1.1,!=8.3.0,>=6.1.0 in /opt/conda/lib/python3.7/site-packages (from scikit-image->efficientnet) (9.1.1)
Requirement already satisfied: packaging>=20.0 in /opt/conda/lib/python3.7/site-packages (from scikit-image->efficientnet) (21.3)
Requirement already satisfied: tifffile>=2019.7.26 in /opt/conda/lib/python3.7/site-packages (from scikit-image->efficientnet) (2021.11.2)
Requirement already satisfied: PyWavelets>=1.1.1 in /opt/conda/lib/python3.7/site-packages (from scikit-image->efficientnet) (1.3.0)
Requirement already satisfied: decorator>=4.3.0 in /opt/conda/lib/python3.7/site-packages (from networkx>=2.2->scikit-image->efficientnet) (5.1.1)
Requirement already satisfied: pyparsing!=3.0.5,>=2.0.2 in /opt/conda/lib/python3.7/site-packages (from packaging>=20.0->scikit-image->efficientnet) (3.0.9)
WARNING: Running pip as the 'root' user can result in broken permissions and conflicting behaviour with the system package manager. It is recommended to use a virtual environment instead:
s/venv class="ansi-yellow-fg">
Testing with  ResNet152V2 and 20
Creating model
Model created
Model compiled
Epoch 1/25
8/8 [==============================] - 21s 793ms/step - loss: 0.6477 - precision 2: 0.6129 - recall 2: 0.3065 - auc: 0.7079 - accuracy: 0.5565 - val loss: 9.2691 - val precision 2: 0.0000
00 - val auc: 0.5000 - val accuracy: 0.5000
Epoch 2/25
8/8 [==============================] - 3s 362ms/step - loss: 0.5500 - precision 2: 0.8913 - recall 2: 0.6613 - auc: 0.8770 - accuracy: 0.7903 - val loss: 689722.5000 - val precision 2: 0.
00e+00 - val auc: 0.5000 - val accuracy: 0.5000
Epoch 3/25
8/8 [==============================] - 3s 343ms/step - loss: 0.5244 - precision 2: 0.8525 - recall 2: 0.8387 - auc: 0.9123 - accuracy: 0.8468 - val loss: 15955472.0000 - val precision 2:
0000e+00 - val auc: 0.5000 - val accuracy: 0.5000
Epoch 4/25
8/8 [==============================] - 3s 335ms/step - loss: 0.5279 - precision 2: 0.8226 - recall 2: 0.8226 - auc: 0.8963 - accuracy: 0.8226 - val loss: 112152.4609 - val precision 2: 0.
00e+00 - val auc: 0.5000 - val accuracy: 0.5000
Epoch 5/25
8/8 [==============================] - 3s 336ms/step - loss: 0.4652 - precision 2: 0.9123 - recall 2: 0.8387 - auc: 0.9489 - accuracy: 0.8790 - val loss: 1111.7107 - val precision 2: 0.37
al auc: 0.4722 - val accuracy: 0.4722
Epoch 6/25
8/8 [==============================] - 3s 335ms/step - loss: 0.4538 - precision 2: 0.9206 - recall 2: 0.9355 - auc: 0.9680 - accuracy: 0.9274 - val loss: 46.6433 - val precision 2: 0.8000
 auc: 0.6651 - val accuracy: 0.6667
Epoch 7/25
8/8 [==============================] - 3s 341ms/step - loss: 0.4543 - precision 2: 0.8966 - recall 2: 0.8387 - auc: 0.9499 - accuracy: 0.8710 - val loss: 8.2658 - val precision 2: 0.7500
auc: 0.6979 - val accuracy: 0.6389
```

LIST OF ACCEPTED PAPER

1-Mohanad S. Al-Mothafar, Ahmed Kareem Abdullah, and Faris Mohammed Ali, "Web Server Self-Examination for Detection of COVID-19 Cases with Fuzzy Classifiers Using Chest X-Ray Image," Scopus - AIP Conference Proceedings (ICASDG- Turkey Istanbul), 2022.

2- Mohanad S. Al-Mothafar, Ahmed Kareem Abdullah, and Faris Mohammed Ali, "Enhancement detect of COVID-19 Based ICA Dimensionality Reduction of CXR images," IEEE International Conference (AEST-2022), 2022.

الملخص

يعد تشخيص فيروس (Coronavirus) COVID-19 مشكلة صحية رئيسية في جميع أنحاء العالم. هناك طرق عديدة لتشخيص هذا المرض، من بينها اختبار تفاعل البوليميرات المتسلسل (PCR) الذي يستخدم على نطاق واسع في جميع أنحاء العالم. لكون هذا الاختبار بطيئًا في نتائجه، كما أن دقته مشكوك فيها، لأنه يرتبط بنتائج سلبية / إيجابية عالية كاذبة. وفقًا لذلك، تعتبر الأشعة السينية للصدر (CXR) طريقة تحقيق مهمة للوصول إلى التشخيص. تتمثل أهداف هذا البحث في تعزيز الكشف عن COVID-19 من خلال تقنية المنطق الضبابي بطريقتين (الكشف عن الحواف، والتعبير عن نسبة تلف الرئة) واستخدام تحليل المكونات المستقلة (ICA) كأداة لتقليل ابعاد الصورة. تتضمن منهجية هذا البحث جمع صور للأشعة السينية الخاصة بالصدر (chest X-Rays) من مصادر مجموعة بيانات موثوقة متعددة ثم استخدام التقنيات المقترحة (المنطق الضبابي ، تحليل المكونات المستقلة) كمعالجة مسبقة للصورة ، بعد ذلك يتم استخدام شبكة الالتفاف العصبية (CNN) ، تحديداً شبكات التعلم العميق . لتدريب البيانات بعد عملية المعالجة المقترحة، ثم دراسة مدى تأثير التقنيات المقترحة المتعلقة بالمرشح ضبابي وICA في شبكات التعلم العميق. في النهاية، تم استخدام اختبار عملي للنموذج المدرب النهائي على جهاز حاسوب صغير (Raspberry Pi) حيث تم استخدامه ك(webserver). حيث تم الحصول على نتائج عالية الدقة عند اختبار النموذج. حيث بلغة الدقة عند الاختبار أكثر من 90%. تُظهر التقنيات المقترحة أداءً عاليًا من حيث AUC والدقة ووقت التدريب عند مقارنتها بالتقنيات الحديثة الموجودة في الأدبيات السابقة. أخيرًا، تم تطبيق النظام المقترح لهذا العمل، من خلال إنشاء تطبيق ويب، حيث يتم إدخال صورة الصدر الخاصة بالمريض على النموذج المدرب باستخدام جهاز ذكي (محمول أو جهاز لوحي) عبر واجهة مستخدم رسومية (GUI).

تحسين الكشف عن كوفيد-19 باستخدام تقنيتي المنطق المضبب وتحليل المركبات المستقلة

الرسالة

مقدمة الى قسم هندسة تقنيات الاتصالات كجزء من متطلبات نيل درجة الماجستير في هندسة تقنيات الاتصالات

تقدم بها

مهند صارم عبد الله

إشراف

ا.م.د. احمد كريم البكري **ا.د. فارس محمد علي الجعيفري**

٢٠٢٢

جمهورية العراق
وزارة التعليم العالي والبحث العلمي
جامعة الفرات الاوسط التقنية
الكلية التقنية الهندسية- نجف

تحسين الكشف عن كوفيد-19 باستخدام تقنيتي المنطق المضبب وتحليل المركبات المستقلة

مهند صارم عبد الله

ماجستير في هندسة تقنيات الاتصالات

٢٠٢٢